AD-A013 181

LOW ANGLE-OF-ATTACK LONGITUDINAL AERODYNAMIC PARAMETERS OF NAVY T-2 TRAINER AIRCRAFT EXTRACTED FROM FLIGHT DATA: A COMPARISON OF IDENTIFICATION TECHNIQUES. VOLUME I. DATA ACQUISITION AND MODIFIED NEWTON-RAPHSON ANALYSIS

A. J. Schuetz

Naval Air Development Center
Warminster, Pennsylvania

23 June 1975

DISTRIBUTED BY:

NTIS

National Technical Information Service
U. S. DEPARTMENT OF COMMERCE

DISCLAIMER NOTICE

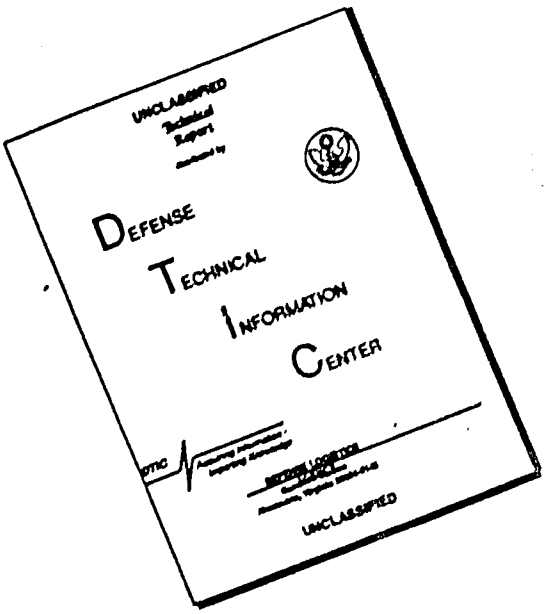

THIS DOCUMENT IS BEST QUALITY AVAILABLE. THE COPY FURNISHED TO DTIC CONTAINED A SIGNIFICANT NUMBER OF PAGES WHICH DO NOT REPRODUCE LEGIBLY.

AD A013181

REPORT NO. NADC-74181-30

225120

LOW ANGLE-OF-ATTACK LONGITUDINAL AERODYNAMIC PARAMETERS OF NAVY T-2 TRAINER AIRCRAFT EXTRACTED FROM FLIGHT DATA: A COMPARISON OF IDENTIFICATION TECHNIQUES

VOLUME I

DATA ACQUISITION AND MODIFIED NEWTON–RAPHSON ANALYSIS

A. J. Schuetz
Air Vehicle Technology Department
NAVAL AIR DEVELOPMENT CENTER
Warminster, Pennsylvania 18974

23 June 1975

FINAL REPORT
IR TASK R000-01-01/MF-9-01

DDC
JUL 31 1975
B

APPROVED FOR PUBLIC RELEASE; DISTRIBUTION UNLIMITED.

Reproduced by
NATIONAL TECHNICAL
INFORMATION SERVICE
U S Department of Commerce
Springfield VA 22151

Prepared for
DIRECTOR OF NAVAL LABORATORIES
Department of the Navy
Washington, D. C. 20390

NOTICES

REPORT NUMBERING SYSTEM - The numbering of technical project reports issued by the Naval Air Development Center is arranged for specific identification purposes. Each number consists of the Center acronym, the calendar year in which the number was assigned, the sequence number of the report within the specific calendar year, and the official 2-digit correspondence code of the Command Office or the Functional Department responsible for the report. For example: Report No. NADC-73015-40 indicates the fifteenth Center report for the year 1973, and prepared by the Crew Systems Department. The numerical codes are as follows:

CODE	OFFICE OR DEPARTMENT
00	Commander, Naval Air Development Center
01	Technical Director, Naval Air Development Center
02	Program and Financial Management Department
03	Anti-Submarine Warfare Program Office
04	Remote Sensors Program Office
05	Ship and Air Systems Integration Program Office
06	Tactical Air Warfare Office
10	Naval Air Facility, Warminster
20	Aero Electronic Technology Department
30	Air Vehicle Technology Department
40	Crew Systems Department
50	Systems Analysis and Engineering Department
60	Naval Navigation Laboratory
81	Administrative and Technical Services Department
85	Computer Services Department

PRODUCT ENDORSEMENT - The discussion or instructions concerning commercial products herein do not constitute an endorsement by the Government nor do they convey or imply the license or right to use such products.

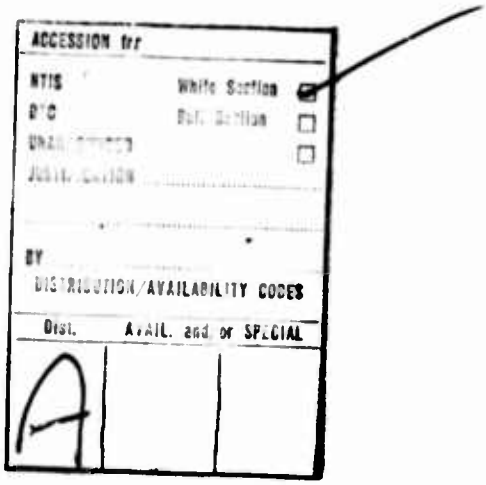

APPROVED BY: P. D. Stoops DATE: 23 June 1975

P. D. STOOPS
Commander, USN
Deputy Director, AVTD

UNCLASSIFIED

SECURITY CLASSIFICATION OF THIS PAGE (When Data Entered)

REPORT DOCUMENTATION PAGE		READ INSTRUCTIONS BEFORE COMPLETING FORM
1. REPORT NUMBER NADC-74181-30	2. GOVT ACCESSION NO.	3. RECIPIENT'S CATALOG NUMBER
4. TITLE (and Subtitle) LOW ANGLE-OF-ATTACK LONGITUDINAL AERODYNAMIC PARAMETERS OF NAVY T-2 TRAINER AIRCRAFT EXTRACTED FROM FLIGHT DATA: A COMPARISON OF IDENTIFICATION TECHNIQUES VOLUME I: DATA ACQUISITION AND MODIFIED NEWTON-RAPHSON ANALYSIS		5. TYPE OF REPORT & PERIOD COVERED Final Report 6. PERFORMING ORG. REPORT NUMBER
7. AUTHOR(s) A. J. Schuetz		8. CONTRACT OR GRANT NUMBER(s)
9. PERFORMING ORGANIZATION NAME AND ADDRESS Air Vehicle Technology Department (Code 30) Naval Air Development Center Warminster, Pa. 18974		10. PROGRAM ELEMENT, PROJECT, TASK AREA & WORK UNIT NUMBERS IR TASK R000-01-01/MF-9-01
11. CONTROLLING OFFICE NAME AND ADDRESS Director of Naval Laboratories Department of the Navy Washington, D. C. 20390		12. REPORT DATE 23 June 1975 13. NUMBER OF PAGES ~~145~~ 144
14. MONITORING AGENCY NAME & ADDRESS(if different from Controlling Office)		15. SECURITY CLASS. (of this report) Unclassified 15a. DECLASSIFICATION/DOWNGRADING SCHEDULE
16. DISTRIBUTION STATEMENT (of this Report) Approved for Public Release, Distribution Unlimited		
17. DISTRIBUTION STATEMENT (of the abstract entered in Block 20, if different from Report)		
18. SUPPLEMENTARY NOTES		
19. KEY WORDS (Continue on reverse side if necessary and identify by block number)		

20. ABSTRACT (Continue on reverse side if necessary and identify by block number)

A Navy T-2 jet trainer aircraft was instrumented to measure and record all motion variables. Motion time histories were recorded for a variety of carefully selected pilot inputs. A unique problem with the data was the high noise level in the measurement of the control input. Longitudinal motion data were analyzed with three digital computer parameter identification techniques: modified Newton-Raphson, Kalman filtering/smoothing, and maximum likelihood. Reported in Volume I are data gathering and modified Newton-Raphson analysis.

DD FORM 1 JAN 73 1473 EDITION OF 1 NOV 65 IS OBSOLETE
S/N 0102-014-6601

UNCLASSIFIED

SECURITY CLASSIFICATION OF THIS PAGE (When Data Entered)

A C K N O W L E D G E M E N T S

As with any research and development program involving full scale experimental work (e.g., flight testing), literature search, and comparison with other current work, analysis, and contractual assistance, this project involved a large number of people. Some of these participants will be authors or co-authors of papers and/or reports related to this project, but for the most the only recognition will be a brief mention here. The author, then, wishes to express his thanks for the cooperation and assistance of the following people who made particularly significant contributions:

Mr. A. Piranian, who served as flight test engineer, performing all the daily tasks essential to gathering the flight data;

Mr. John Eney, who conceived this program while project engineer for the variable stability T-2;

Messrs. Joe Dapkiewicz, Joe Ozer, and Al Ortiz, who operated the aging telemetry and recording equipment to the best of their abilities;

LCDR Dennis Laack, principal pilot for the project, who also served as unofficial liaison between the engineers and the military personnel involved in the flight testing;

Mr. Larry Taylor of NASA-Langley Research Center and Mr. Ken Iliff of NASA-Flight Research Center, who provided advice and counsel concerning the identification process;

Messrs. Ed Rynaski and Robert Chen of Calspan Corp., and Messrs. James Tyler, Dave Stepner, and Earl Hall of Systems Control, Inc., who patiently awaited the arrival of the flight data while providing guidance on identification techniques, flight instrumentation, and pilot control input selection; and

Mr. Steve Williams of NAVAIRTESTCEN, who performed the analog to digital conversion of the flight data.

While this program began under Independent Research and Development funding from the Technical Director of NAVAIRDEVCEN, substantial delays in gathering the flight data pushed the program into FY74, and the program could not be fully supported by IR&D money any longer. Consequently, the completion of the program was financed largely under the Naval Air Systems Command High Angle of Attack Aircraft Parameter Identification Program (one task area under the Combat Effectiveness and Safety AIRTASK). Without the cooperation and understanding of the program sponsor, Mr. Ray Siewert, NAVAIR-320D, it is unlikely that this research could have been completed.

SUMMARY

A Navy T-2 jet trainer aircraft was instrumented to measure and record all airframe motion variables. Motion time histories were recorded for small perturbation responses to a variety of carefully selected pilot inputs. Two flight conditions were considered: a relatively high speed power approach configuration and a high speed cruise condition. Noise levels in the data were found to be significant, and it was determined that measurement noise was a larger problem in this case than process noise. A unique noise problem was the high level of measurement noise on the control inputs.

Although all motion variables were recorded, only longitudinal motion time histories were used for analysis. Three digital computer parameter identification techniques were applied to the data: modified Newton-Raphson (in-house at NAVAIRDEVCEN), Kalman filtering/smoothing (Calspan Corp.), and maximum likelihood (Systems Control, Inc.). The objective was the determination of the relative accuracy and utility of the three techniques. Volume I reports the data gathering effort and the modified Newton-Raphson analysis.

For the in-house analysis, a linear mathematical model was used, containing nine stability derivatives to be identified. In general, the identification effort was successful in matching model response to flight data and obtaining consistent sets of stability derivatives from the various data segments, but the time history matches are far from perfect and some anomalies do exist in the stability derivative results.

TABLE OF CONTENTS

LIST OF FIGURES

LIST OF TABLES

LIST OF SYMBOLS

Symbol	Definition	Dimension
A	angle of attack	deg
A/D	analog/digital	-
AX	longitudinal acceleration	ft/sec^2
AZ	normal acceleration	ft/sec^2
a_x	AX	-
a_z	AZ	-
C_D	drag coefficient	-
C_L	lift coefficient	-
$C_{m_{\delta_e}}$	$\partial C_m/\partial \delta_e$	1/deg
C_{D_α}	$\partial C_D/\partial \alpha$	-
CDC	Control Data Corp.	-
c	mean aerodynamic chord	ft
c.g.	center of gravity	%c
DE	elevator deflection	deg
DEZ	elevator deflection set to zero after significant input	-
F	matrix of stability derivatives	-
FM	frequency modulation	
G	matrix of control derivatives	-
g	acceleration due to gravity	$32.2\ ft/sec^2$
h	altitude	ft
I_x	moment of inertia about roll axis	$slug/ft^2$
I_y	moment of inertia about pitch axis	$slug/ft^2$
I_z	moment of inertia about yaw axis	$slug/ft^2$

LIST OF SYMBOLS (CON'T)

Symbol	Definition	Dimension
L	roll moment	ft-lb
L_p	$1/I_x \; \partial L/\partial p$	1/sec
L_r	$1/I_x \; \partial L/\partial r$	1/sec
L_θ	$1/I_x \; \partial L/\partial \theta$	$1/sec^2$
$L\delta_a$	$1/I_x \; \partial L/\partial \delta_a$	$\frac{1}{sec^2\text{-deg}}$
$L\delta_r$	$1/I_x \; \partial L/\partial \delta_r$	$\frac{1}{sec^2\text{-deg}}$
M	pitching moment	ft-lb
M_q	$1/I_y \; \partial M/\partial q$	1/sec
M_u	$1/I_y \; \partial M/\partial u$	$\frac{1}{ft\text{-sec}}$
M_α	$1/I_y \; \partial M/\partial \alpha$	$1/sec^2$
$M_{\dot{\alpha}}$	$1/I_y \; \partial M/\partial \dot{\alpha}$	1/sec
$M\delta_e$	$1/I_y \; \partial M/\partial \delta_e$	$\frac{1}{sec^2\text{-deg}}$
m	mass	slugs
N	yawing moment	ft-lb
NASA	National Aeronautics and Space Administration	-
NAVAIRDEVCEN	Naval Air Development Center	-
N_p	$1/I_z \; \partial N/\partial p$	1/sec
N_r	$1/I_z \; \partial N/\partial r$	1/sec
N_θ	$1/I_z \; \partial N/\partial \theta$	$1/sec^2$
$N\delta_a$	$1/I_z \; \partial N/\partial \delta_a$	$\frac{1}{sec^2\text{-deg}}$

LIST OF SYMBOLS (CON'T)

Symbol	Definition	Dimension
N^{δ}_{r}	$1/I_z \; \partial N/\partial \delta_r$	$\frac{1}{sec^2\text{-deg}}$
n_x	longitudinal acceleration	g
n_y	lateral acceleration	g
n_z	normal acceleration	g
PAM	pulse amplitude modulation	-
p	roll rate	rad/sec
Q	pitch rate	rad/sec
QD	pitch acceleration	rad/sec^2
q	Q	-
r	yaw rate	rad/sec
S	wing area	ft^2
S	number of smoothing iterations	-
SCI	Systems Control Inc.	-
TH	pitch angle	deg
U	airspeed	ft/sec
u	perturbation airspeed	ft/sec
u	control vector	-
W	number of weighting iterations	-
X	longitudinal (fore-aft) force	lb
X_u	$1/m \; \partial X/\partial u$	1/sec
X_{α}	$1/m \; \partial X/\partial \alpha$	ft/sec^2
X^{δ}_{e}	$1/m \; \partial X/\partial \delta_e$	$\frac{ft}{sec^2\text{-deg}}$

LIST OF SYMBOLS (CON'T)

Symbol	Definition	Dimension
x	state vector	--
Y	sideforce	lb
Y_p	$1/m\ \partial Y/\partial p$	ft/sec
Y_r	$1/m\ \partial Y/\partial r$	ft/sec
Y_β	$1/m\ \partial Y/\partial \beta$	ft/sec^2
Y_{δ_a}	$1/m\ \partial Y/\partial \delta_a$	$\frac{ft}{sec^2\text{-deg}}$
Y_{δ_r}	$1/m\ \partial Y/\partial \delta_r$	$\frac{ft}{sec^2\text{-deg}}$
Z	vertical (normal) force	lb
Z_q	$1/m\ \partial Z/\partial q$	ft/sec
Z_u	$1/m\ \partial Z/\partial u$	1/sec
Z_α	$1/m\ \partial Z/\partial \alpha$	ft/sec^2
$Z_{\dot{\alpha}}$	$1/m\ \partial Z/\partial \dot{\alpha}$	ft/sec
Z_{δ_e}	$1/m\ \partial Z/\partial \delta_e$	$\frac{ft}{sec^2\text{-deg}}$
α	A	-
β	sideslip angle	deg
γ	flight path angle	deg
δ_a	aileron deflection	deg
δ_b	speed brake deflection	deg
δ_e	elevator deflection	deg
δ_r	rudder deflection	deg
θ	TH	-
ρ	air density	$slug/ft^3$
ϕ	roll angle	deg

INTRODUCTION

The problem of extracting aerodynamic parameters, such as stability derivatives, from aircraft flight data has been the subject of considerable study over the years. In the past decade, however, the use of digital computer parameter identification techniques has given new impetus to the technology. The state of the art, except for the most recent developments, is summarized in reference (a).

The primary objective of this program was the assessment of the relative accuracy and utility of several existing parameter identification techniques. Secondary objectives were the establishment of one consensus set of stability derivatives for the T-2 aircraft, development of one identification technique for continuing in-house use at NAVAIRDEVCEN, and the establishment of a carefully and completely documented file of flight data to be made available to anyone pursuing parameter identification technique development. Although not part of the original objectives, the most significant result of this current work may be the development of NAVAIRDEVCEN expertise (in data acquisition and use of identification techniques) which will be essential in the current effort on development of high angle of attack (stall/post-stall/spin) parameter identification processes.

It should be emphasized that no attempt was planned or made to originate new identification techniques or even substantially modify existing ones. Rather, existing techniques were used, modified only slightly for adaptation to this particular application. In recent years, the opinion that the low angle of attack aircraft identification problem had been "solved" has been expressed by numerous investigators in various forums. Thus there seemed to be no need to attempt to develop any new identification techniques for this program.

Since a portion of the program objective was the establishment of an in-house identification capability for the future, the existing telemetry and data recording equipment at NAVAIRDEVCEN was used for the project, although this equipment was by no means state-of-the-art. This constraint conflicted with the desire of producing carefully controlled, low noise level flight data - a type of flight data which has been essentially unavailable to many investigators in the parameter identification field. The most significant problem with generally available flight data in the past, however, has been a lack of documentation. For this project all relevant information pertaining to flight circumstances and instrumentation has been recorded.

The need for an in-house capability in parameter identification perhaps merits further comment. Although it has not been active in in-house experimental flight dynamics research programs prior to the effort reported here, NAVAIR-DEVCEN is designated (reference (b)) as the lead laboratory for flight dynamics research and development work in the Navy. Consequently, it would be appropriate and desirable for NAVAIRDEVCEN to have a capability for in-house experimental flight dynamics work, and parameter identification would probably be required in such work.

In particular, NAVAIRDEVCEN has planned to construct a variable stability research aircraft and prototype trainer based on the T-2. A parameter identification capability is necessary for the calibration and verification of such a simulator. A consensus set of T-2 stability derivatives as a function of flight condition would be necessary for the programming of the variable stability control system, so two portions of the results of this work have application to the variable stability project.

Volume I of this report concerns the acquisition of the flight data and the in-house identification effort, while Volume II reports on the contractor identification efforts.

SELECTION OF IDENTIFICATION TECHNIQUES

It is generally recognized that modern, digital computer, identification techniques can be divided into two types: maximum likelihood and Kalman filtering. Reference (c) provided an explanation of this division. Within these two broad divisions there exist many techniques which are somewhat different in specifics although similar in principle, and in fact there are numerous techniques which are quite similar although referred to by different names. All these techniques are "output error" types; equation of motion error techniques and non-digital (i.e., analog matching) techniques were not considered in this study.

Probably the most popular of the digital techniques today is the modified Newton-Raphson technique, which is a member of the maximum likelihood "family", and in fact becomes a maximum likelihood method if a properly calculated weighting matrix is used. Considering the relatively straightforward nature and the wide acceptance of the modified Newton-Raphson technique, it was decided to use this technique in-house at NAVAIRDEVCEN.

Processing of the data by the most advanced identification technique at NASA-Ames Research Center, NASA-Langley Research Center, and NASA-Flight Research Center was considered highly desirable, but pressures of other work and limited manpower, and delays in the gathering of the data by NAVAIRDEVCEN, made NASA participation uncertain. To ensure that at least three different identification techniques would be used, two contractors were selected to perform analysis concurrently with the in-house effort.

Systems Control, Inc., of Palo Alto, California, was contracted to use their version of maximum likelihood (reference (d)); Calspan Corp. of Buffalo, New York, was paid to apply their Kalman filtering/smoothing (reference (e)) method to the data.

It was decided that the in-house analysis effort would have a different philosophy than the contracted efforts. In-house, the data would be run through the identification procedure without any substantial operator interface - the program would simply be "on its own". The contractors, however, would be free to make minor modifications to their programs as they desired,

and to use any level of human involvement which they felt appropriate. Major modifications to the programs were rendered impossible by cost and time constraints, in addition to being contrary to the philosophy of the program.

EXPERIMENTAL EQUIPMENT AND CONDITIONS

THE AIRCRAFT

The flight data used in this report were obtained with YT-2B BuNo 144218, shown in Figures 1 and 2. The aircraft was constructed by Rockwell International, Columbus Division (formerly North American), as a prototype of the model T-2B, and is essentially identical to the T-2B and T-2C with respect to aerodynamics. The geometric parameters of the aircraft are given in Table I.

The most significant features of the aircraft configuration are the straight, mid-fuselage wing and the conventional elevator mounted on a fixed cruciform tail. The flaps are semi-Fowler single-slotted.

Naval Air Facility, Warminster, was the base of the aircraft throughout the flight program, and the majority of flights were conducted in the south-eastern Pennsylvania and southern New Jersey areas.

INSTRUMENTATION

A complete set of motion transducers was installed in the YT-2B for the sole purpose of obtaining flight time histories for parameter identification analysis. The locations and serial numbers of the transducers, as originally installed, are given in Table II. The measurement ranges of the transducers are presented in Table III. As of 10 May 1973, the changes listed in Table IV became effective.

In addition to the transducers listed in the tables, the aircraft was equipped for the measurement of airspeed, altitude, angle of attack, sideslip, and control positions. For the purposes of this project, the YT-2B was re-equipped with the noseboom constructed by North American at the time of the original flight testing. The boom included a pitot-static system and α and β vanes.

The pressure altitude transducer was intended to measure perturbation altitudes ±1200 feet about a reference altitude, which was "locked in" when the pilot selected the "altitude reference engage" control. The transducer malfunctioned, however, and would measure only +1200, -600 feet from reference. A reference-and-climb procedure was used to make the effective range ±900 feet.

Airspeed was also calculated from the dynamic pressure transducer at the tip of the noseboom. Two independent transducers were used for "coarse" and "fine" measurements. Coarse airspeed had a range of 0-500 kt, while 0-50 kt was the range for fine airspeed which was automatically reset to zero at each 50 kt upper limit, thus describing a "sawtooth" function. This resetting

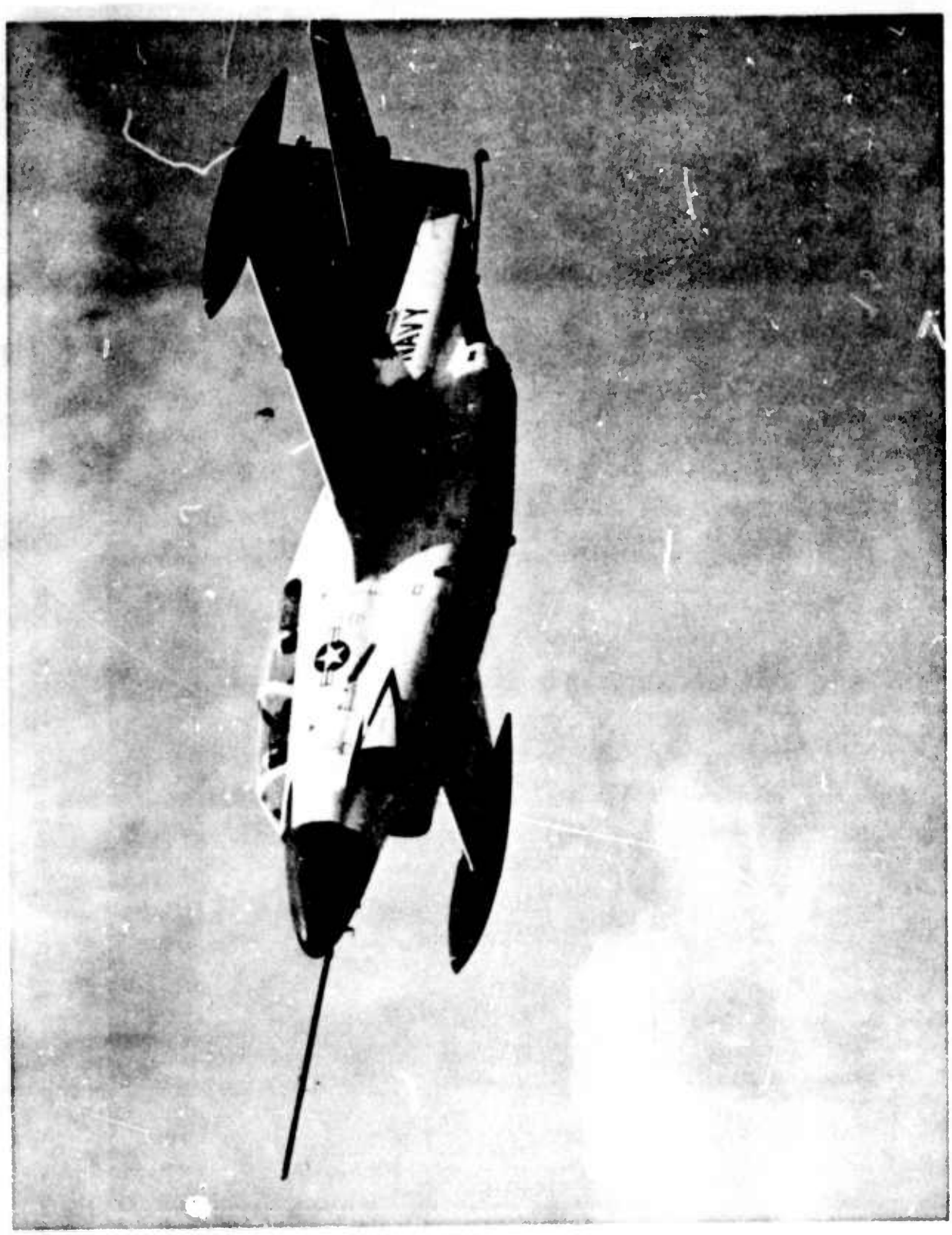

FIGURE 1. YT-2B BuNo 144218, CLEAN CONFIGURATION

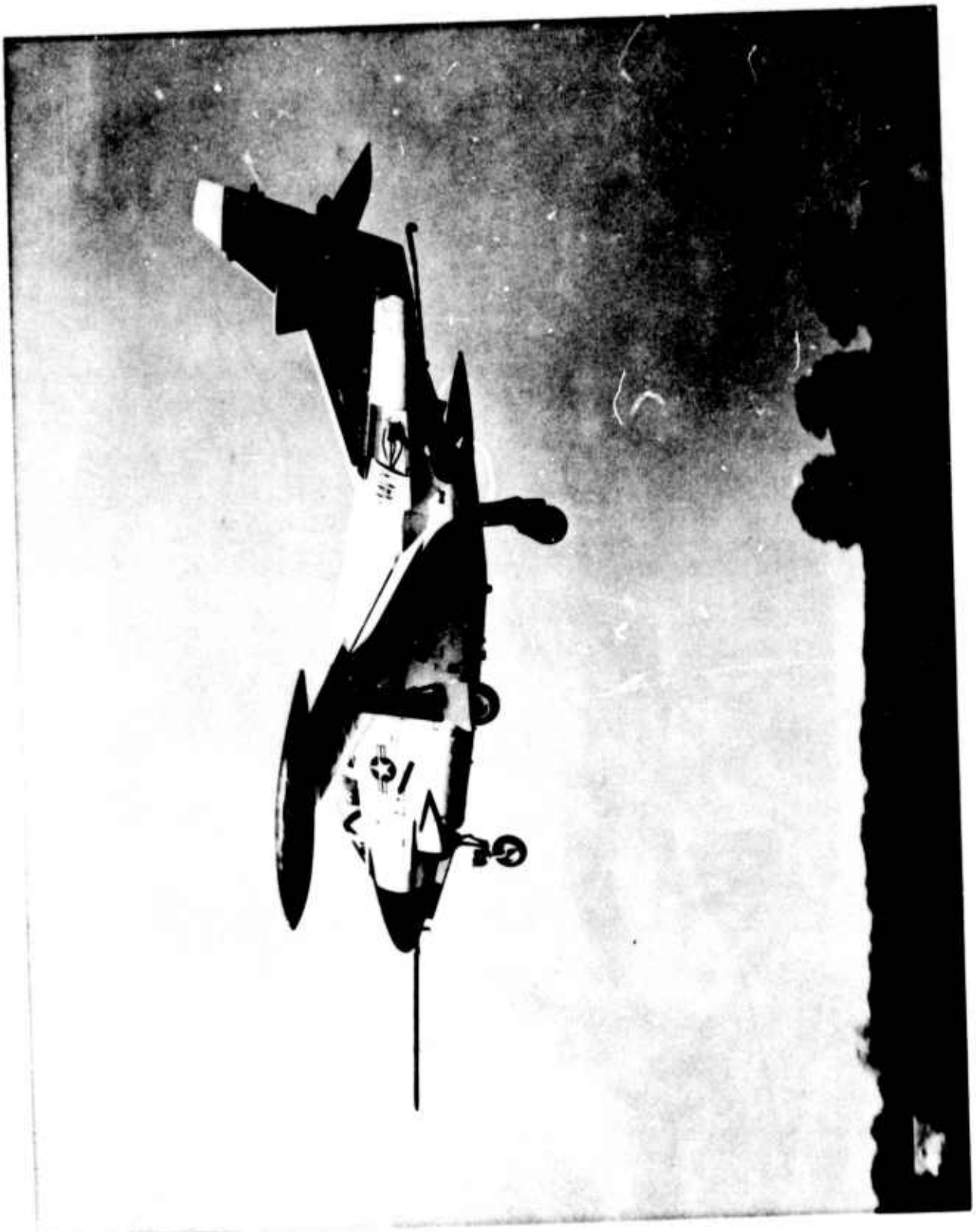

FIGURE 2. YT-2B BuNo 144218, POWER APPROACH CONFIGURATION

TABLE I
GEOMETRIC PARAMETERS OF FULL-SCALE T-2
(from reference (f))

WING		
S_W	Total area (includes flap, aileron and 39.39 ft^2 covered by fuselage)	254.86 ft^2
A_W	Net surface area (wetted)	424.85 ft^2
b_w	Span (perpendicular to plane of symmetry) including tiptanks	38.13 ft
AR_w	Aspect Ratio	5.07
λw	Taper Ratio	.496
Γw	Dihedral Angle	+3°
	Chord (in streamline direction)	
c_r	Root (Wing Sta. 0)	114.20 in
c_t	Tip Chord (Wing Sta. 214.242)	56.63 in
	(Equivalent)	
$\bar{c}_w$	Mean aerodynamic chord	88.88 in
	(Wing Sta. 95.078)	
	Location of 25% MAC	F.S. 219.697
Λ_w	Sweepback of 25% element	2°17'
i_w	Incidence angle	
	Root Chord	2°
	Tip Chord	-1°
	Airfoil Section (root and tip in streamline direction)	NASA641A212 a = .8*(MOD) (flaps and ailerons rigged 3° up)
	*NAA Modified	

TABLE I (CON'T)
GEOMETRIC PARAMETERS OF FULL-SCALE T-2
(from reference (f))

Ω_w	Rate of Taper	0.2671
FLAP (Data for One)		
	Type	Single Slotted
S_f	Area	22.78 ft^2
b_f	Span (perpendicular to plane of symmetry)	101.75 in
c_i	Inboard chord (Wing Sta. 27.09)	39.39 in
c_o	Outboard chord (Wing Sta. 127.54)	29.63 in
c_f/c_w	Ratio flap chord to wing chord (avg.)	.37
$b_f/b_{\frac{w}{2}}$	Ratio flap span to wing semi-span	.475
δ_f	Flap deflection, maximum (from uprigged position)	33°
	Flap in neutral position	3° Up
AILERON		
	Type	Straight Sided
S_a	Area (aft of hinge line and including tab)	9.5 ft^2
b_a	Span (perpendicular to plane of symmetry)	79.57 in
c_i	Inboard chord (Wing Sta. 128.69)	20 in
c_o	Outboard chord (Wing Sta. 208.26)	14.66 in
c_a/c_w	Ratio aileron chord (aft H.L.) to wing chord	.25
$b_a/b_{\frac{w}{2}}$	Ratio aileron span to wing semi-span	.374

TABLE I (CON'T)
GEOMETRIC PARAMETERS OF FULL-SCALE T-2
(from reference (f))

δ_a	Aileron deflection, maximum (from neutral position)	-12° Up, +13° Dn
	Aileron in neutral position	3° Up
	Aerodynamic Balance	Sealed paddle balance
S_b	Balance area forward of the H.L. (including 50% of fabric seal)	4.45 ft^2
c_b/c_a	Ratio balance chord to aileron chord	.42
	Static balance	Weighted paddle balance
	Irreversible full power system	Hydraulic
AILERON TRIM TAB		
	Ground adjustable fixed tab on each aileron	
S_a	Area (each)	.07 ft^2
HORIZONTAL TAIL*		
S_h	Total area (includes 3.07 ft^2 covered by vertical tail and fairing)	72.29 ft^2
S_{net_h}	Net area	146.38 ft^2
A_h	Net surface area (wetted)	146.38 ft^2
b_h	Span	17.91 ft
AR_h	Aspect Ratio	4.42
λ_h	Taper Ratio	0.50
Γ_h	Dihedral angle	0°
Λ_h	Sweepback of 25% element	15°

*Percent lines base on horizontal prior to addition of trailing edge extension.

TABLE I (CON'T)
GEOMETRIC PARAMETERS OF FULL-SCALE T-2
(from reference (f))

	Chord (in streamline direction)	
c_r	Root (H.T. Sta. 0)	64.61 in
c_t	Equivalent tip chord	33.05 in
	(H.T. Sta. 106.483)	
$\bar{c}_h$	Mean aerodynamic chord	50.447 in
	(H.T. Sta. 47.78)	
i_h	Incidence angle	0°
	Airfoil section (root and tip in streamline direction)	NASA 65A012
l_h	Tail length (.25 $\bar{c}_w$ to .25 $\bar{c}_h$)	202.58 in
HORIZONTAL STABILIZER		
S_s	Area stabilizer, total	42.5 ft^2
i_s	Stabilizer incidence angle	0°
ELEVATOR		
S_e	Total area (excluding balance area forward of the hinge line)	21.00 ft^2
b_e	Span (between equivalent chords) (one elevator only)	101.97 in
c_i	Inboard chord (B.P. 3.906)	18.85 in
c_o	Outboard chord (B.P. 105.877)	10.52 in
c_e/c_h	Ratio elevator chord (aft H.L.) to horizontal tail chord	.310
b_e/b_h	Ratio elevator span to horizontal tail span	0.936

TABLE I (CON'T)
GEOMETRIC PARAMETERS OF FULL-SCALE T-2
(from reference (f))

δ_e	Elevator deflection maximum	27° Up, 15° Dn
	Boost: Push force 2.95:1	Hydraulic
	Pull force 2.95:1 to 8 lbs	
	then 6.0:1	
	Static balance	Weighted Leading Edge
	Aerodynamic balance	Overhang
S_b	Balance area forward of hinge line	5.72 ft^2
c_b/c_e	Ratio balance chord to elevator chord	0.322
	Nose factor	0.60
	Point of tangency for nose factor is at elevator hinge line	
ELEVATOR TRIM TAB		
S_t	Area (each)	2.36 ft^2
b_t	Span, Equivalent (B.P. 8.93 to 54.53)	46.10 in
c_t	Chord, constant	6.5 in
b_t/b_e	Ratio tab span to elevator span	0.462 in
δ_t	Tab deflection	L.H. 10° Up, 13° Dn R.H. 0° Up, 13° Dn
VERTICAL TAIL		
S_v	Total area (includes 4.38 ft^2 blanketed by fuselage plus 2.14 ft^2 blanketed by horizontal tail)	40.33 ft^2
S_{net_v}	Net area	33.86 ft^2

TABLE I (CON'T)
GEOMETRIC PARAMETERS OF FULL-SCALE T-2
(from reference (f))

A_v	Net surface area (wetted)	79.18 ft^2
A_d	Net surface area of dorsal fin (wetted)	18.12 ft^2
b_v	Span, unblanketed	8.04 ft
AR_v	Aspect ratio	1.80
λ_v	Taper ratio	.375
c_r	Chord (in streamline direction)	
	Root (W.P. + 33.000)	78.14 in
c_t	Equivalent Tip Chord (W.P. + 129.41)	29.38 in
$\bar{c}_v$	Mean aerodynamic chord (W.P. + 73.92)	58.47 in
Λ_v	Sweepback (25% chord)	30°
	Airfoil Section	NASA 63A012
l_v	Tail length (.25 $\bar{c}_w$ to .25 $\bar{c}_v$)	194.05 in
VERTICAL FIN		
S_f	Area (including 2.14 ft^2 blanketed by horizontal tail and excluding dorsal fin)	29.87
i_f	Angle with respect to airplane plane of symmetry	0°
RUDDER		
S_r	Total area	9.13 ft^2
	S_{r_u} Upper surface	3.23 ft^2
	S_{r_l} Lower surface	5.90 ft^2

TABLE I (CON'T)
GEOMETRIC PARAMETERS OF FULL-SCALE T-2
(from reference (f))

b_r	Span, equivalent	
	b_{r_u} Upper surface	31.94 in
	b_{r_l} Lower surface	42.99 in
c_{r_u}	Upper chord (W.P. 96.00)	12.59 in
c_{r_l}	Lower chord (W.P. + 9.91)	22.45 in
c_r/c_v	Ratio rudder chord (aft H.L.) to vertical tail chord	
	c_r/c_v Upper surface @ W.P. 96.00	.266
	c_r/c_v Lower surface	.250
δ_r	Rudder deflection, maximum	25° Rt, 25° Lt
	Boost	None
	Aerodynamic balance	Overhang
S_b	Balance area forward of hinge line	2.41 ft^2
c_b/c_r	Ratio balance chord to rudder chord	
	c_b/c_{r_u} Upper surface @ W.P. 96.00	.234
	c_b/c_r Lower surface	.24
	Static balance	Weighted leading edge
	Nose factor	0.40
	Point of tangency for nose factor is at rudder hinge line	
RUDDER TRIM TAB		
S_t	Area	1.60 ft^2

TABLE I (CON'T)
GEOMETRIC PARAMETERS OF FULL-SCALE T-2
(from reference (f))

b_t	Span, equivalent (W.P. 14.94 to W.P. 53.00)	38.06 in
c_t	Chord, constant	6.0 in
b_t/b_r	Ratio tab span to rudder span	.508
δ_t	Tab deflection, maximum	7° Rt, 7° Lt
FUSELAGE		
l_f	Length (actual)	34.58 ft
F_f	Maximum frontal area (basic fuselage)	15.75 ft^2
w_f	Maximum width (basic fuselage) F.S. 169	54 in
h_f	Maximum depth	
	Basic fuselage over canopy (F.S. 169)	88.1 in
	Including ducts (F.S. 214)	73.9 in
A_f	Net surface area	221.11 ft^2
L/D	Fineness ratio (actual)	5.91
CANOPY		
l_c	Length (actual)	19.75 ft
F_c	Maximum frontal area	3.70 ft^2
A_c	Net surface area	73.10 ft^2
L/D_c	Fineness ratio (actual)	8.8
NACELLE		
l_n	Length (actual)	23.71 ft
F_n	Maximum frontal area	10.50 ft^2

TABLE I (CON'T)
GEOMETRIC PARAMETERS OF FULL-SCALE T-2
(from reference (f))

A_n	Net surface area	206.0 ft^2
	Inlet area (includes gutters)	3.1 ft^2
L/D_n	Fineness ratio (actual)	5.025
SPEED BRAKE (Data for one side only)		
	Type	One Piece
	Location	Side of Aft Fuselage
	Number	Two
S_j	Area (Planform)	8.00 ft^2
F_j	Area (frontal)	4.24 ft^2
δ_j	Maximum deflection	32°*
TIP TANK (Data for one tank only)		
l_{tt}	Overall length	142.75 in
d_{tt}	Maximum diameter (Tank Sta. 61.875)	20.00 in
L/D	Fineness ratio	7.14
Ss_{tt}	Side area (projected)	14.1 ft^2
Sp_{tt}	Planform area (projected)	14.2 ft^2
	Volume	15.3 ft^2
A_{tt}	Total Surface Area	44.30 ft^2
$A_{net_{tt}}$	Net Surface Area (wetted)	42.40 ft^2

*Note: Manufacturers specification is 32°. By actual measurement, test A/C maximum speedbrake deflection is 50°. Reference (g) states that AFC 103 ordered extension of speed brake deflection to 50° for production T-2 aircraft.

TABLE II

INSTRUMENT LOCATIONS ON YT-2B FOR AIRFRAME DYNAMICS IDENTIFICATION PROGRAM
(prior to 10 May 73)

Function	Name	Fuselage Station	Wing Station	Water Line
n_x	Greenleaf Serial 1655000-A #674	37.	-4.	-11.
n_z (c.g.)	Giannini #1816 24117P-3.5-20	207.	-1.	-21.
n_z nose (for $\dot{q}$)	Giannini #1819 24117P-3.5-20	34.	-6.	-11.
n_z tail (for $\dot{q}$)	Giannini #1837 24117P-3.5-20	366.5	0	+9.
$\dot{q}$	Staham Ang. Acc. AA196-8-350	230.	0	-23.5
θ	Giannini Model Serial 5812 3416	56.	0	5.
ϕ	Giannini Model Serial 3812 3416	56.	0	5.
r	Gyro Dynamics Serial #62	47.	0	3.5
p	Norden RG 228 Serial #185	52.	0	2.5
q	Norden RG 228 Serial #183	196.	0	-22.5
n_y nose (for $\dot{r}$)	Edelcliff Model 7-30 Serial #367	31.5	-6.	-11.
n_y tail (for $\dot{r}$)	Edelcliff Model 7-30 Serial #366.5	366.5	0	+9.
n_y (c.g.)	Edelcliff Model 7-30 Serial #4444	204.	-1.5	-19.
n_z wing tip (for $\dot{p}$)	Giannini #1685 24117P-3.5-20	249.	206.5	15.
n_z wing tip (for $\dot{p}$)	Giannini #1860 24117P-3.5-20	249.	-206.5	15.

NOTE: Negative wing stations are toward left wing. Negative water line positions are below fuselage reference line.

TABLE III
MEASUREMENT RANGES FOR YT-2B TRANSDUCERS

Measurement	Range
n_z	±3.5g
n_x	±1.0g
n_y	±1.0g
q	±20 deg/sec
θ	±15 deg
r	±20 deg/sec
$\dot{q}$	±450 deg/sec^2
ϕ	±90 deg
p	±20 deg/sec (prior to 5/10/73)
	±45 deg/sec (effective 5/10/73)

TABLE IV

YT-2B INSTRUMENTATION CHANGES EFFECTIVE 10 MAY 1973

Measurement	Transducer Removed	Transducer Substituted
p	Norden RG 228 SN 185	Humphrey G20-1021-00 SN 328
r	Gyro Dynamics SN 62	Norden RG 228 SN 185
n_z (port wing tip)	----Giannini 24117-3.5-20---------- SN 1860	SN 1681

function developed problems, however, and caused some noise in the velocity signal at the switching points. A position error correction for the airspeed measurement was supplied by the manufacturer in reference (h).

The angle of attack and sideslip vanes were located 23.1 feet and 23.4 feet, respectively, forward of the nominal center-of-gravity. The ranges of the measurements from these vanes were adjustable, but were set at $\pm 10^{\circ}$ for both vanes throughout this flight program.

While all gyros and accelerometers were aligned with respect to the fuselage reference line indicated by the aircraft manufacturer, the α vane was referenced to the noseboom. It was calculated that the noseboom itself was inclined -4.0° relative to the wing chord line, from which true angle of attack should be measured.

Aileron, rudder, elevator, flap, and speedbrake positions were measured via potentiometers covering the full range of available movement.

Note that pitch angular acceleration was measured twice: once directly with the Statham angular accelerometer and once via differential normal acceleration between nose-mounted and tail-mounted normal accelerometers.

TELEMETRY, RECORDING, AND DATA REDUCTION

Transducer signals were simultaneously recorded onboard the aircraft and broadcast to the ground station. The telemetry system was of the FM-FM type and the onboard recorder was an Astro-Science Corporation MARS 2000. Since only 12 discrete IRIG-standard subcarrier frequencies were available, many of the channels had to be assigned to a pulse amplitude modulation system and then sampled at 30 samples/sec by a commutator, with the commutator output modulated on the 70 KHZ subcarrier. Table V lists channel assignments. The various subcarrier signals were then modulated together and recorded as a single channel on the tape.

Demodulation and analog-to-digital conversion could not be accomplished at NAVAIRDEVCEN without procurement of additional equipment, so these operations were performed at Naval Air Test Center. The digital data tapes were then provided as input to the NAVAIRDEVCEN digital computer facility.

A digital computer program for data reduction purposes was developed. This program transformed the digital information into CDC 6600 format, corrected for aircraft instrumentation offsets, decalibrated the data into physical units, and referenced all motion variables to trim values. A printout of this program, configured for a typical run, is given as Appendix A.

The calibration constants used in this process for the gyros and accelerometers were developed from tests at NAVAIRDEVCEN using rate tables and similar equipment. Every transducer was tested independently. Control surfaces and α and β vanes were calibrated using an inclinometer. Airspeed and altitude transducers were calibrated in accordance with procedures recommended by manufacturers using pressurized air sources.

TABLE V

CHANNEL ASSIGNMENTS FOR YT-2B TELEMETRY AND RECORDING

Channel	Assigned Variable
FM 1.3KHZ	angle of attack
FM 1.7KHZ	sideslip angle
FM 2.3KHZ	heading
FM 3.0KHZ	pitch angle
FM 3.9KHZ	pitch rate
FM 5.4KHZ	roll rate
FM 7.35KHZ	roll angle
FM 10.5KHZ	normal acceleration (port wingtip)
FM 14.5KHZ	pitch angular acceleration
FM 22.0KHZ	normal acceleration (starboard wingtip)
FM 40.0KHZ	aileron position
FM 70.0KHZ	PAM
PAM1	zero reference
PAM2	full scale reference
PAM3	flap position
PAM4	speed brake position
PAM5	flight path acceleration
PAM6	side acceleration (cg)
PAM7	normal acceleration (cg)
PAM8	normal acceleration (nose)
PAM9	normal acceleration (tail)
PAM10	side acceleration (nose)
PAM11	side acceleration (tail)
PAM12	airspeed (coarse)
PAM13	airspeed (fine)
PAM14	altitude
PAM15	elevator position
PAM16	-
PAM17	rudder position
PAM18	yaw rate

All of the calibrations mentioned above were static in nature, except that the angular accelerometer was exposed to a sinusoidal input because no practical method of providing steady-state angular acceleration was available. A byproduct of this calibration method was the capability of measuring phase shift. It was assumed that the oscillation table itself contributed no lag, so that all phase shift from input command to accelerometer signal can be attributed to the accelerometer. The results are shown in Figure 3. The transducer apparently develops significant phase lags at high frequencies, but the phase shift is only 10° to 15° in the highest frequency region of interest. The phase lead at very low frequencies is difficult to explain. Either the indication of phase lead is an error, or the transfer function for the transducer is considerably more complex than the simple lag usually assumed. If the data found in these tests are accurate, it must be concluded that the unit has been designed well, since the phase shift is zero in the frequency region of greatest interest.

One rate gyro was selected at random to be tested for phase shift in the manner described above. Results are shown in Figure 4. Again, zero phase shift seems to occur in the frequency range of most interest, and a phase lead of as much as 10° exists at low frequencies. Thus phase shift on rate gyros should not cause any serious problems.

FLIGHT DATA CHARACTERISTICS

Flight data were collected for a wide variety of pilot control inputs for eight flight conditions. For the purposes of the current parameter identification effort, however, 17 sets of time histories, including only the two most significant flight conditions, were selected. A list of the characteristics of each time history set (referred to by "Data Run Number") is given in Table VI. A detailed discussion of elevator control inputs is given elsewhere in this report. Furthermore, the pilot's record of the circumstances of each flight (from which data were taken) are presented in Table VII. The details of the two flight conditions are listed in Table VIII.

The trim angle of attack was calculated by first calibrating the vane relative to the boom, and then measuring the angle between the noseboom and the wing chord line (in the vicinity of the mean aerodynamic chord). Trim angles of attack referenced to wing chord line cannot have negative values for the T-2, yet negative values are shown in Table VI. It seems, therefore, that an error exists in the angle of attack reference. Such an error should not affect the perturbation angle of attack measurement significantly.

PILOT CONTROL INPUTS

It is generally recognized (see, for example, reference (j)) that system identification is impossible if the test input does not excite the principal natural modes of system response. Moreover, several investigators (see references (k) and (l)) have determined that an input can be found which will improve identification performance substantially relative to traditional flight test inputs.

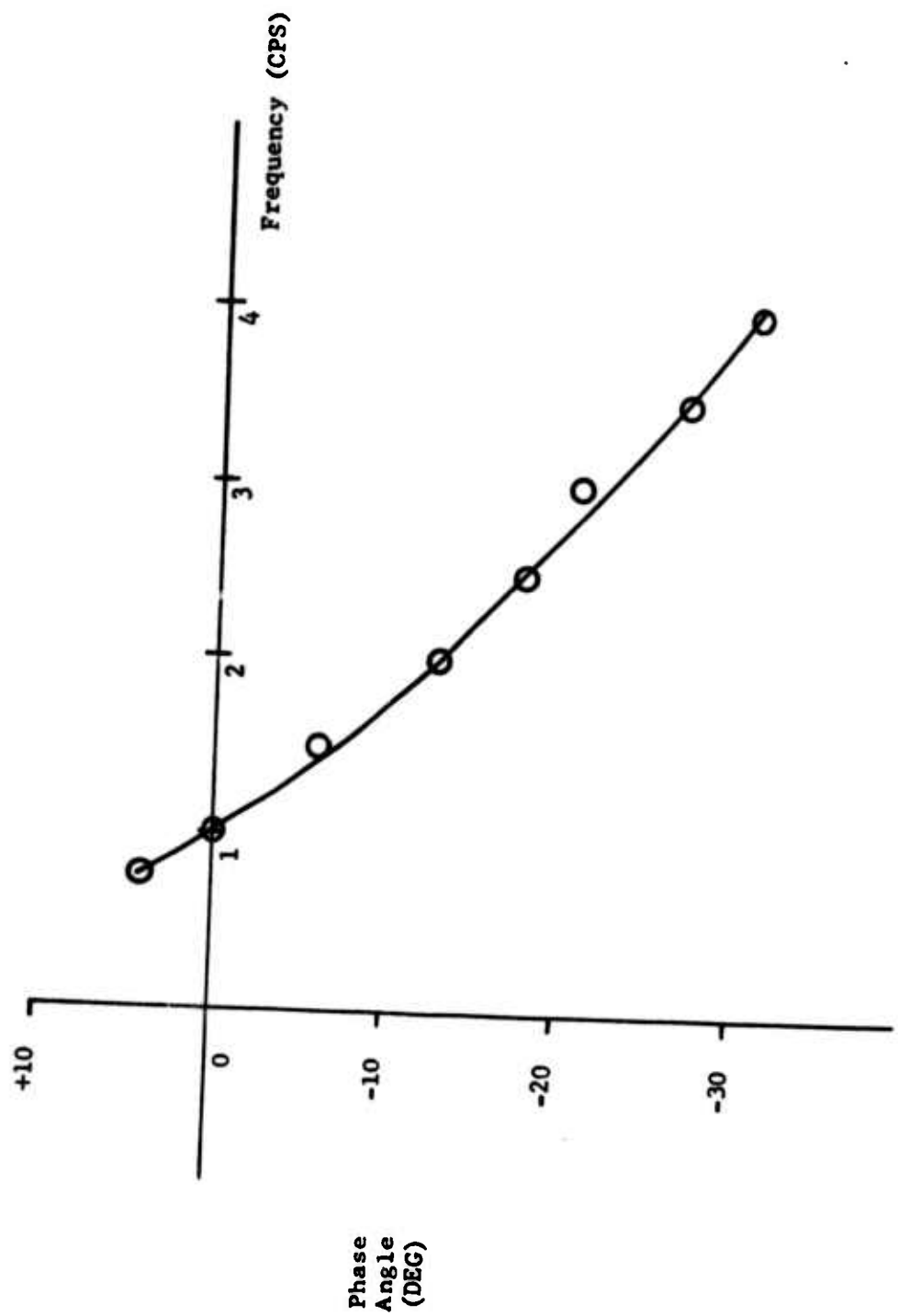

FIGURE 3. PHASE SHIFT TESTS OF STATHAM ANGULAR ACCELEROMETER (AA196-8-350)

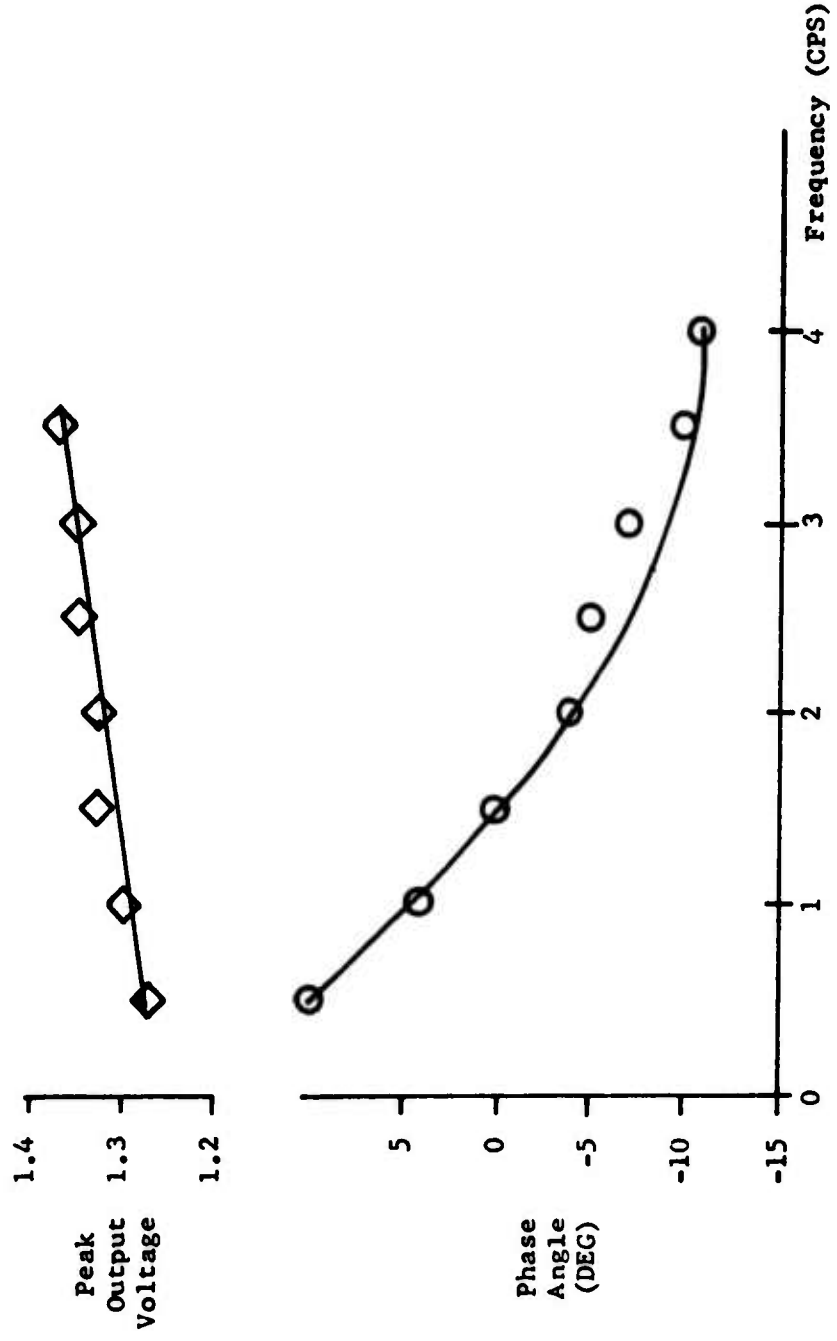

FIGURE 4. RATE GYRO FREQUENCY RESPONSE, NORDEN RATE GYRO MODEL RG228, SERIAL NO. 183

TABLE VI
FLIGHT DATA CHARACTERISTICS

Data Run Number	Date	Flight Condition	Trim Velocity (ft/sec)	Trim Angle-of-Attack (deg)	Elevator Input
2	3/14/73	1	266.5	5.8	(2-cycle sine wave short period frequency)
3	3/14/73	1	246.7	7.1	pulse
4	3/21/73	1	253.2	6.0	(1-cycle sine wave short period frequency)
5	3/21/73	1	255.7	5.2	(2-cycle sine wave short period frequency)
6	3/21/73	1	251.6	5.9	pulse
7	3/23/73	2	685.7	0.1	(1-cycle sine wave short period frequency)
8	3/23/73	2	685.5	0.1	(3-cycle sine wave short period frequency)
9	5/10/73	2	699.3	0.3	pulse
10	5/10/73	2	683.7	0.3	pulse
11	5/10/73	2	679.2	0.1	pulse
12	5/10/73	2	669.9	0.2	step
13	5/10/73	2	680.8	0.1	SCI optimum
14	5/10/73	2	687.2	-0.1	SCI optimum
16	5/16/73	2	683.9	-0.6	step
17	5/16/73	2	689.6	-0.7	step
18	5/16/73	2	682.8	-0.7	SCI optimum
19	5/16/73	2	690.0	-0.8	white noise

TABLE VII
PILOT'S RECORD OF FLIGHT CIRCUMSTANCES

Date	3/14/73	3/21/73	3/23/73	5/10/73	5/16/73
Calibrated Airspeed (kt)	140	140	351	351	351
Power Setting (%)	78-79	78-79	90	93	93
Pressure Altitude (ft)	1500	1500	10,000	10,000	10,000
Clouds	10,000' Overcast	3000' scattered	None	3500' scattered	3500' scattered
Turbulence	Light	None	None	None	None
Altimeter Setting	30.02	30.00	30.12	29.85	30.03
Fuel Level (lb)	2200→1300	2100→1800	2200→1000	2400→600	2300→600
Wind Velocity (kt)	5	8	2	4	27
Time Out/Back	1005/ 1115	0710/ 0824	1015/ 1118	1450/ 1550	1335/ 1435
Temperature (°F)	52	32	48	78	57
Gear	Down	Down	Stowed	Stowed	Stowed
Flaps	50%	50%	Up	Up	Up

TABLE VIII
SELECTED YT-2B FLIGHT CONDITIONS

Flight Condition Number	1	2
Nominal Mach Number	0.212	0.63
Nominal True Airspeed (ft/sec)	236	679
Nominal Pressure Altitude (ft)	0	10,000
Gear Position	down	up
Flap Position (deg)	16	0
Speed Brake Position	closed	closed
Approximate Weight (lb)	11,000	11,000
Approximate CG Position (% $\bar{c}$)	20	20
Approximate I_y (slug-ft^2)	14,600	14,600
Approximate I_x (slug-ft^2)	9,000	9,000
Approximate I_z (slug-ft^2)	19,000	19,000
Estimated Trim Angle-of-Attack (deg)	4.7	1.2

NOTE: Weight and moment of inertia approximations were based on reference (i).

To maximize the identifiability of the aircraft from the current flight data and to provide a basis for the determination of the effects of input type on identification performance, it was decided that a variety of pilot inputs would be used. The classic step, pulse, and doublet inputs were included. The frequencies of the principal longitudinal modes of motion (short period and phugoid) were estimated, and sine waves at those frequencies were used also. The number of cycles of the sine waves was also varied.

Systems Control, Inc., calculated inputs which they believed to be optimum for identification of parameters which have significant effect on the short period mode. These inputs are shown in Figures 5 and 6. The shape of such inputs is dependent upon the flight condition and the estimated short period characteristics. On the theory that all possible frequencies should be represented in the input, a pseudo-white noise input was also selected.

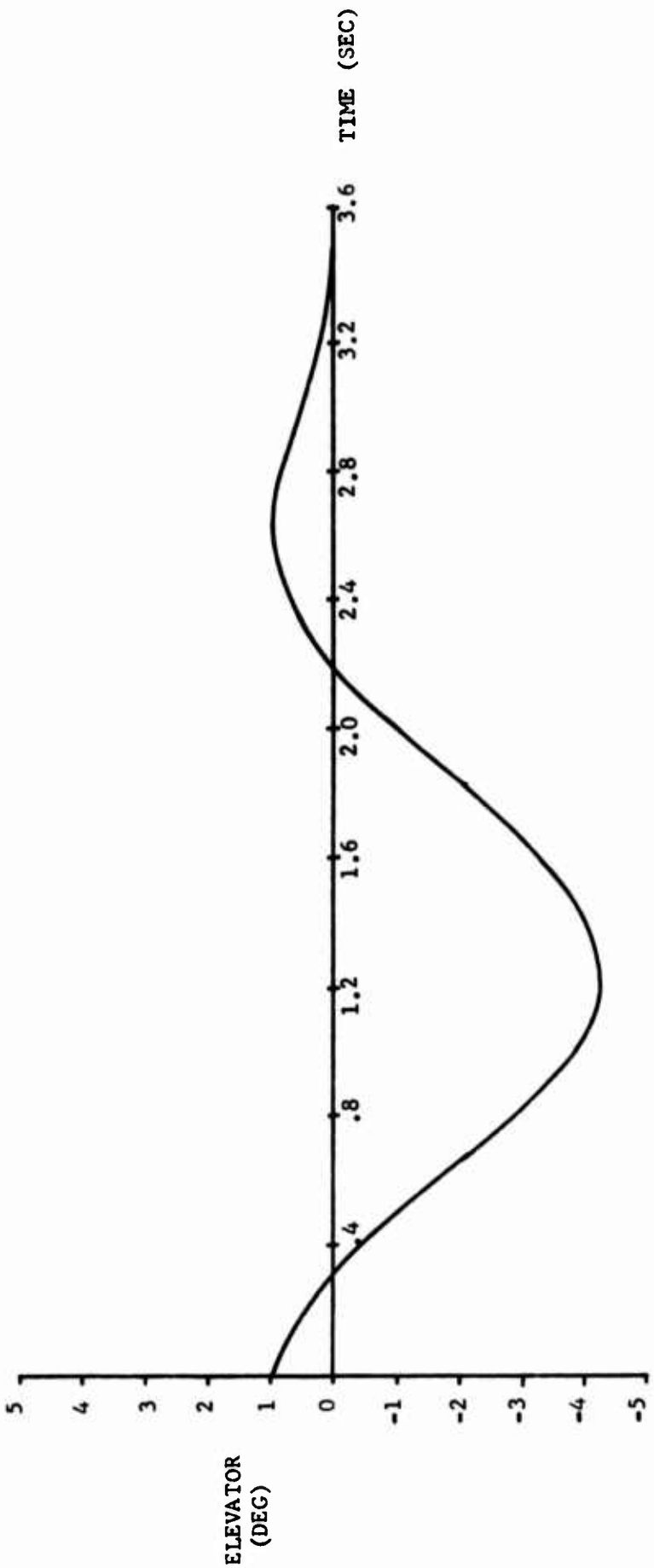

FIGURE 5. SCI OPTIMAL INPUT FOR T-2 SHORT PERIOD, FLIGHT CONDITION #1

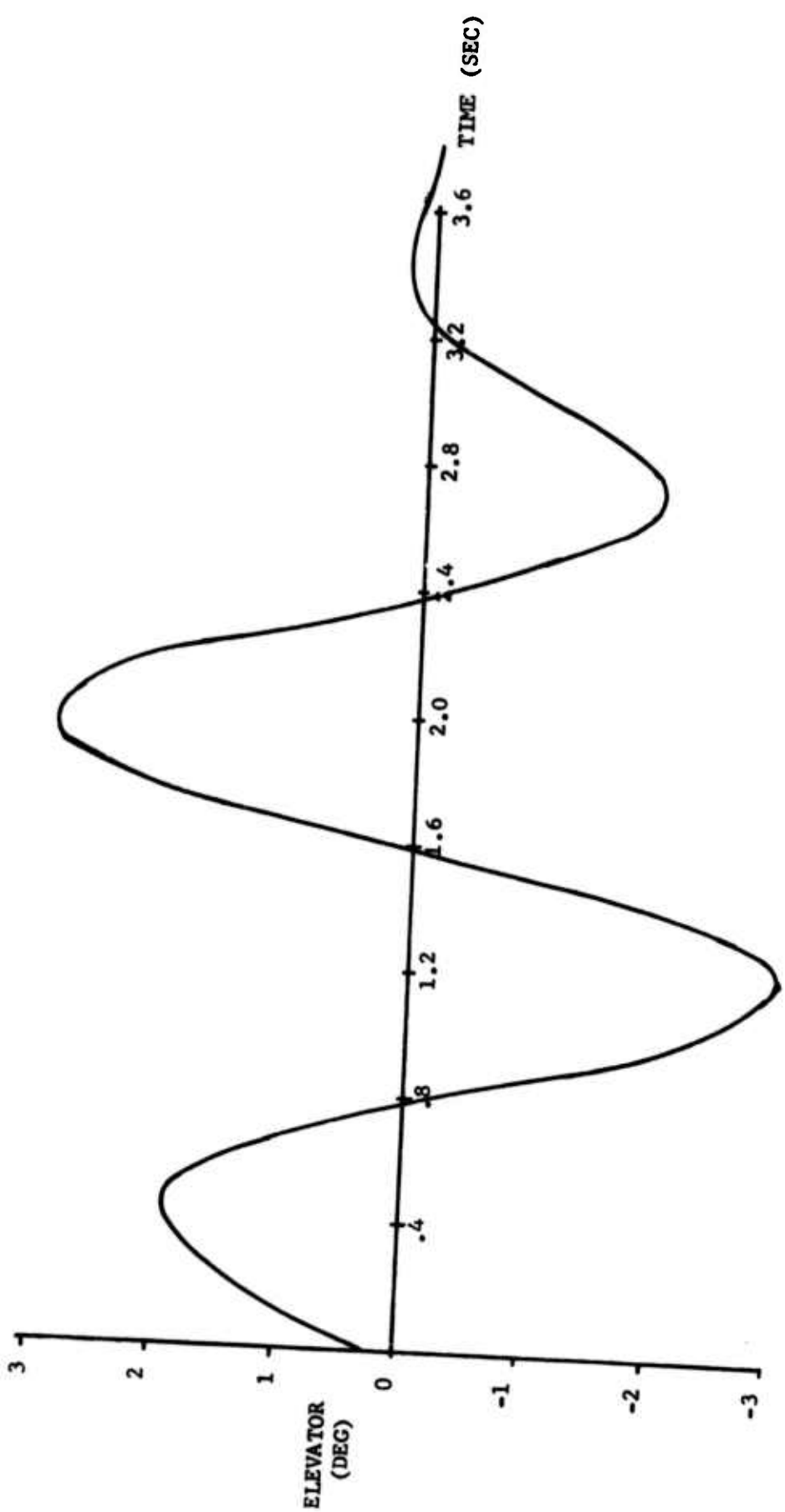

FIGURE 6. SCI OPTIMAL INPUT FOR T-2 SHORT PERIOD, FLIGHT CONDITION #2

The actual shape of the pilot input was, of course, not always identical to the requested command since no automatic equipment was available to aid the pilot in making these relatively complex stick movements. After some practice, however, the pilots (who were not test pilots) developed a high degree of skill in executing the planned inputs. Whenever the real-time telemetry system was in operation, the pilot inputs could be observed at the ground station in graphical form and corrections could be dictated to the pilot immediately. This iterative process would quickly converge to an acceptable approximation of the requested input.

The amplitudes of the inputs were also determined iteratively. Acceptable amplitudes were difficult to obtain in some cases. The goal in the selection of input size was to force all significant output variables to be large enough for a reasonable signal-to-noise ratio while remaining small enough to permit the use of the linear approximations to the equations of motion and to remain within the ranges of the transducers. An additional problem existed at flight condition #1, since the pilots were reluctant to permit significant altitude variations while in proximity to the ground. Unfortunately, altitude variations are inherent in the phugoid mode, and it was therefore difficult to find any input which would generate a phugoid output without exceeding any of the constraints placed on the tests.

The rapid doublet input was eventually abandoned since too large an elevator deflection was required for sufficient excitation of aircraft response. The SCI optimum input was never successfully generated in flight condition #1, and cannot be evaluated.

SOURCES OF NOISE

The scope of this effort did not permit any attempt at quantitative analysis of noise contributions from various sources, nor of the sensitivity of identification performance to levels of noise of different types. It is possible, however, to list the known sources of noise and evaluate their importance subjectively based on the experiences of the investigators.

It is generally recognized that noise can be broadly divided into two types: process noise and measurement noise. In theory, the modified Newton-Raphson identification technique used in this in-house investigation is more affected by process noise. Given sufficient quantities of data, this algorithm will produce unbiased estimates even in the presence of measurement noise, but the technique does not tolerate significant process noise. The theoretical sensitivity of various types of identification techniques to different noise types has been discussed many times (see, for instance, reference (m)), and will not be discussed in this report.

Process noise can be further subdivided into turbulence and modeling error. Atmospheric turbulence was not noticeable on any flight at flight condition #2, but was present for the low altitude flight condition #1. Every effort was made to fly early in the day to minimize turbulence. As can be seen in Table VII, the flight of 3/21/73 occurred rather early in the day and the turbulence level was such that the pilot termed it "none", given

a choice of "none", "light", "moderate", and "heavy". On 3/14/73 the flight did not occur until late morning and turbulence was "light". Several additional flights were launched at 0700 or earlier, but data from these flights was found unacceptable for reasons other than turbulence considerations. Turbulence, then, should not be a factor in analysis of flight condition #2 data, but might have a degrading influence on identification at condition #1.

The mathematical model (equations of motion) used in this analysis is discussed elsewhere in this report. Substantial errors in the longitudinal equations per se are unlikely, but one must consider the validity of the assumption that the longitudinal and lateral-directional motions are independent. Although the lateral-directional motions occurring during the longitudinal maneuvering are not large, there are noticeable excursions in sideslip. It would have been possible to include in the model some sideslip effects and consider the sideslip as an external input (i.e., an additional control), but this work was judged to be outside the scope of the current program. In summary, the investigators suspect that process noise is present, but not in sufficient degree to impede the identification process, in spite of the theoretical sensitivity of the identification technique to process noise.

In theory, every change in the nature or the format of the flight motion data introduces some measurement noise. It is clearly desirable to minimize the number of transformations in the process of changing physical aircraft motions into digital computer identification program inputs. However, it was necessary that already available NAVAIRDEVCEN equipment be used in this investigation, and the number of data transformations became rather large. The recording and data reduction procedures have been described in a previous section of this report, and the various transformations will only be summarized here. The physical motions were sensed by transducers, which output electrical signals in analog form. These signals were frequency modulated and multiplexed for single channel recording. They were then demultiplexed, demodulated, sampled (at 20 samples/second), and recorded as digital information. These digital data were read from tape, re-organized to a form compatible with the NAVAIRDEVCEN CDC 6600 computer, decalibrated (converted to physical units), transformed to the stability axis system, and written onto a disk file to be available for input to identification programs. Based on the investigators' observations of the data throughout the processes outlined above, it seems that substantial noise was introduced by these repeated transformations.

Specifically, "bad points" arose in the data both from the commutator and the analog/digital conversion. These saturated data points had to be deleted, and their places occupied by interpolated information. Zero and full-scale reference values for both modulation and analog/digital conversion were subject to drifting. Each recording/playback process introduced noise from the recording device.

Although no transducer is perfect, only three of the longitudinal flight motion transducers in the YT-2B caused noticeable problems: elevator position, airspeed, and angle of attack. Every transducer selection involves some coarse/fine trade-off. In the case of elevator position, it was determined that the entire range of deflection would have to be included, so a potentiometer

was installed on the actuator and calibrated for the entire -27° to +15° deflection range. At high dynamic pressure flight conditions, however, the elevator movement about its trim position was quite small (on the order of magnitude of 1°), and the resulting signal-to-noise ratio for the data was rather poor. No straightforward solution was found to this problem because the elevator trim position varied considerably with flight condition. The noise level in elevator data was high even for flight conditions in which large elevator deflections were used, indicating that sources of noise other than resolution difficulties are also contributing.

Airspeed measurement presented a problem analagous to the elevator position measurement problem: small perturbations about a large trim value. For airspeed measurement, however, two sensors were used - a 0-500 kt coarse transducer and a 0-50 kt resetting fine transducer. This system worked well except that the fine transducer was "undecided" about resetting between 48 and 50 knots. At, and just below, any multiple of 50 knots airspeed, the airspeed measurement becomes useless as the transducer continuously switches between full scale and zero readings. This problem is strictly a hardware phenomenon, but no other hardware was available.

A filter on the velocity signal was used to process some of the data. This digital filter simply eliminated velocity values which were excessively different from a previous data point, and reset the excessive value to equal the previous data point. Thus the bursts of sharp peaks in the signal were reduced to constant value "flap spots". For the in-house identification effort, however, this filter was applied only to the worst data cases because extensive use would have compromised the principle of minimizing the engineering interaction with the details of the identification process.

Angle of attack was measured by a vane mounted on a noseboom. The vane mounting position was sufficiently forward of the wing for upwash effects to be negligible. However, the vane appeared to have dynamic characteristics which varied from day to day as the friction on the pivot changed with weather, time, etc. Unfortunately, no means of dynamic calibration for the vane was available.

In summary, the investigators suspect that most of the noise in the flight data was measurement noise. It is especially significant that measurement noise was considerable in the control input, since theoretical parameter identification studies generally consider the input as a noise-free measurement.

SELECTION OF MATHEMATICAL MODEL

The general equations of motion for aircraft flight are quite complex, but numerous assumptions are often made to justify simplification of the equations for a particular application. Two simplifying assumptions were implicit in the definition of this project: (1) longitudinal equations may be decoupled from lateral-directional equations, and (2) small perturbation theory and small angle approximations are applicable to the flight motions. Equations based on these assumptions are developed in many texts, but reference (n) was used for this project.

The modified Newton-Raphson computer program (and most other identification schemes) requires that the model be in the state vector form

$$\dot{x} = Fx + Gu$$

where x is the vector of the motion states, u is the control vector, F is the matrix of stability derivatives, and G is the matrix of control derivatives. The equations of motion are not usually written in such a form when used for dynamics analysis, but they can be manipulated to the proper form. The resulting equations are listed in Table IX.

During the identification process, the equations were simplified even further, as $Z_{\dot{\alpha}}$, Z_q, X_{δ_e}, and γ_o were all taken to be zero. The quantities $\dot{u}$ and $\dot{\alpha}$ were not measured, but were calculated from a_x and a_z using auxilliary equations.

With the equations of motion in the state vector form, it is clear that no straightforward solution for $M_{\dot{w}}$ is possible. Various schemes were considered, including the use of the auxilliary relationship M_{δ_e} = tail length X Z_{δ_e} and obtaining data at large γ_o, to permit separation of $M_{\dot{w}}$ from the lumped parameters, but all were eventually discarded as grossly inaccurate or impractical. To separate the identified derivatives for comparison to estimates, either the $M_{\dot{w}}$ estimate can be assumed correct or the estimates can be combined into lumped parameters and the comparisons done with those quantities.

DEVELOPMENT OF A PRIORI PARAMETER SET

Despite occassional claims that various parameter identification techniques will function without any a priori or start-up parameter estimates, it is generally agreed that the use of such estimates substantially increases the chances of success. A priori parameter estimates which merit a high level of confidence may also serve as a basis of comparison for results, but should never be considered the "right answers". Indeed, if a priori estimates were to be considered the "right answers", then there would be no need for parameter identification from flight data.

A priori parameter estimates for the T-2 for the flight conditions of current interest were developed from information in references (f), (i), and (o). The methods used by the aircraft manufacturer to generate this original information are not known, but a reasonable level of confidence would seem appropriate for any information released to the public by the aircraft design team.

The estimated parameters are given in Table X in several forms. Only one set of information is presented, but several formats were used as a convenience to the user. This information has been supplied to all parties receiving the flight data.

TABLE IX

T-2 LONGITUDINAL EQUATIONS OF MOTION IN STATE VECTOR FORMAT

$$\dot{\alpha} = \left[\frac{Z_u}{U_o - Z_{\dot{\alpha}}}\right] u + \left[\frac{Z_\alpha}{U_o - Z_{\dot{\alpha}}}\right] \alpha + \left[\frac{U_o + Z_q}{U_o - Z_{\dot{\alpha}}}\right] q - \left[\frac{g \sin \gamma_o}{U_o - Z_{\dot{\alpha}}}\right] \theta + \left[\frac{Z_{\delta_e}}{U_o - Z_{\dot{\alpha}}}\right] \delta_e$$

$$\dot{u} = X_u u + X_\alpha \alpha - (g \cos \gamma_o)\, \theta + X_{\delta_e} \delta_e$$

$$\dot{q} = \left[M_u + \frac{M_{\dot{\alpha}} Z_u}{U_o - Z_{\dot{\alpha}}}\right] u + \left[M_\alpha + \frac{M_{\dot{\alpha}} Z_\alpha}{U_o - Z_{\dot{\alpha}}}\right] \alpha + \left[M_q + M_{\dot{\alpha}} \left[\frac{U_o + Z_q}{U_o - Z_{\dot{\alpha}}}\right]\right] q - \left[\frac{M_{\dot{\alpha}} g \sin \gamma_o}{U_o - Z_{\dot{\alpha}}}\right] \theta + \left[M_{\delta_e} + \frac{M_{\dot{\alpha}} Z_{\delta_e}}{U_o - Z_{\dot{\alpha}}}\right] \delta_e$$

$$\dot{\theta} = q$$

TABLE X
A PRIORI VALUES FOR YT-2B AERODYNAMIC PARAMETERS

Parameter	Dimensions	Flight Condition 1	Flight Condition 2
C_L	-	0.642	0.106
C_D	-	0.110	0.018
C_{L_α}	-	4.62	5.50
C_{D_α}	-	0.172	0.228
$C_{L_{\delta_f}}$	1/rad	1.049	-
$C_{L_{\delta_e}}$	1/rad	0.486	0.401
C_{L_u}	-	0	0.031
C_{D_u}	-	0	0
C_{m_u}	-	0	0.011
C_{m_α}	-	-0.597	-0.429
$C_{m_{\dot{\alpha}}}$	-	-3.95	-5.50
C_{m_q}	-	-10.59	-11.86
$C_{m_{\delta_e}}$	1/rad	-1.13	-0.994
X_u	1/sec	-0.046	-0.016
X_α	ft/(sec^2 - rad)	-23.23	-36.91
Z_u	1/sec	-0.269	-0.122
Z_α	ft/(sec^2 - rad)	-233.75	-1669.24
Z_{δ_e}	ft/(sec^2 - rad)	-24.02	-121.30
M_u	1/(ft - sec)	0	0.0017
M_α	1/(sec^2 - rad)	-5.11	-22.50
$M_{\dot{\alpha}}$	1/(sec - rad)	-0.53	-1.57
M_q	1/(sec - rad)	-1.42	-3.39
M_{δ_e}	1/(sec^2 - rad)	-9.68	-52.12
$-g\ (\cos \gamma_o)/U_o$	1/sec	-0.134	-0.047
$Z_u\ U_o/(U_o - Z_{\dot{\alpha}})$	1/sec	-0.27	-0.12
$Z_\alpha/(U_o - Z_{\dot{\alpha}})$	1/sec	-0.974	-2.46
$(U_o + Z_q)/(U_o - Z_{\dot{\alpha}})$	-	1.0	1.0
$-g\ (\sin \gamma_o)/(U_o - Z_{\dot{\alpha}})$	1/sec	0	0

TABLE X (CON'T)
A PRIORI VALUES FOR YT-2B AERODYNAMIC PARAMETERS

Parameter	Dimensions	Flight Condition 1	Flight Condition 2
X_α/U_o	1/sec	-0.097	-0.054
$X\delta_e/U_o$	1/sec	0	0
$(U_o X_u + M_\alpha Z_u/U_o - Z_{\dot{\alpha}}))$	$1/sec^2$	1.43	1.34
$M_\alpha + (M_{\dot{\alpha}} Z_\alpha/(U_o - Z_{\dot{\alpha}}))$	$1/sec^2$	-4.59	-18.6
$M_q + M_{\dot{\alpha}} ((U_o + Z_q)/(U_o - Z_{\dot{\alpha}}))$	1/sec	-1.95	-4.96
$-(M_{\dot{\alpha}} g \sin \gamma_o)/(U_o - Z_{\dot{\alpha}})$	$1/sec^2$	0	0
$Z\delta_e/(U_o - Z_{\dot{\alpha}})$	1/sec	-0.102	-0.18
$M\delta_e + (Z\delta_e M_{\dot{\alpha}}/(U_o - Z_{\dot{\alpha}}))$	$1/sec^2$	-9.63	-51.8

The conditions of each actual data run are, of course, slightly different from each other and from the nominal flight condition. For the in-house identification analysis, a separate set of combined start-up parameters was generated for each run reflecting the differences in trim velocity.

IN-HOUSE IDENTIFICATION COMPUTER PROGRAM

ACQUISITION

The identification technique used in this effort was a modified Newton-Raphson algorithm. The computer program was provided (informally) by Mr. Larry Taylor of NASA-Langley Research Center. The rationale of the program and an example of its application are given in reference (p). Reference (q) is a "user's guide" for the program. In fact, the computer program has been documented so thoroughly that it would be redundant to discuss it in this report. Minor changes were made to the program in accordance with references (r) and (s), and some modifications had to be made to adapt the program to the current NAVAIRDEVCEN CDC 6600 computer operating system.

VERIFICATION

At the time of its acquisition by NAVAIRDEVCEN, the computer program had been configured for analysis of lateral-directional dynamics. To minimize the number of immediate programming changes, it was decided that the program would first be applied to lateral-directional "flight data" generated by a digital computer simulation of the T-2, and then the program would be tried on longitudinal data. Results of the first run on lateral-directional data are shown in Table XI. Since the data are theoretically noiseless and the same equations of motion were used in both the simulation and identification computer programs, the identification should be perfect if all controls are used. Both aileron and rudder were applied in the simulation program.

Run 1 results indicate that the parameter identification was excellent, but not perfect. Small errors existed in almost all parameters, and N_p, Y_p, and Y_{δ_a} were not identified at all. It is customary to neglect Y_{δ_a} and Y_p in most applications, and N_p was very small in this case, although N_p can be an important derivative in some cases. It is clear, then, that some noise was present after all. The investigators suspect that the source of the noise was an incompatibility in the integration schemes used in the digital computer programs for identification and flight simulation. Any quantification error resulting from integration algorithm mismatch was a phenomenon unique to application of the identification method to digitally simulated flight data, so that the problem should not exist in applications of the program to true flight data, and no further investigation was made.

Several types of gusts were added to the flight data to test the reaction of the identification program to process noise. The characteristics of runs 2 through 5 are given in Table XII. It can be seen from the results, given

TABLE XI
RESULTS OF
IDENTIFICATION OF COMPUTER-GENERATED
LATERAL-DIRECTIONAL T-2 DATA

	Actual Parameter Value	Run Number 1	2	3	4	5	6	7
L_p	-6.67	-6.69	-6.66	-6.79	-7.35	-7.43	-6.71	-6.40
L_r	1.38	1.38	1.41	1.44	.64	.60	1.70	1.59
L_β	-46.	-46.2	-45.5	-46.9	-48.1	-48.9	-46.4	-44.6
$L\delta_a$	-82.3	-82.3	-82.9	-83.8	-85.8	-86.8	-82.3	-80.4
$L\delta_r$	8.	8.1	8.2	7.3	7.4	7.8	8.1	8.3
N_p	-.0087	+.0016	-.0026	.036	.37	.42	.015	-.07
N_r	-.931	-.923	-.946	-.937	-.474	-.473	-1.10	-.867
N_β	24.9	25.0	24.7	25.2	26.3	26.6	25.0	24.5
$N\delta_a$	-1.78	-1.72	-1.30	-1.12	.40	.99	-1.70	-1.94
$N\delta_r$	-13.9	-13.9	-14.0	-13.4	-13.7	-13.8	-13.9	-13.9
Y_p	-.679	.01	-8.1	-7.4	-3.9	1.26	1.93	-9.9
Y_β	-268.6	-266.0	-296.8	-254.7	-383.7	-353.9	-134.6	-381.
Y_r	4.116	5.91	-6.43	2.62	-4.08	3.47	4.41	-.17
$Y\delta_a$	0	10.8	-63.2	-155.0	-26.6	27.8	27.7	-106.
$Y\delta_r$	41.6	43.8	43.6	2.6	122.9	124.	-24.5	75.9

TABLE XII
NOISE CHARACTERISTICS OF COMPUTER-GENERATED
T-2 FLIGHT TIME HISTORIES

Run No.	Characteristics
1.	Noiseless. Should be perfect identification. Used as reference.
2.	Low amplitude, low frequency, sinusoidal β and r gusts. No p gusts.
3.	Moderate amplitude, moderate frequency, sinusoidal β and r gusts; and low amplitude, high frequency p gusts.
4.	Amplitude and spectral characteristics of β gusts per MIL-F-8785B. No r or p gusts.
5.	Amplitude and spectral characteristics of β and r gusts per MIL-F-8785B. No p gusts.
6.	No gusts. Lag with .098 second time constant introduced in β vane.
7.	No gusts. Pseudo-random noise in all measurements. Noise amplitudes selected on basis of Cornell Aeronautical Laboratory experience in X-22 identification program.

in Table XI, that the the quality of the identification process deteriorates rapidly as gust intensity is increased. The presence of turbulence, having the characteristics set forth in section 3.7 of military specification MIL-F-8785B (ASG) for ambient atmospheric turbulence, is sufficient to seriously degrade the performance of the identification method. The results obtained by the computer program from flight data acquired under such turbulence conditions could be used only to specify ±10% estimates of L_β, $L\delta_a$, $L\delta_r$, N_β, and $N\delta_r$, a ±15° estimate of L_p, and no estimates of the other parameters. These poor results are not unexpected, since the modified Newton-Raphson algorithm is known to give biased results in the presence of process noise. Whenever a consistent set of turbulence characteristics of a particular level (e.g., light turbulence, moderate turbulence, MIL-F-8785 ambient turbulence) is present, the β gusts are far more damaging to identification quality than r or p gusts.

Run 6 was made to evaluate the effect of a lag in the β-vane, and all other noise was temporarily deleted to isolate this effect. The presence of this small uncompensated time lag in the sideslip vane seriously corrupts estimation of Y_β, $Y\delta_r$, N_r, and L_r, and has a lesser effect on the other derivatives. This result is curious, since the four listed derivatives are not those which one would expect to be affected most, but the important conclusion is that the existence of the lag is sufficient to seriously disrupt the identification process.

In theory, the operation of the modified Newton-Raphson algorithm is not biased by the presence of zero mean white Gaussian measurement noise. While the results from the application of the identification method to any individual set of time histories may be corrupted by the presence of measurement noise, the mean value of the parameter estimates will approach the true parameter values during repeated analysis of different sets of time histories for the same flight condition. No source of truly white noise was available for data generation, so a zero-mean approximation was developed. The noise amplitudes were selected on the basis of Calspan Corporation experience with flight testing of the X-22 aircraft in reference (e).

The results from the identification program operating in the presence of such pseudo-random measurement noise may be described as fair. The L_p, L_β, $L\delta_a$, $L_{\delta r}$, N_r, N_β, $N\delta_a$, and $N\delta_r$ parameters are estimated within ±10% error. These results are presented as run 7 in Table XI.

The longitudinal form of the identification program was also tested, albeit briefly. When the initial parameter values are identical to the correct results, the first iteration of the program has a very low fit error. If the program is allowed to continue to iterate, a slightly smaller fit error is obtained with a set of stability derivatives somewhat different from the correct value. Presumably, this problem is analogous to the slight disparities found in the lateral-directional data identification.

It must be noted that the weighting matrix in the identification program was not used during these applications of the program. These experiments were performed immediately after acquisition of the program, and it was felt at that time that use of the weighting matrix would be difficult and would violate the concept of an "off-the-shelf" program to be used in "cookbook" fashion. Later experiences, described elsewhere in this report, revealed that the weighting matrix could be used easily and in straightforward manner, and that its use would substantially improve the performance of the program on noisy data.

IN-HOUSE IDENTIFICATION PROCEDURES

A number of "data runs" were selected from the original flight data. These runs were processed by program MASSAGE (see listing, Appendix A) to a reduced form. The runs were then analyzed individually by program NEWTON (see listing, Appendix B). In most cases 350 data points were extracted from the input data file for each identification run. The time location of these points was selected to place the control input several seconds from the beginning. For some runs, less than 350 points were available (data run 6. for instance, only had 200 data points before occurrence of excessive noise). At 20 data points per second, these 350 point data sets were 17.5 seconds in length. In an attempt to extract velocity derivatives from longer data runs, a mechanism was provided in the program for reading only every second, or third, or fourth data point, so that 350 data points were still used, but the time interval was multiplied.

A bad point filter was used in the identification program, which substituted a reasonable value (calculated by extrapolation from previous points) for any data point which was completely off scale. A somewhat more restrictive filter was applied to airspeed in those instances where spikes existed from transducer switching. This filter also operated with the substitution/extrapolation method. These were the only filters used on the flight condition #1 data - there was no general, lowpass filtering done during A/D conversion.

The very low signal/noise ratios in the elevator flight data for flight condition #2 led to the use of several relatively extreme measures. The elevator signal was treated with a weighted average smoothing routine. Only a three point width smoothing interval was used to prevent excessive loss of high frequency signal content, and the signal was smoothed either once or twice. The suppression of the elevator signal to zero following the significant portion of the control input was also done for the data sets containing "spikes". The smoothing was done after the suppression to maintain a smooth transition.

The identification program contained a weighting matrix which weighted the importance of the time history matches in the parameter update iteration process. The program printout lists the weighted contributions to the overall time history fit error, and the diagonal elements of the weighting matrix should each be the inverse of the corresponding weighted fit error term. This process of adjusting the weighting matrix thus became an outer iterative loop - the inner loop being the parameter determination with a fixed weighting matrix.

The weighting matrix was updated manually, and after two or three iterations the weighted fit error terms would usually all be nearly equal to 1 (between 0.9 and 1.1), which of course was a terminal condition since further inversion would yield no changes. The process of correcting the weighting matrix clearly could be included in the program itself if one wished to make the necessary effort. The effect of the weighting matrix was to compensate for the dimensional differences in the time histories (in effect a normalization) and to proportion the significance of each time history inversely with its noise level.

In most cases, all the identifiable derivatives were left as variables, but on the longer time (such as 52.5 seconds) runs, the short period derivatives were held constant at the values determined for those derivatives by analysis of the first 17.5 seconds of the same data run.

The variables read into the identification program from the data massage program were δ_e, α, θ, q, $\dot{q}$ (calculated from linear accelerations), $\dot{q}_2$ (measured directly), u, a_x, a_z, h, δ_b. Of these variables, $\dot{q}$, h, and δ_b were not usually used by the identification program. The $\dot{q}$ signal appeared far more noisy than the $\dot{q}_2$ signal and therefore was abandoned. The mechanization of the computer program had no provision for use of altitude information, and speed brakes simply were not used by the pilot during any of the selected data runs.

Since the equations of motion in the program are in state variable format, a_x and a_z were used to calculate, respectively, $\dot{u}$ and $\dot{\alpha}$, which were the matched variables along with α, u, θ, q, and $\dot{q}$.

According to reference (q), the output from the computer program includes "the approximate standard deviation if the inverse of the noise covariance matrix is used" for the weighting matrix. The investigators on this project felt, however, that the method of calculation of this "approximate standard deviation" was not necessarily valid. It was decided not to attempt to use this quantity as a measure of estimation quality, and no other confidence level indicator was developed.

IN-HOUSE IDENTIFICATION RESULTS

SUMMARY OF FLIGHT CONDITION NO. 1

Flight condition #1 time history data included data runs 2 through 6. A tabular summary of the stability derivatives obtained from the various modified Newton-Raphson identification attempts with these data is given in Appendix C. A tabular summary of the results of significant runs, reduced with respect to velocity and reduced with an assumed $M_{\dot{\alpha}}$ and $Z_{\dot{\alpha}}$, is given in Table XIII. The reduced form will be used for most discussions because it is more universal and more easily compared to estimates, even though some inaccuracy is clearly introduced by the assumption of a known $M_{\dot{\alpha}}$. Although

TABLE XIII
FLIGHT CONDITION #1 FINAL RESULTS

Run	X_u	X_α	Z_u	Z_α	M_u	M_α	M_q	Z_{δ_e}	M_{δ_e}
A Priori	-0.046	-23.23	-0.27	-233.8	0	-5.11	-1.42	-24.	-9.68
Data Run 3									
1W2	-0.046	-5.7	-0.28	-235.3	-0.001	-4.97	-1.22	-21.7	-7.20
1W1DEZ	-0.044	+0.4	-0.22	-198.3	+0.003	-5.11	-1.50	-22.7	-7.71
2W2	-0.047	-7.4	-0.37	-201.6	-0.003	-4.77	-1.66	-22.0	-7.15
U2W1	-0.054	-5.7	-0.41	-235.3	-0.004	-4.97	-1.22	-22.2	-7.20
U3W2	-0.046	-5.7	-0.39	-235.3	-0.004	-4.97	-1.22	-22.2	-7.20
Data Run 2									
1W3	-0.076	-10.92	+ .069	-311.8	+0.002	-5.64	-1.24	-21.6	-9.32
Data Run 4									
1W4	-0.036	-10.63	-0.22	-222.6	-0.004	-4.69	-1.28	-23.0	-8.26
Data Run 5									
1W3	+0.034	+5.11	-0.35	-240.6	+0.004	-5.36	-1.32	-26.3	-8.65
Data Run 6									
1W3SH	0	-8.55	-0.24	-233.2	+0.001	-4.90	-1.33	-21.6	-8.15

the trim velocity has been eliminated as a direct effect on the identified derivatives, it is still true that velocity varies significantly among the five data runs, and some variation in the dimensional stability derivatives is to be expected with variation in trim velocity. Time history matches for all of the runs included in Table XIII, as well as some other matches from preliminary runs, are shown in Figures 7 through 16.

EFFECT OF WEIGHTING MATRIX AND START-UP VALUES

The first identification attempt was made on data run 3 with an identity weighting matrix and all zero start-up values, but only a divergence was obtained. A converging run was eventually obtained using a set of start-up values which were the "best guess" a priori stability derivatives, based on the trim velocity of data run 2 (which had also been tried with zero start-up values but diverged). Under these circumstances, the program converged, but the stability derivatives were virtually unchanged from the start-up values and the time history matches (see Figure 7) showed significant problems. Also visible in Figure 7 are the poor signal-to-noise ratio for the elevator input and a typical unfiltered velocity transducer switching problem. This first identification run, however, did provide sufficient information to calculate a weighting matrix. The next run (Figure 8) showed significant improvement, and a second iteration (Figure 9) brought about a respectable time history match and a series of weighted fit error contributions nearly equal to one.

EFFECT OF ZEROED CONTROL INPUT

In an effort to assess the damage caused to the identification process by the noisy elevator input, a run was made with δ_e set to zero after the pilot control input was clearly completed. Unfortunately, an overzealous velocity filter set questionable velocity data to zero as well, rather than simply smoothing. This distortion of the velocity time history was felt to be relatively insignificant, however. The time history matches (see Figure 10) are quite similar, but comparison of run DR3-1W2 and run DR3-1WDEZ results in Table XIII shows that noticeable changes occur in the identified derivatives, so control noise clearly was a factor.

One identification run was accidentally made with the control input zeroed for the entire time history with the time histories of the other variables intact. Such an exercise is only of academic interest, of course, but the results do reveal some interesting aspects of the operation of the identification algorithm. The program returned values for the control derivatives which were equal to the a priori values, rather than calculating very large numbers or refusing to find a solution. The implication is clearly that the algorithm tends to retain the a priori parameter values when given insufficient information to estimate the parameters. This behavior may explain the phenomenom of reasonable estimation of the speed derivatives from short data records with little or no speed variation.

KEY TO TIME HISTORY COMPARISONS

Solid lines are flight data. Dotted lines are calculated responses. For elevator time history, solid line is measured input data while dotted line is smoothed version actually used as input for identification program.

DE = elevator deflection, degrees, positive trailing edge up

A = angle of attack, degrees, positive for airplane nose up

U = airspeed, ft/sec

TH = pitch angle, degrees, positive for airplane nose up

Q = pitch rate, radians/seconds, positive clockwise viewed from port side of aircraft

AX = longitudinal acceleration, ft/sec^2, positive forward

AZ = normal acceleration, ft/sec^2, positive down

QD = pitch acceleration, $radians/sec^2$, positive clockwise viewed from port side of aircraft

TIME = elapsed time, seconds

Run number coding:

1. Digit after "DR" is data run number.

2. "U" after hyphen indicates that only speed derivatives were variables.

3. First digit is time length in multiples of 17.5 seconds.

4. Digit after "W" is number of iterations to obtain satisfactory weighting matrix.

5. Digit after "S" is number of times smoothing applied to input data.

6. Absence of "W" or "S" indicates absence of weighting or smoothing, respectively.

7. "DEZ" indicates elevator set to zero following significant control input.

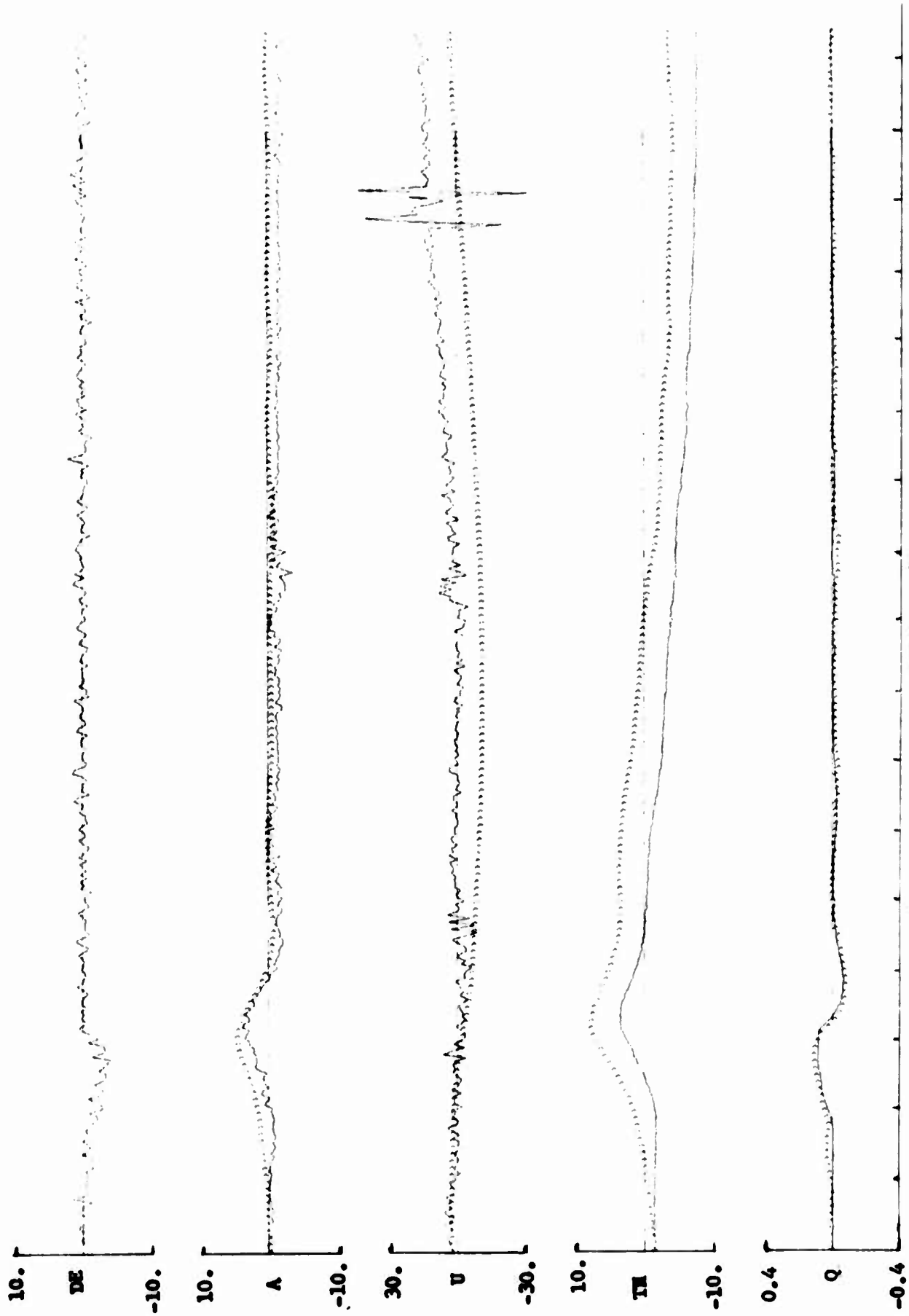

FIGURE 7. TIME HISTORY COMPARISON DR3-1

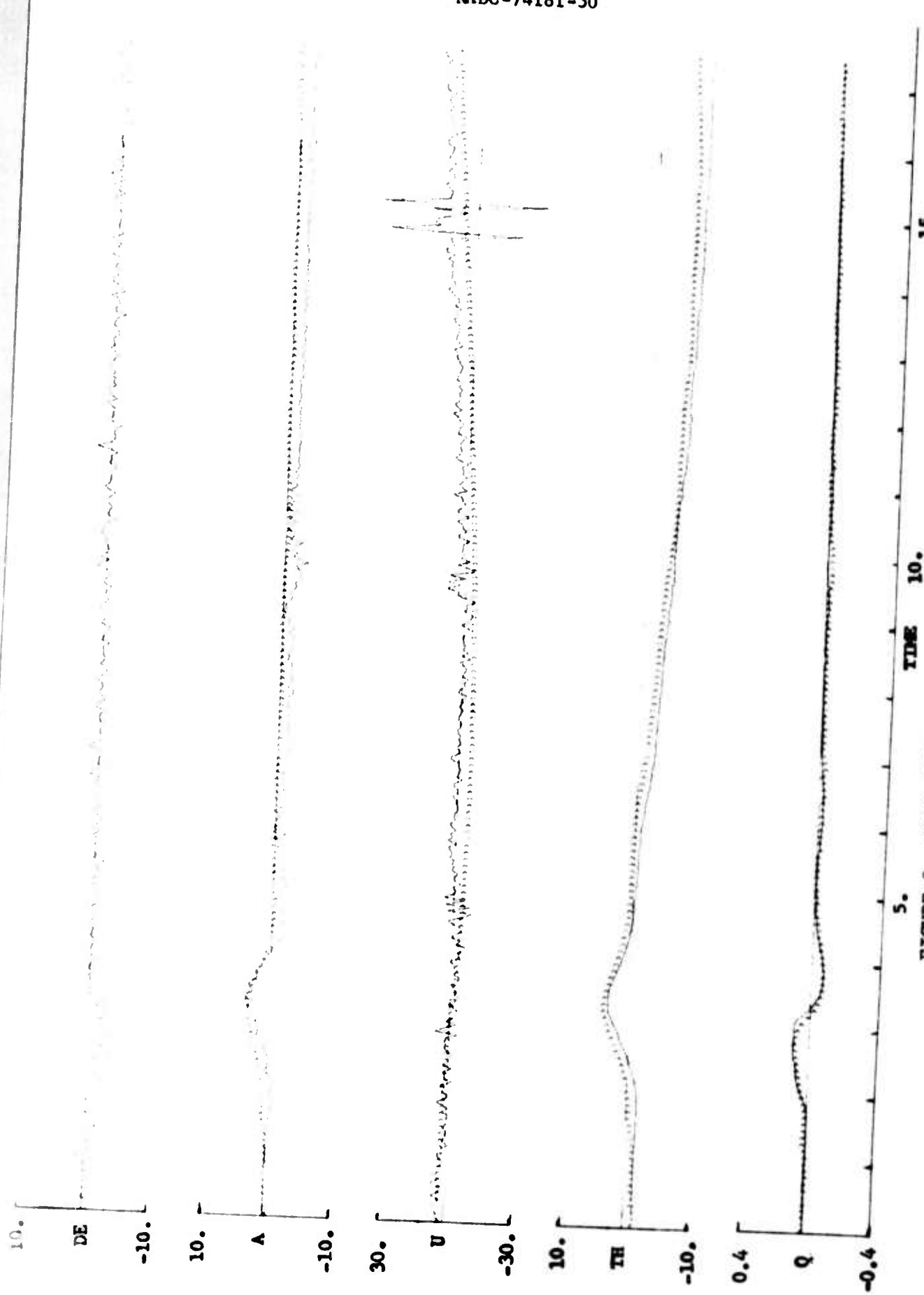

FIGURE 8. TIME HISTORY COMPARISON DR3-1W1

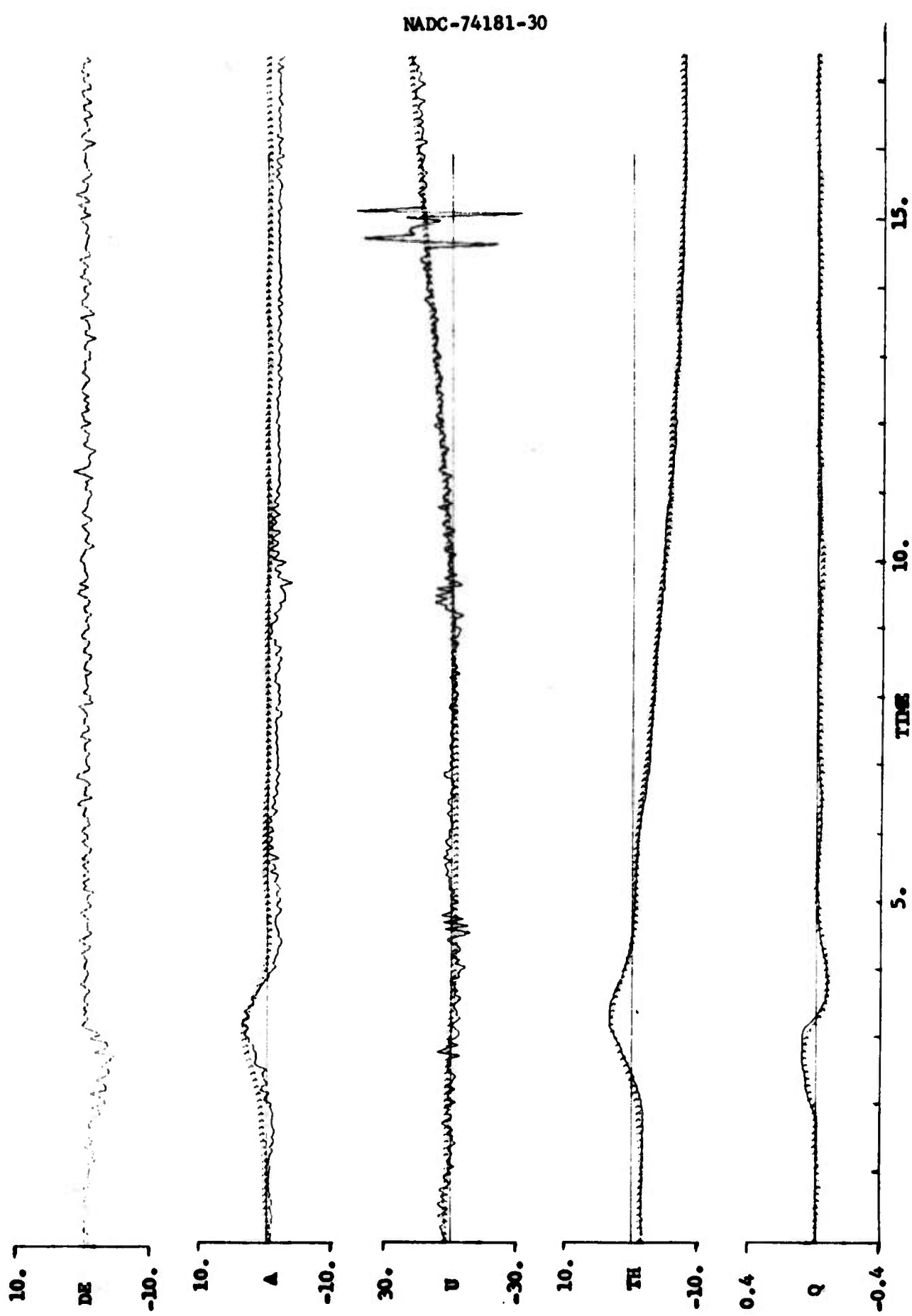

FIGURE 9. TIME HISTORY COMPARISON DR3-1W2

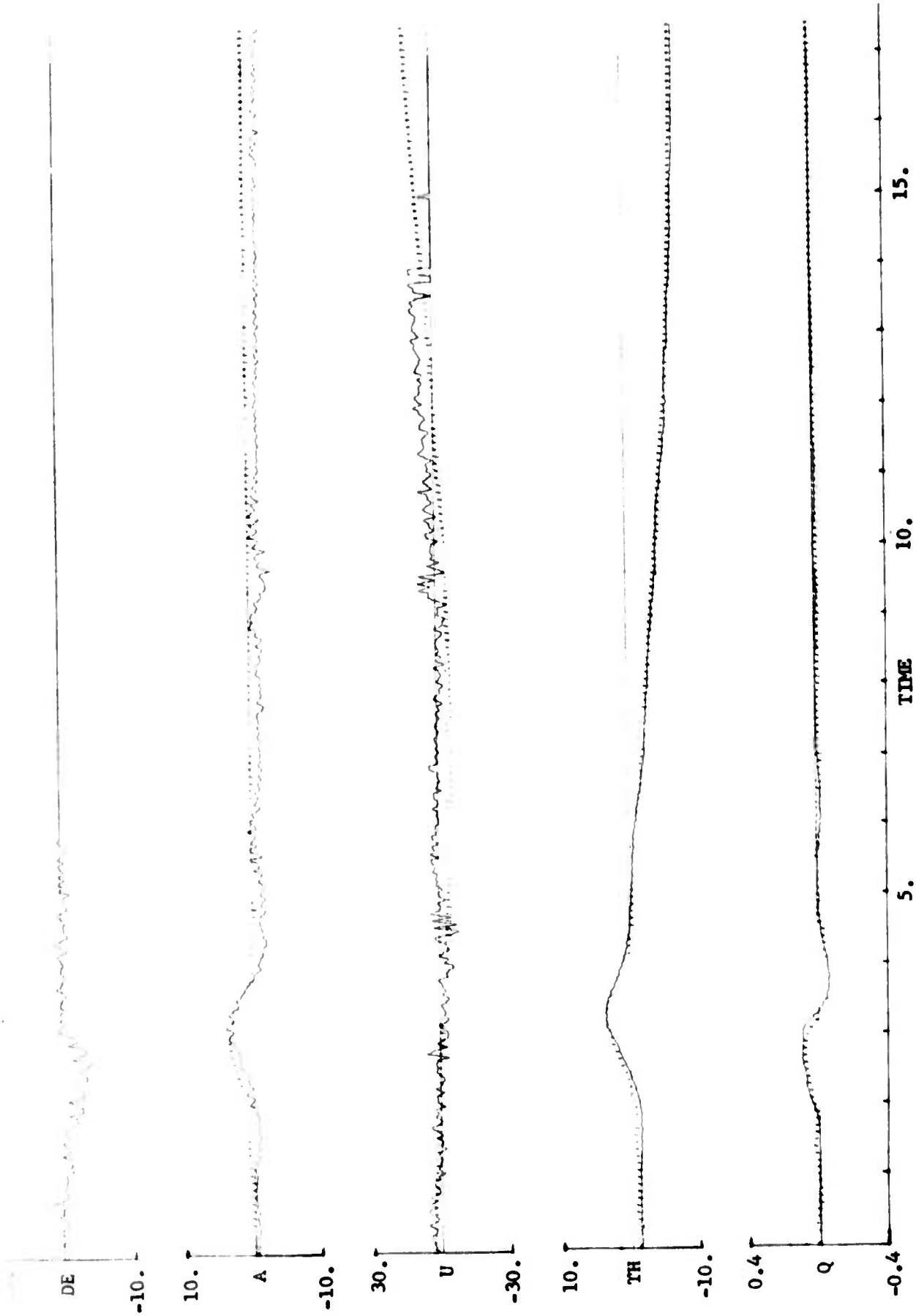

FIGURE 10. TIME HISTORY COMPARISON DR3-1W1DEZ

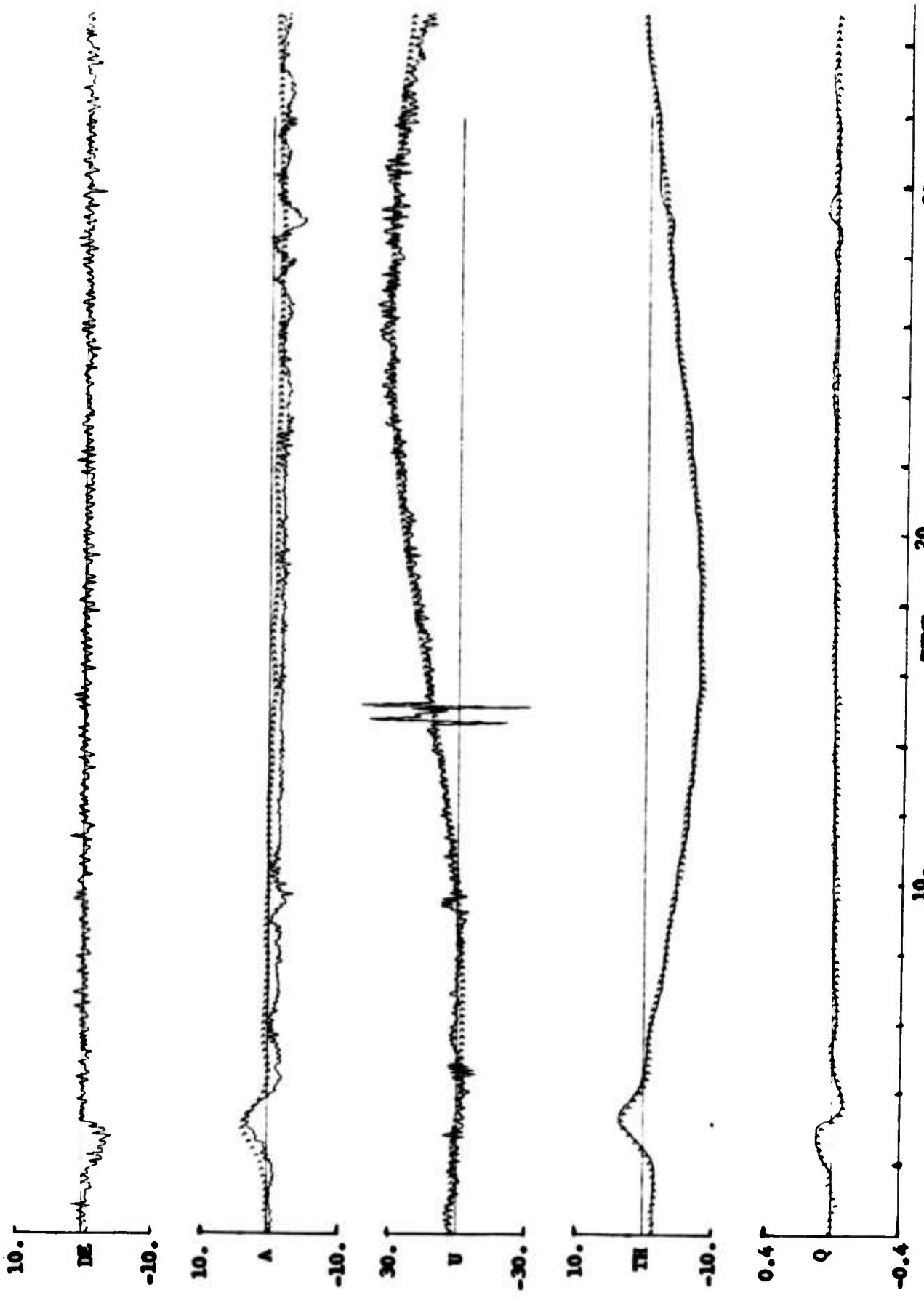

FIGURE 11. TIME HISTORY COMPARISON DR3-2W2

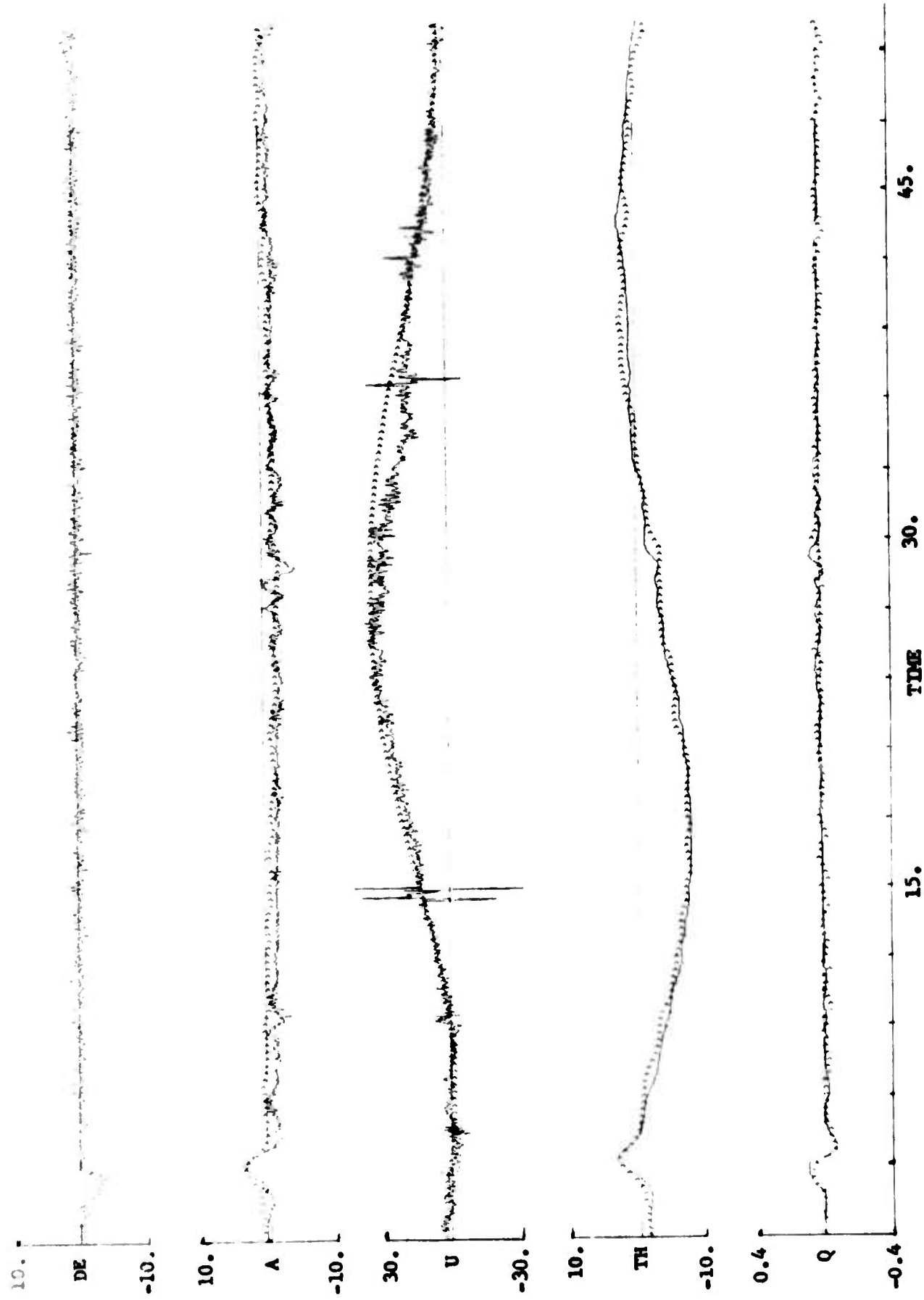

FIGURE 12. TIME HISTORY COMPARISON DR3-U3W2

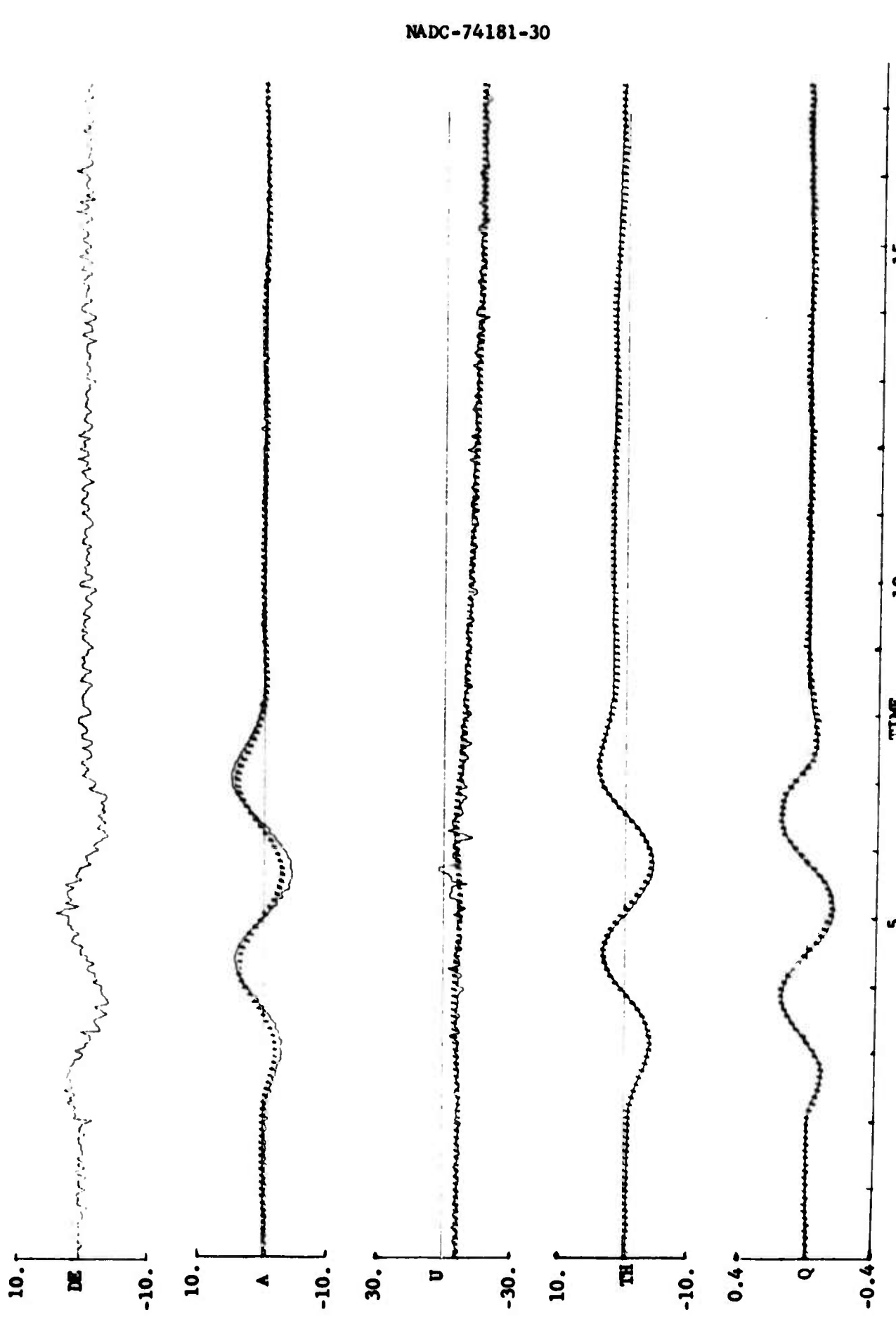

FIGURE 13. TIME HISTORY COMPARISON DR2-1W3

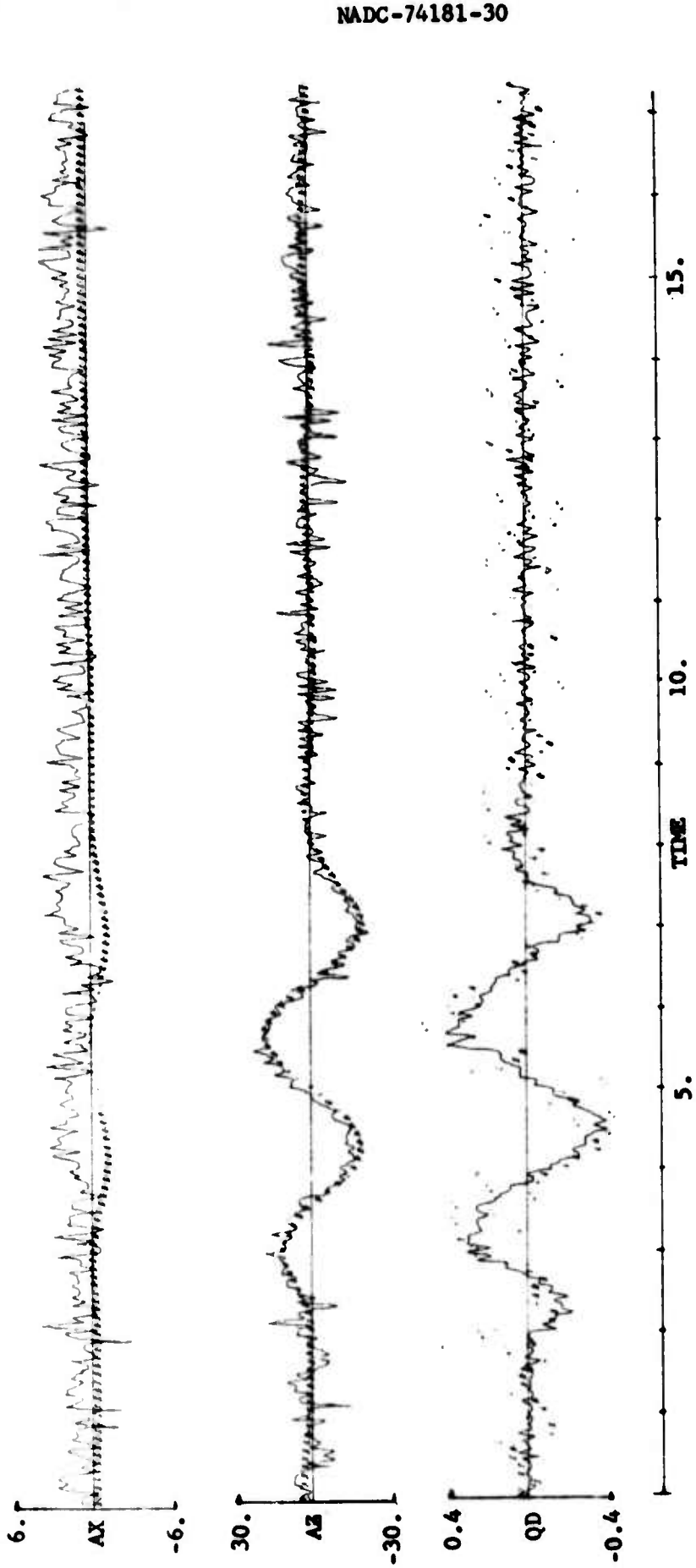

FIGURE 13 (CONT). TIME HISTORY COMPARISON DR2-1W3

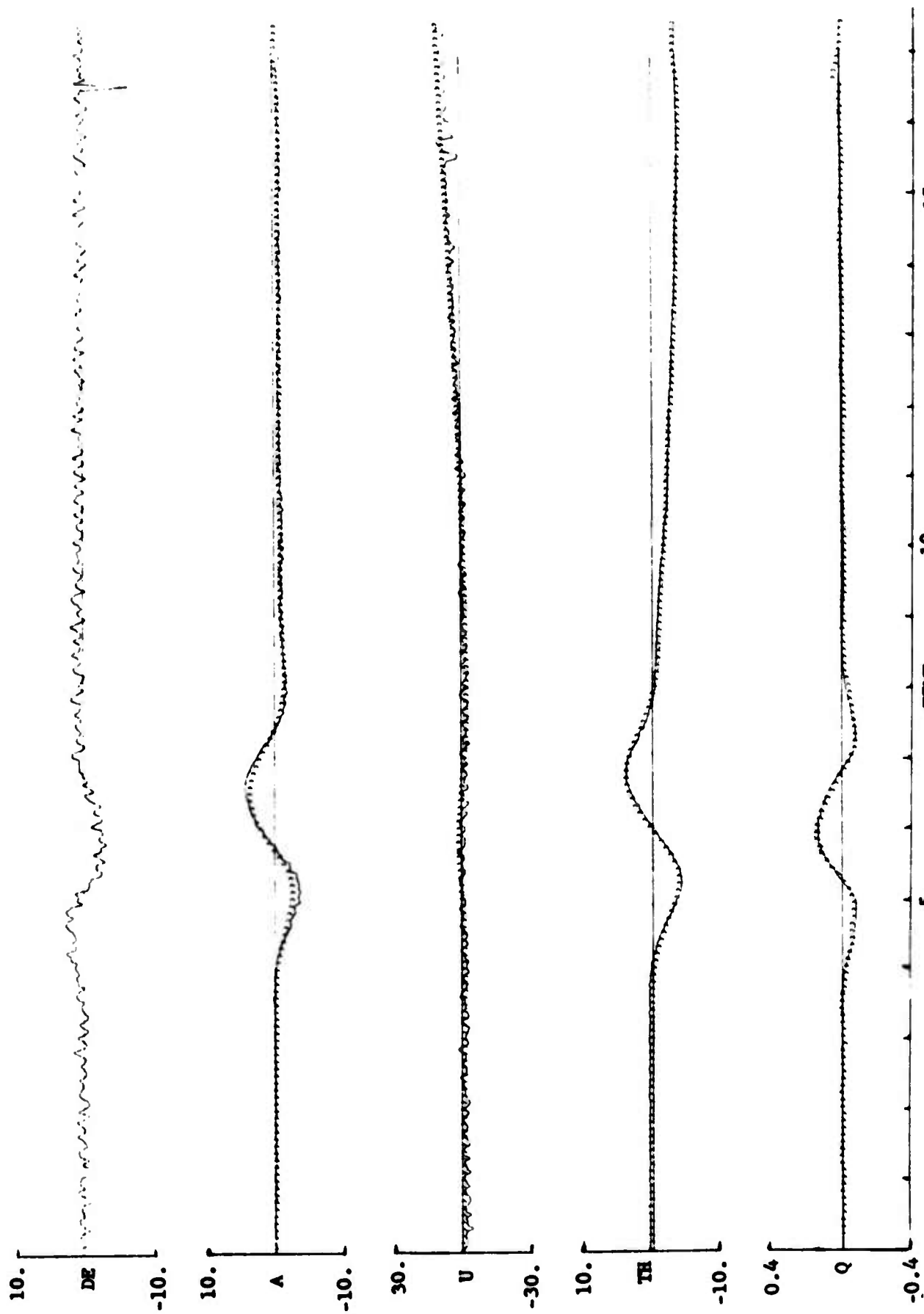

FIGURE 14. TIME HISTORY COMPARISON DR4-1W4

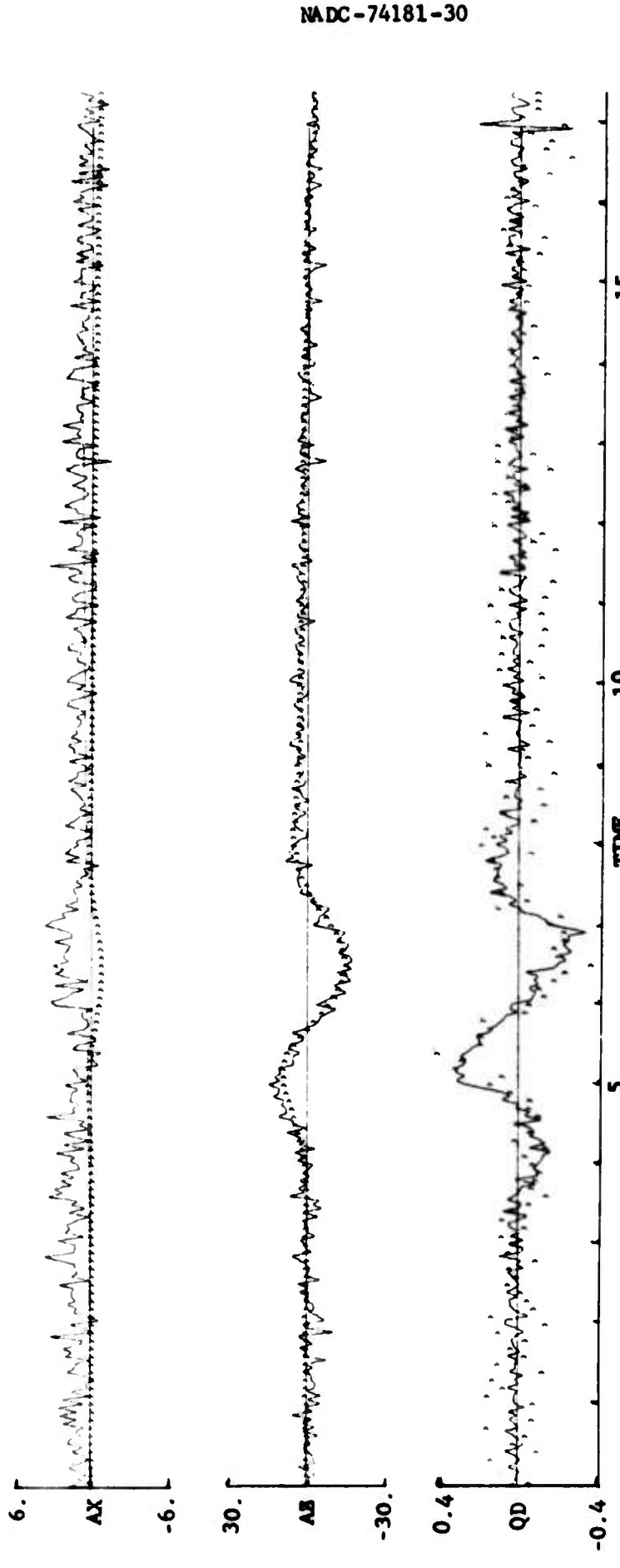

FIGURE 14 (CONT). TIME HISTORY COMPARISON DR4-1W4

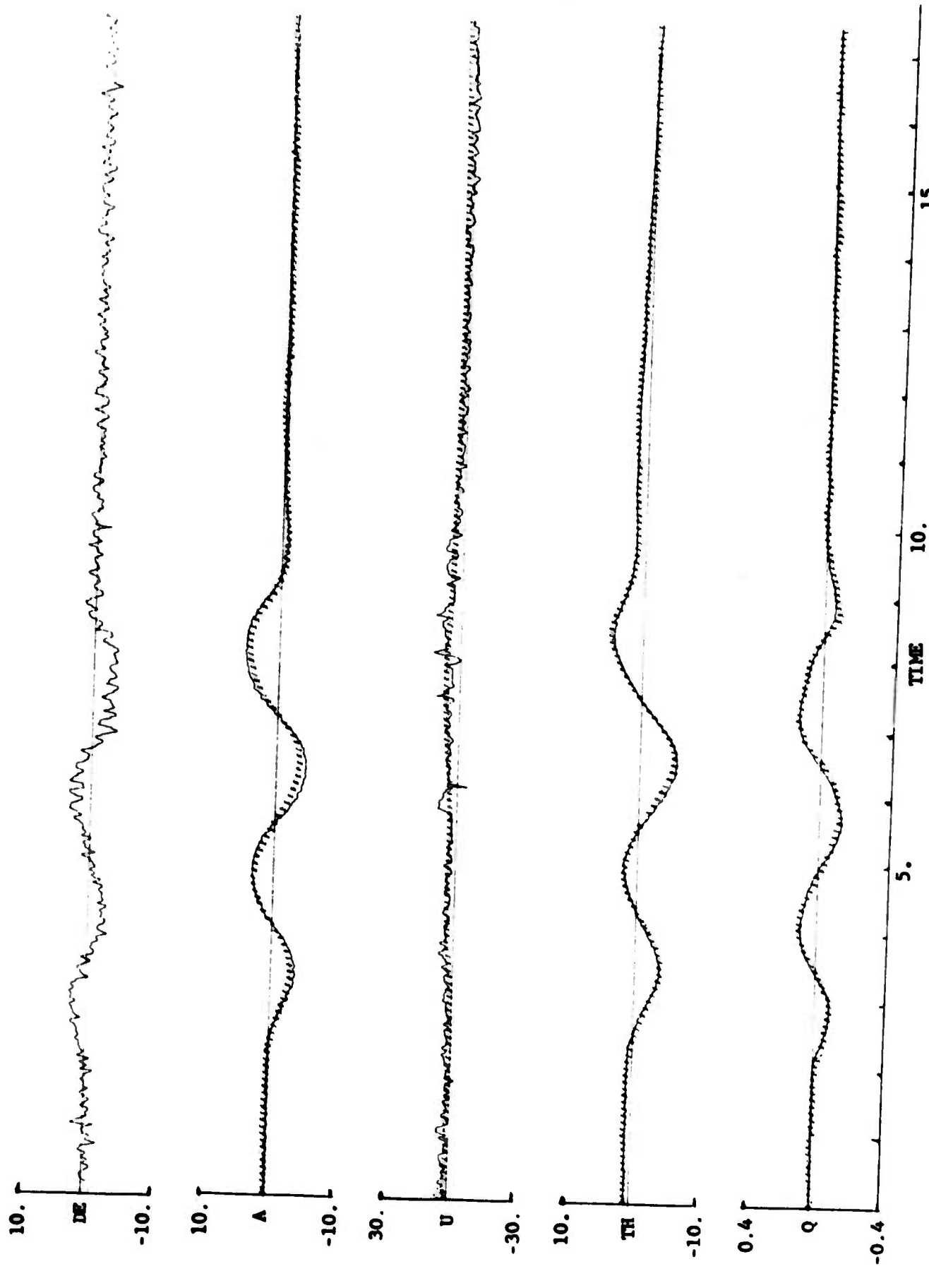

FIGURE 15. TIME HISTORY COMPARISON DR5-1W3

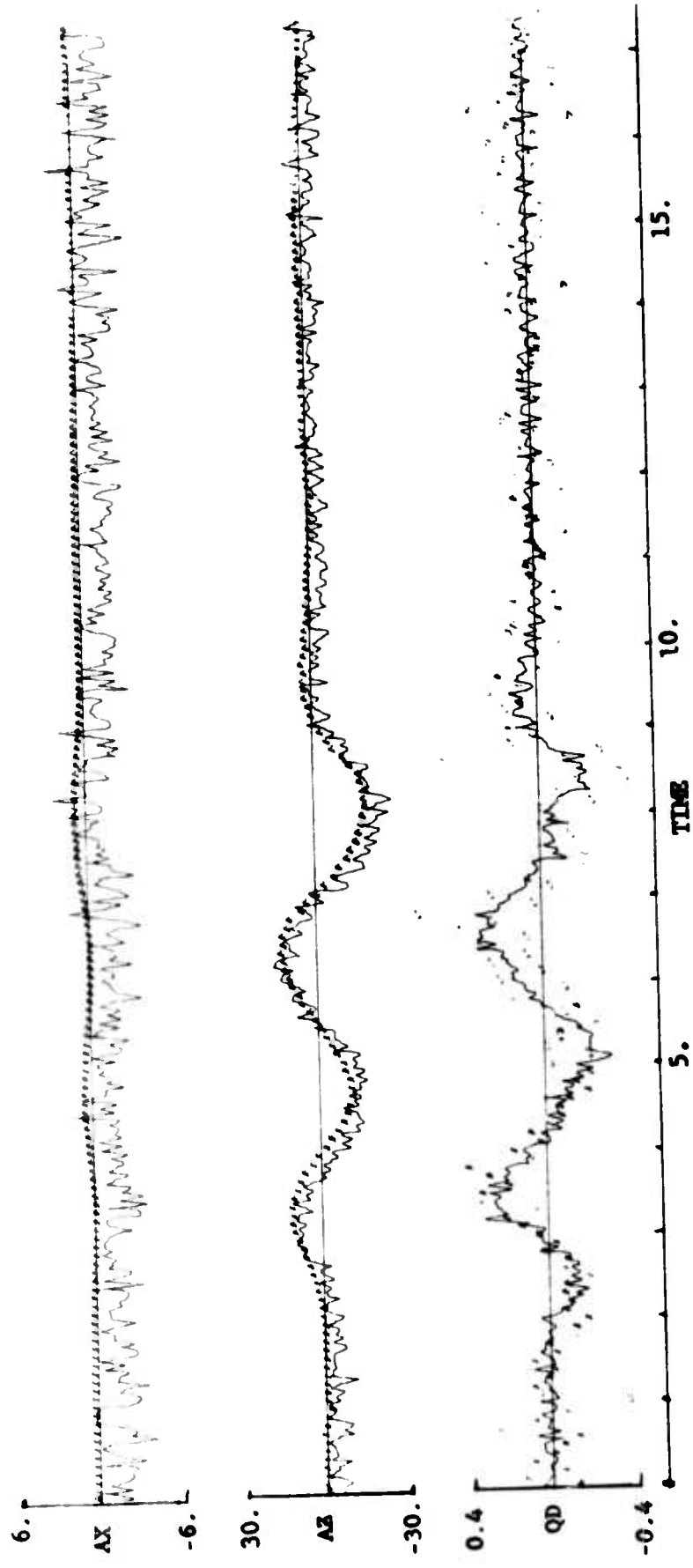

FIGURE 15 (CONT). TIME HISTORY COMPARISON DR5-1W3

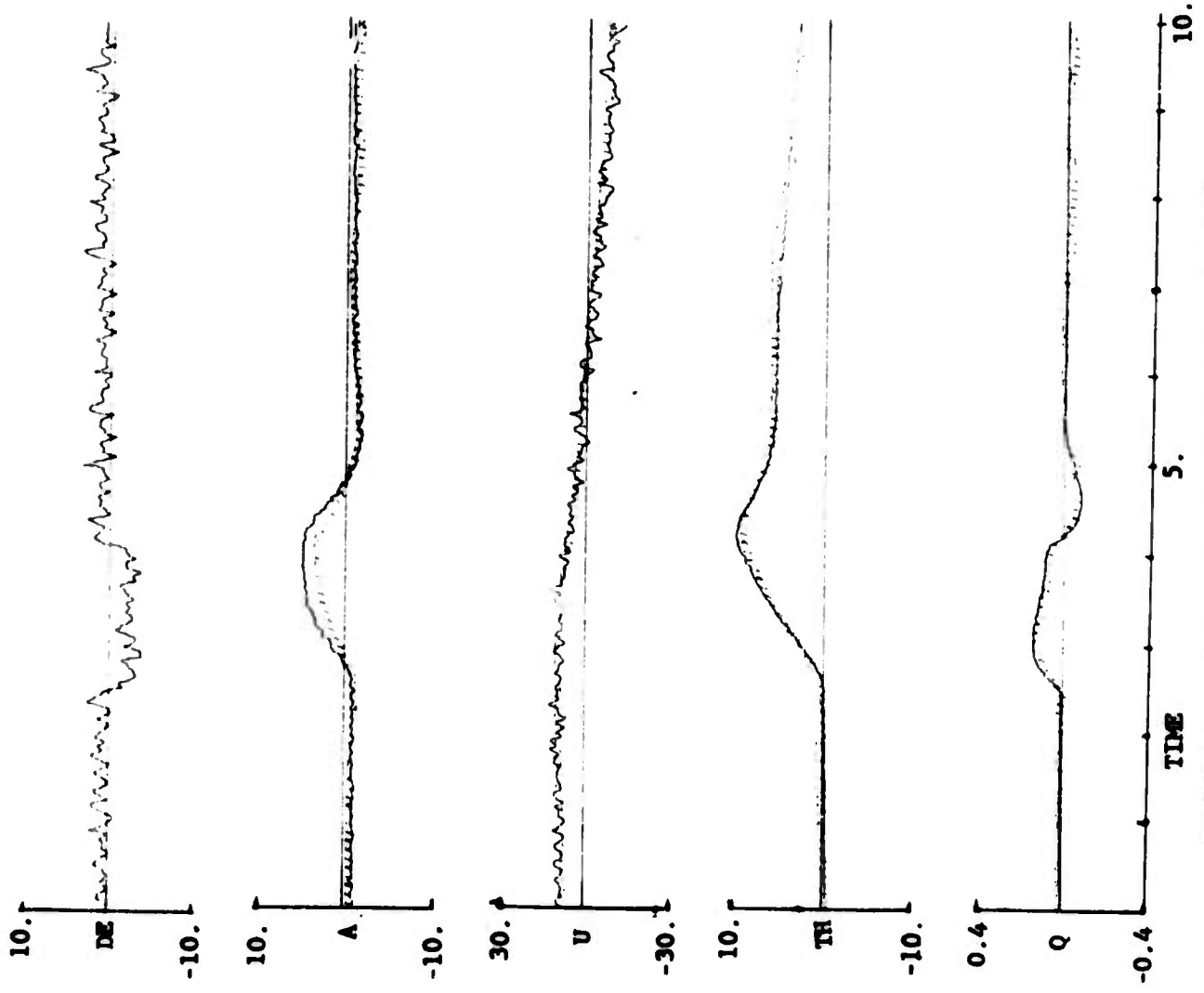

FIGURE 16. TIME HISTORY COMPARISON DR6-1W3SH

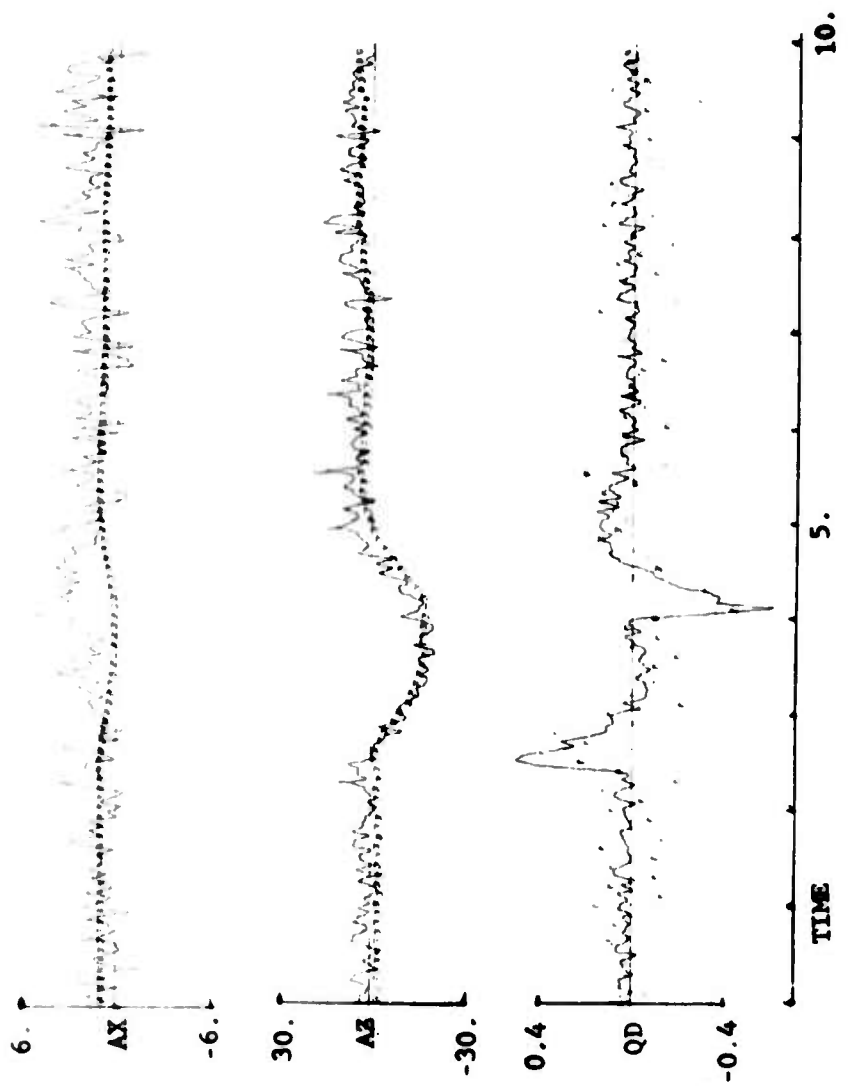

FIGURE 16 (CONT). TIME HISTORY COMPARISON DR6-1W3SH

If the algorithm does tend to keep parameters at their a priori values when faced with insufficient data, then parameter results would be a strong function of their start-up values if the flight data were incomplete or inappropriate. This theory was not tested because all radical changes in start-up values lead to divergence.

EFFECT OF HOLDING SHORT-PERIOD DERIVATIVES CONSTANT

Utilizing a 35 second section of data run 3, two different identification procedures were used. One run (DR3-2W2) had all derivatives as variables while the other (DR3-U2W1) had short period derivatives held fixed at the values determined by the best 17.5 second run (DR3-1W2) and only the speed derivatives variable.

Only M_q was significantly different in the two sets of results. As can be seen in Table XIII, the speed derivatives were essentially identical. The time history match (Figure 11) is for run DR3-2W2, but an identical plot was generated for DR3-U2W1. Both time history matches were disturbed by apparent atmospheric turbulence. At approximately 10 seconds and 28 seconds significant variations in angle of attack occur without any visible change in δ_e. Pitch rate and pitch angle also change at this time, but not as severely as angle of attack. On the 52.5 second run with the same data (see Figure 12) even more turbulence is obvious, and a large disturbance in velocity is visible lagging significantly behind angle of attack. The model equations of motion have neither gust inputs nor nonlinear terms, so the model insists on creating smooth time histories. The velocity time history, for instance, rejoins the flight data after the gust disturbance.

DATA RUN #3

Several identification attempts using data run 3 have already been discussed for other purposes, but it remains necessary to take an overall look at data run 3 results. The principal results (DR3-1W2) agree well with the a priori values except for $X_{\sim}$, which is negative but much smaller, and M_{δ_e}, which is about 25% below the a priori value. The other runs (DR3-1WDEZ and DR3-2W2) which had variable short period derivatives had a similarly low M_{δ_e}, and M_q higher than the a priori value (and about 25% higher than DR3-1W2), and a widely varying X_{α}. The speed derivatives are surprisingly consistent from the short runs to the long runs, and also similar to the a priori values.

The time history match (Figure 9) for angle of attack seems to be both slightly out of phase and offset somewhat. The offset may be due to a poorly defined trim condition on angle of attack due to the atmospheric turbulence. The time history matches for the other variables are quite good except for the previously discussed areas of turbulence.

DATA RUN #2

As can be seen from Table XIII, the results from data run 2 are significantly different from the other data runs. Specifically, Z_u has an incorrect sign (although it would be foolish to expect to estimate speed derivatives from a short data record), Z_α and M_α are unusually large, and M_{δ_e}, although smaller than the a priori value, is much larger than that obtained from any other runs. Run 2 has a higher trim velocity than any other data run, but this factor alone is not enough to explain the difference. Considering C_{L_α} as independent of trim velocity, for instance, Z_α for data run 2 should be -275.6 (based on a value of -235.3 for Z_α from data run 3) but was estimated at -311.8.

Figure 13 shows the time history matches for data run 2, including a_x, a_z, and $\dot{q}$ in addition to the δ_e, α, u, θ, and q shown for data run 3. The angle of attack time history match is far from perfect. Some phase shift seems to exist, with the modeling leading the flight data, and the model response is smaller in amplitude than the flight data. The flight data is nearly symmetric with respect to positive and negative excursions in angle of attack; the model response has smaller negative excursions than positive, creating a noticeable fit error.

The a_x time history match is not a match at all - the model response has a large lead relative to the flight data and the principal response is in the opposite direction. As stated previously, the program performs a match on $\dot{u}$, not on a_x itself, and $\dot{u}$ contains a $g\theta$ term which in this case is much larger in magnitude than a_x. Thus the $\dot{u}$ match is largely a repeat of the θ match for this data set. The opposite sign trend in the response nevertheless motivated a thorough investigation of sign convention relative to a_x, but no mistakes were found.

The a_z situation is similar to the a_x problem mentioned above, in that the $\dot{\alpha}$ match is partially a repeat of the q match rather than a_z alone, but the a_z time history match is really quite good. Of course the level of excitation is quite different - a_z is approximately ± 30 ft/sec^2 while a_x is ± 2 ft/sec^2.

The $\dot{q}$ time history comparison is quite unusual, since the model response is much noisier than the flight data. The flight data for $\dot{q}$ are taken from the angular accelerometer, which was less noisy than expected. The other $\dot{q}$ measurement, calculated from nose and tail linear accelerometers, was far too noisy to be of any use. The model response, which is directly proportional to elevator deflection, is quite noisy since the elevator deflection is so noisy. Although the measured fit error is quite large for this time history pair, the trends are clearly correct and it seems fair to judge that $\dot{q}$ is matched.

DATA RUN #4

The stability derivatives extracted from data run 4 are quite similar to the a priori values (and hence to data run 3 results). The widely varying X_{α} has essentially the same value here as for data run 2. $M_{\dot{\alpha}}$ is unusually small for data run 4, however, being 8% below the a priori value. The value of M_q is noticeably (10%) below the a priori value, but it is very close to the results from previous data runs. The M_{δ_e} extracted for this run is a compromise, almost evenly spaced between the results of run 3 and run 2. The extracted derivatives are listed in Table XIII.

Time history comparisons for data run 4 are shown in Figure 14. The comments made for data run 2 (above) apply almost exactly to data run 4 as well. Angle of attack time shift and amplitude, a_x time shift and direction of excursion, and $\dot{q}$ model response noise were still problems.

DATA RUN #5

The control input for data run 5 was similar to that of data run 2, except that the former was somewhat lower in frequency and amplitude than the latter. The trim airspeed for data run 5 is 11 ft/sec less than data run 2, which could lead to some differences in parameter values, but the data run 5 trim airspeed is essentially in the center of the range of trim airspeeds covered by the data, so overall comparisons of results without consideration of airspeed should be possible.

The most obvious feature of the results for data run 5 is that both X_u and X_{α} are estimated to be positive, while all other estimates for these derivatives were negative. The estimate for M_{α} is somewhat large, but not as large as the estimate from data run 2. The M_{δ_e} estimate falls near the center of the range defined by previous estimates.

The time history matches for data run 5, shown in Figure 15, appear to be slightly different from those for previous runs. The angle of attack phase and amplitude problems are slightly smaller than for the runs, but the a_z fit has deteriorated noticeably. The a_x flight data seems to have a steady-state offset, but the model and flight data excursions seem to be approximately equal in magnitude, identical in direction, and nearly in phase.

DATA RUN #6

Excessive noise rendered the latter portion of data run 6 useless, so only 200 data points were used. The results for the shortened run 6 are given in Table XIII. A reasonable value for X_{α} was obtained, while X_u was exactly zero. The remainder of the stability derivatives were very similar to the results from previous runs. Although it may seem unlikely that the speed derivatives could be estimated from a 10 second data run, the magnitude of the velocity

perturbation is actually larger (about 20 ft/sec) in data run 6 than in several other data runs.

Time history comparisons for data run 6 are shown in Figure 16. The angle of attack time history match is in phase, but a serious amplitude error exists. The model response is approximately 75% of the in-flight response. The a_z match is good. The a_x model response leads the flight data slightly and the excursion is once again in the opposite direction.

INTERPRETATION OF X_α RESULTS

Two stability derivatives, X_α and M_{δ_e}, vary more widely than anticipated in the results discussed above, and it would be desirable to identify reasons for this behavior. Although this report generally deals in dimensional derivatives, which are considered more meaningful, an examination of the nondimensional forms may be useful.

According to reference (n), $X_\alpha = \frac{\rho S U^2}{2m}(C_L - C_{D_\alpha})$. For flight condition #1, $\frac{\rho S}{2m} = 8.469 \times 10^{-4}$. Some uncertainty exists in the determination of trim C_L due to previously discussed difficulties with angle of attack reference, but $(C_L)_{trim} = \frac{2mg}{\rho U^2 S}$ is probably sufficient for the purposes of this portion of the investigation. Table XIV lists X_α reduced to nondimensional form, and C_{D_α} extracted from the combined form, for all "final" runs of short time length. Unfortunately, it seems clear that neither $(C_L - C_{D_\alpha})$ nor C_{D_α} are much closer to being consistent than X_α itself. Nor is C_{D_α} a consistent function of $(C_L)_{trim}$.

Reference (t) found that a $(C_L)_{trim}$ of 0.6 corresponds to an $(\alpha)_{trim}$ of approximately 6°, and that a C_{D_α} of 0.287 was indicated for this condition (without consideration of drag due to elevator required for trim). This value of C_{D_α} is considerably smaller than those determined by the identification program. Reference (t) does indicate that C_{D_α} increases rapidly with increasing $(\alpha)_{trim}$, having a value of 0.573 at $(\alpha)_{trim} = 10°$, and 1.123 at $(\alpha)_{trim} = 12.5°$.

INTERPRETATION OF M_{δ_e} RESULTS

The equation (reference (n)) $M_{\delta_e} = \frac{\rho S c U^2}{2I_y} C_{m_{\delta_e}}$ can be used to find the $C_{m_{\delta_e}}$ equivalents of the identified δ_e values. Table XV lists the results of these calculations.

TABLE XIV
FLIGHT CONDITION #1 RESULTS FOR C_{D_α}

Run	X_α	$(C_L - C_{D_\alpha})$	$(C_L)_{trim}$	C_{D_α}
A Priori	-23.23	-0.492	0.683	1.175
DR3-1W2	-5.7	-0.111	0.625	0.736
DR3-1W1DEZ	+0.4	+0.008	0.625	0.617
DR2-1W3	-10.92	-0.182	0.535	0.717
DR4-1W4	-10.63	-0.196	0.593	0.789
DR5-1W3	+5.11	+0.092	0.582	0.490
DR6-1W3S	-8.55	-0.159	0.601	0.760

TABLE XV
FLIGHT CONDITION #1 RESULTS FOR $C_{m\delta_e}$

Run	M_{δ_e}	$C_{m\delta_e}$
A Priori	-9.68	-1.18
DR3-1W2	-7.20	-0.803
DR2-1W3	-9.32	-0.891
DR4-1W4	-8.26	-0.875
DR5-1W3	-8.65	-0.899
DR6-1W3S	-8.15	-0.875

Reduction to nondimensional forms tends to reduce the differences between the identified parameters. The smallest $C_{m_{\delta_e}}$ is only an 11% reduction from the largest identified $C_{m_{\delta_e}}$, while the smallest M_{δ_e} was a 23% decrease from the largest identified M_{δ_e}. However, observation of the $C_{m_{\delta_e}}$ results reveals that the identified results are all quite different from the a priori value. The $C_{m_{\delta_e}}$ determined by the wind tunnel tests reported in reference (t) is 1.29 for δ_e between -10° and -15°, which is slightly higher than the a priori value and much different from the identified parameters. However, the wind tunnel tests also indicate that elevator effectiveness drops off rapidly with increasingly negative δ_e beyond $\delta_e = -15°$, suggesting that a linear $C_{m_{\delta_e}}$ might not be appropriate. Yet the reference (t) wind tunnel data are for a no-flaps configuration, while the flight data were taken for a half-flaps configuration. The deflection of the flaps certainly could change the elevator effectiveness and the elevator angle at which effectiveness decreases. Thus, the comparison of the reference (t) data and the flight results may not be meaningful, but the a priori information was generated for the half-flap case and no simple explanation exists for the discrepancy between this value and the flight results.

SUMMARY OF FLIGHT CONDITION #2

Identification results for flight condition #2, reduced with respect to an assumed known $M_{\dot{\alpha}}$, are given in Table XVI. In general, the results are consistent within themselves, although not necessarily in agreement with the a priori values. Unreduced results are given in Appendix C.

DATA RUN 19

Data run 19 featured a pseudo-white noise elevator input with approximately zero mean. The continuous reversal movements of the control allowed the control deflection magnitude to be relatively large without causing any motion variables to exceed the range for which linear dynamics may reasonably be considered. Thus the signal to noise ratio for the elevator signal was high enough to permit processing without first smoothing the control data. The resultant time history matches are shown in Figure 17. General agreement seems evident although the matches are by no means perfect. The largest discrepancy occurs due to an elevator noise spike at approximately four seconds. The angle of attack match has a persistent offset problem, however, and the normal acceleration response of the model seems to consistently lag the flight data. The pitch acceleration response of the model is too noisy to permit any conclusions.

DATA RUN 10

The time history matches for data run 10 are shown in Figure 18. The signal/noise ratio for the elevator data (solid line) is clearly poor. Shown dotted on the elevator trace is the smoothed elevator time history actually used as input to the identification program. The time history match is rather good, but the maneuver is so small that it would seem dangerous to place too much weight on the results.

TABLE XVI
FLIGHT CONDITION #2 FINAL RESULTS

Assuming $Z_{\dot{\alpha}} = 0$, $M_{\dot{\alpha}} = -1.57$

Run #	X_u	X_α	Z_u	Z_α	M_u	M_α	M_q	Z_{δ_e}	M_{δ_e}
A Priori	-0.016	-36.91	-0.122	-1669.2	0.0017	-22.5	-3.39	-121.3	-52.12
Data Run 10 1W2S2	0.001	6.84	0.155	-1381.1	-0.0006	-22.2	-6.47	-129.9	-50.10
Data Run 11 1W2S2DEZ	-0.006	11.55	0.175	-1358.4	0.0008	-22.4	-7.12	-135.8	-49.61
U4W2S2DEZ	-0.099	11.55	-0.011	-1358.4	0.0016	-22.4	-7.12	-135.8	-49.61
Data Run 12 U5W3S2DEZ	-0.038	11.39	-0.233	-1339.8	0.0018	-22.4	-7.12	-134.0	-49.61
Data Run 14 1W3S2SH	0.053	28.17	-0.021	-1656.2	0.0013	-23.0	-8.08	-123.7	-49.00
Data Run 18 1W3S2	0.024	32.77	0.005	-1119.8	0.0015	-21.9	-7.05	-143.4	-49.73
Data Run 19 1W2	-0.075	24.84	-0.013	-1366.2	0.0004	-22.7	-7.94	-138.0	-48.51
Data Run 13 1W2S2	-0.027	19.06	0.093	-1348.0	0.0012	-22.5	-7.72	-136.2	-48.91

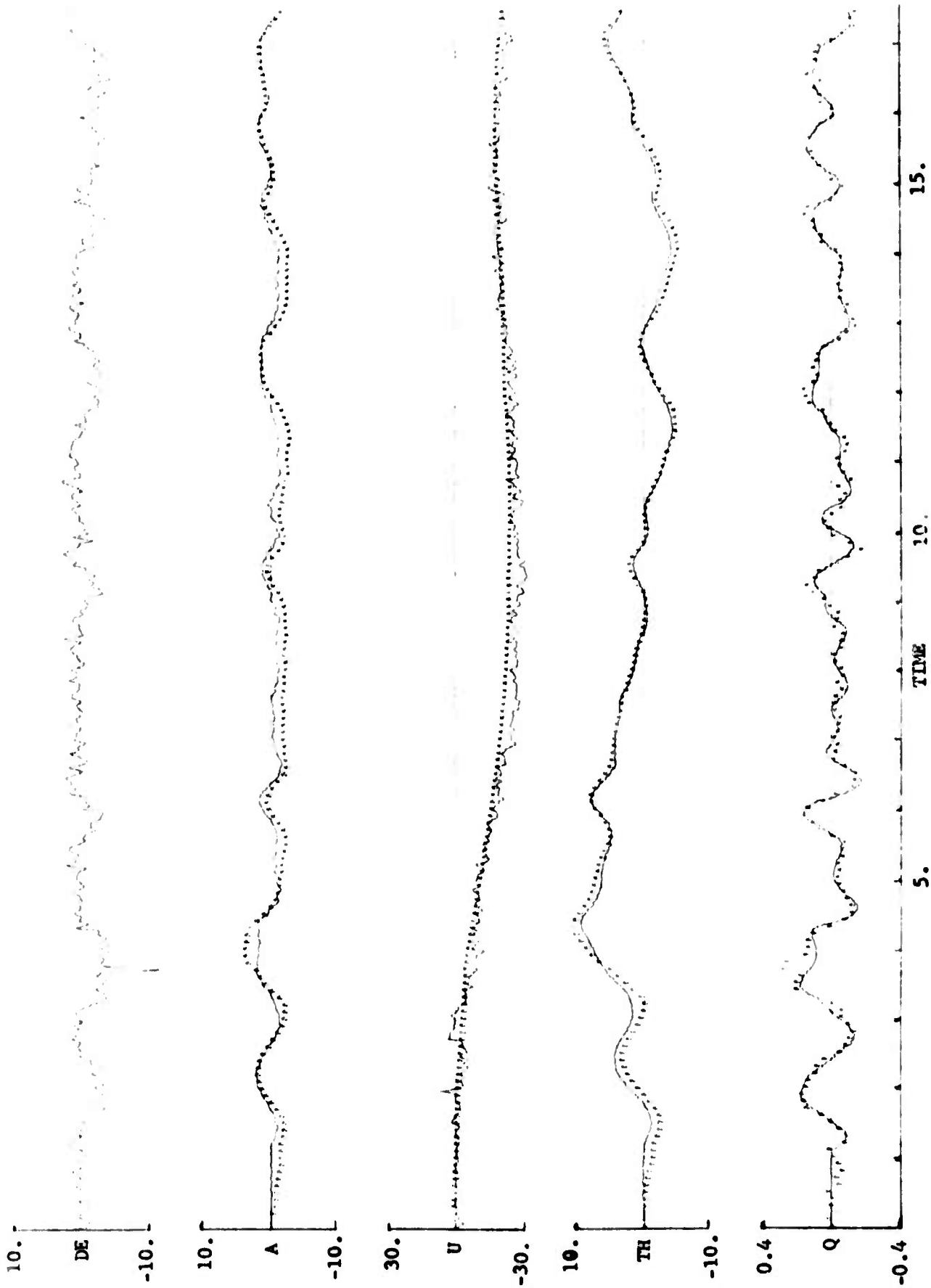

FIGURE 17. TIME HISTORY COMPARISON DR19-1W2

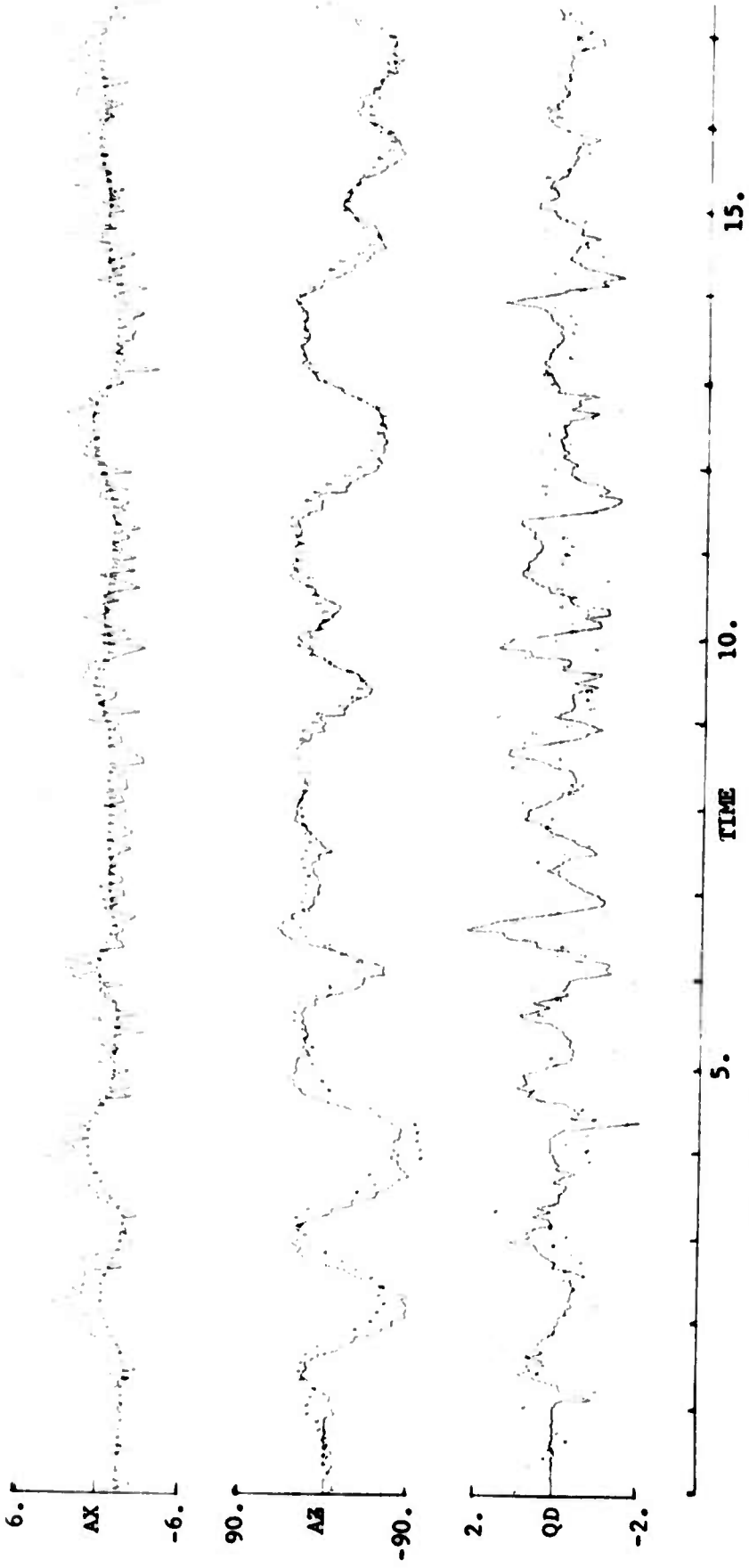

FIGURE 17 (CONT). TIME HISTORY COMPARISON DR19-1W2

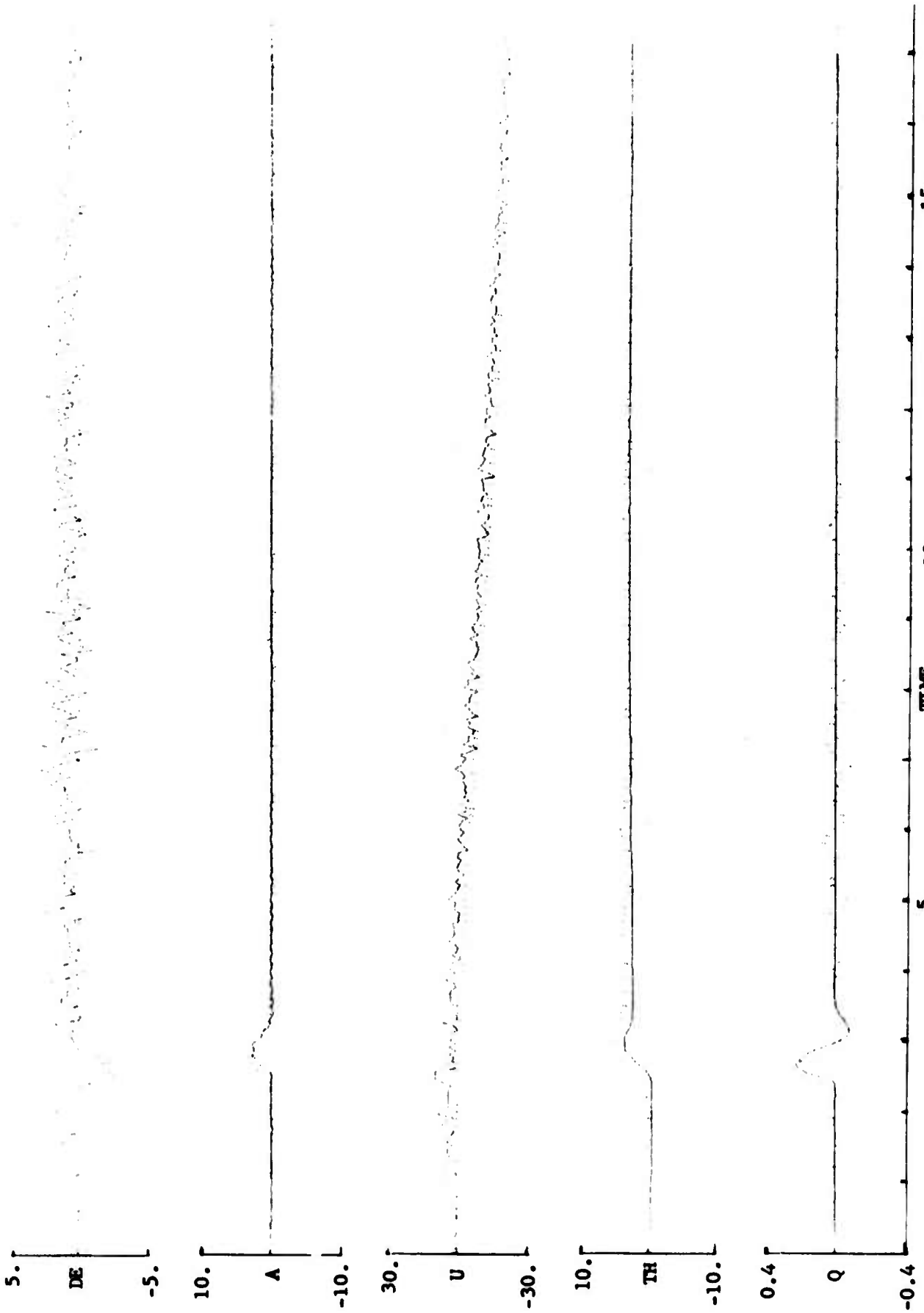

FIGURE 18. TIME HISTORY COMPARISON DR10-1W2S1

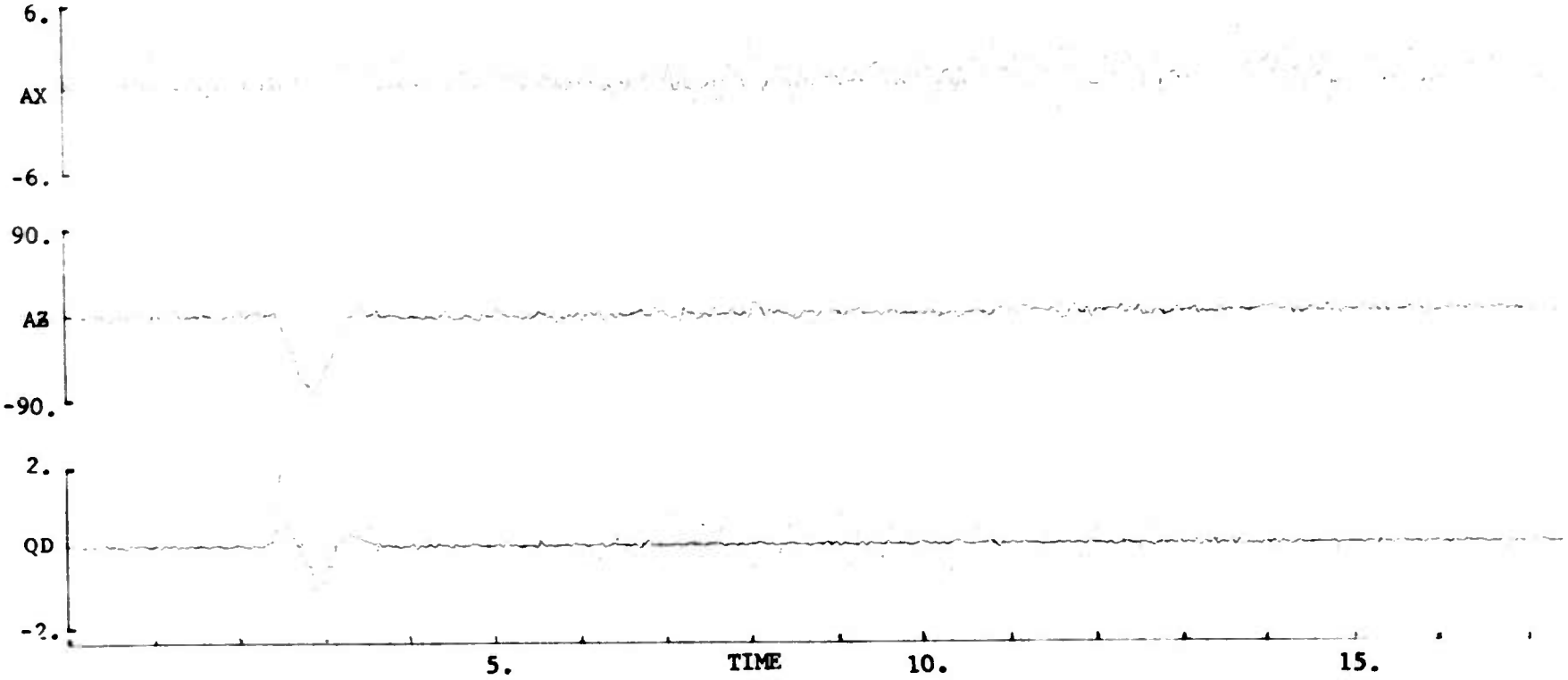

FIGURE 18 (CONT). TIME HISTORY COMPARISON DR10-1W2S1

DATA RUN 14

Only 15 seconds of data were available in data run 14. The time history matches obtained for the shortened run are shown in Figure 19. The magnitudes of the peaks of the angle of attack and pitch angle responses in their positive directions are significantly larger for the model than for the flight data. Also, the model normal acceleration response again seems to lag the flight data.

Although the results for individual stability derivatives will be discussed in later sections, it is worth noting here that the largest values of Z_{α}, $M_{\dot{\alpha}}$, and M_q, and the smallest value of Z_{δ_e}, were obtained from this data run. In particular, the Z_{α} value of -1656. is the only identified result approaching the a priori Z_{α} value of -1669.

DATA RUN 13

The control input shape, and the errors in the resulting time history match, for data run 13 are nearly identical to data run 14. Yet the identified Z_{α} for data run 13 is 19% lower than that obtained from data run 14, and X_{α}, $M_{\dot{\alpha}}$, and M_q are also lower. The time history comparisons for data run 13 are shown in Figure 20.

DATA RUN 18

Time history comparisons for data run 18 are shown in Figure 21. The model responses for angle of attack and pitch angle are roughly correct in shape but have a substantial bias in the direction of positive response. This phenomenom is not a simple shift of the entire response curves, because the model response curves and the flight data are similar at both the beginning and end of the data run. The normal acceleration shows that the model response lags the flight data and the amplitude of the model response is insufficient in the positive direction to match the flight data.

The a_x time history comparison in this data run, as well as all the previously discussed data runs for flight condition #2, contains little information because of the high noise level in the a_x flight data and the relatively low level of excitation. It is quite significant, however, that the model and flight responses are in the same direction. It should be recalled that the responses tended to be in opposite directions in flight condition #1 time history comparisons, leading to speculation that a sign error existed in either the model or the measurement system. The somewhat larger a_x excitations in the data runs of flight condition #2 reveal that the signs are correct in general, although the a_x matching problems in flight condition #1 may indicate a deficiency in the model for that configuration.

The results from data run 18 feature the smallest Z_{α}, $M_{\dot{\alpha}}$, and M_q, and the largest value of Z_{δ_e}, of any flight condition #2 data run. This situation is exactly opposite that of data run 14.

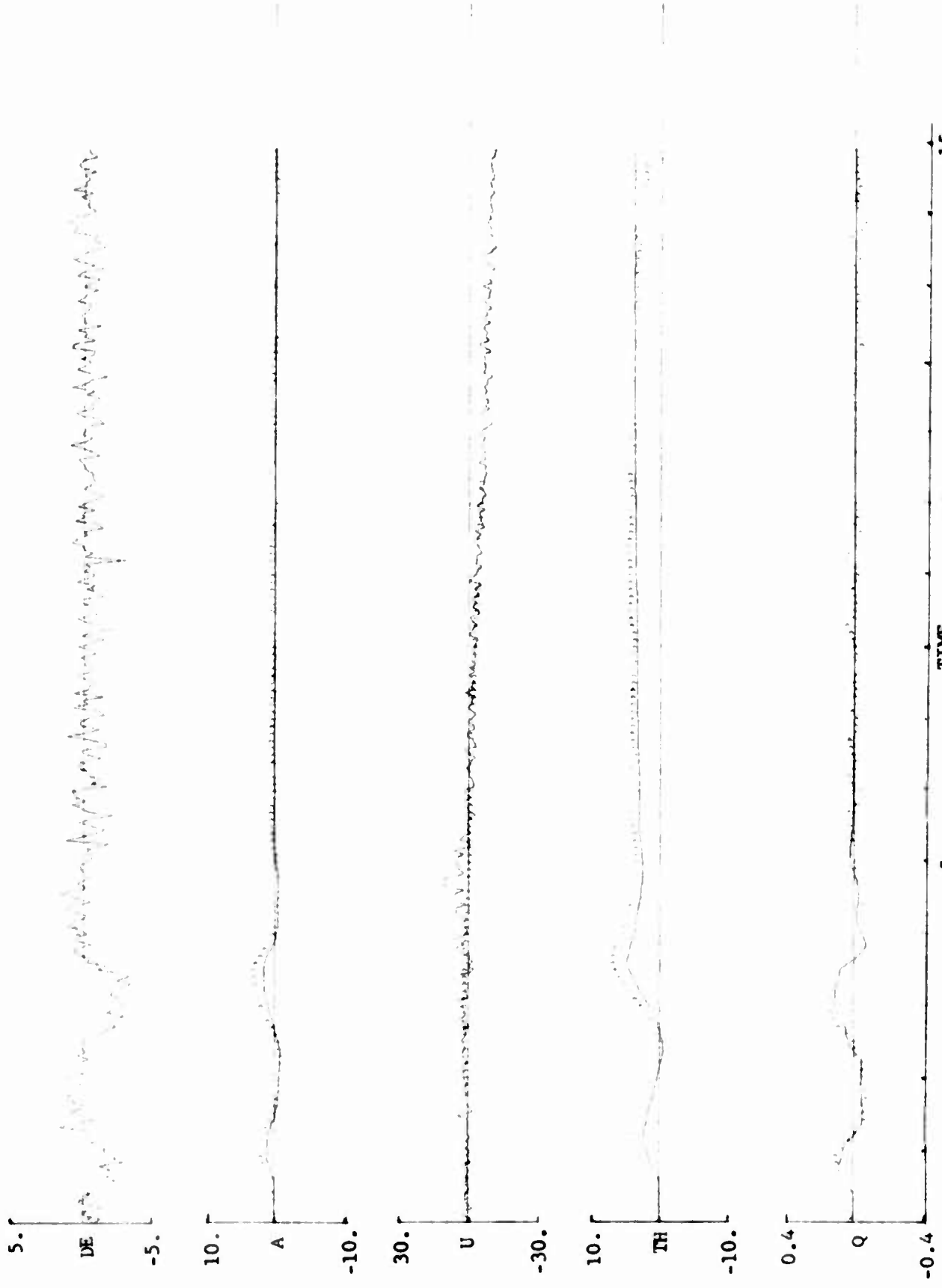

FIGURE 19. TIME HISTORY COMPARISON DR14-1W3S2SH

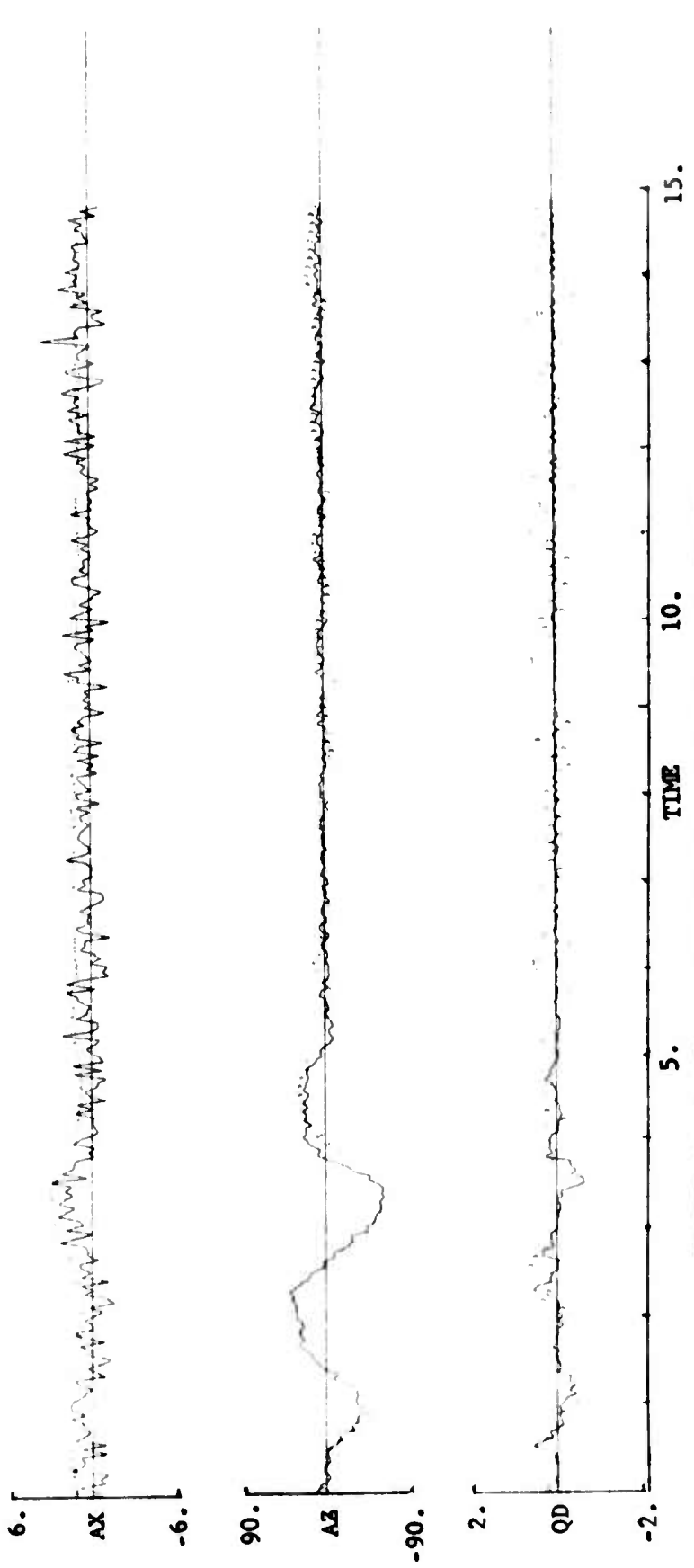

FIGURE 19 (CONT). TIME HISTORY COMPARISON DR14-1W3S2SH

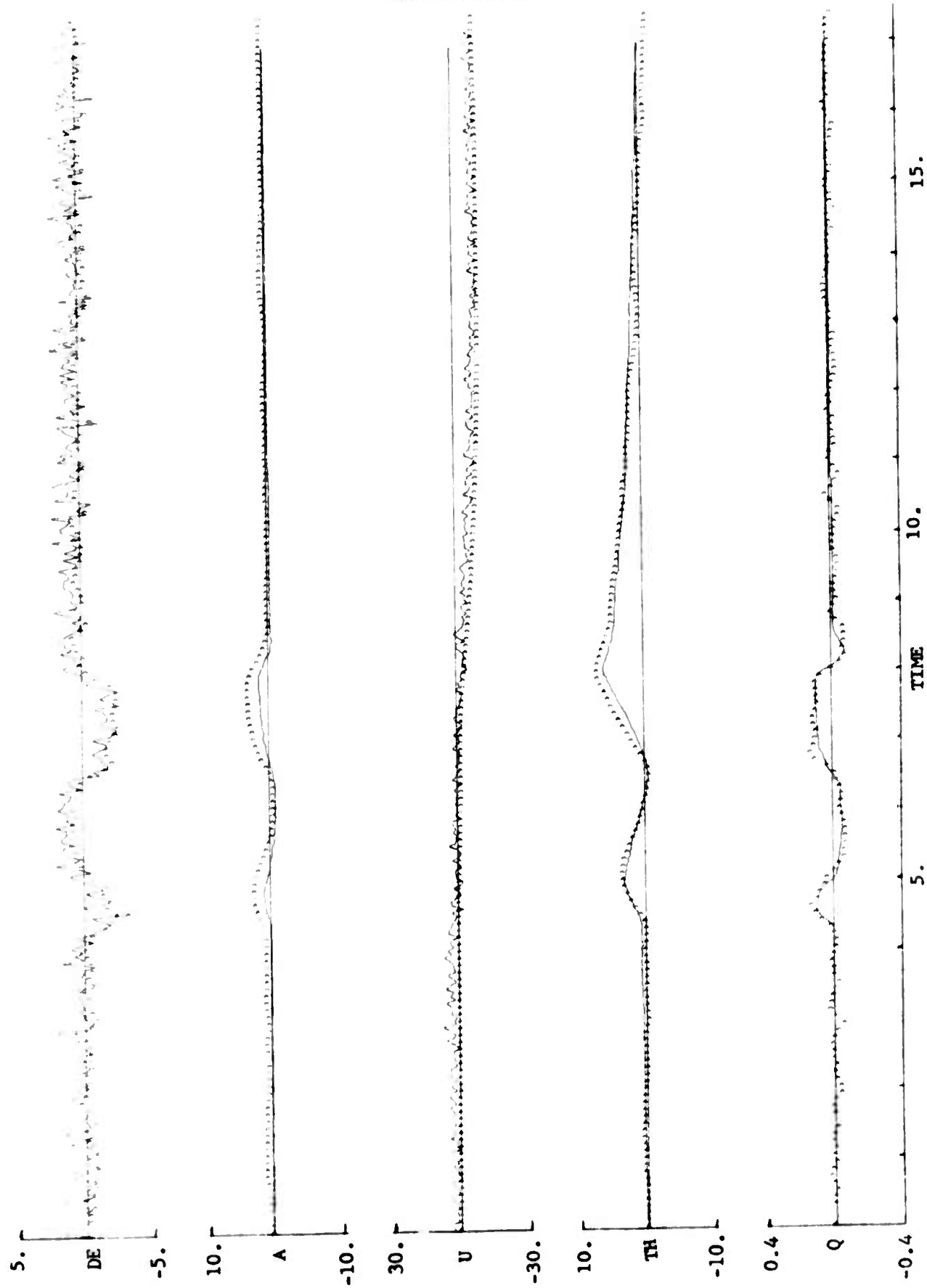

FIGURE 20. TIME HISTORY COMPARISON DR13-1W2S2

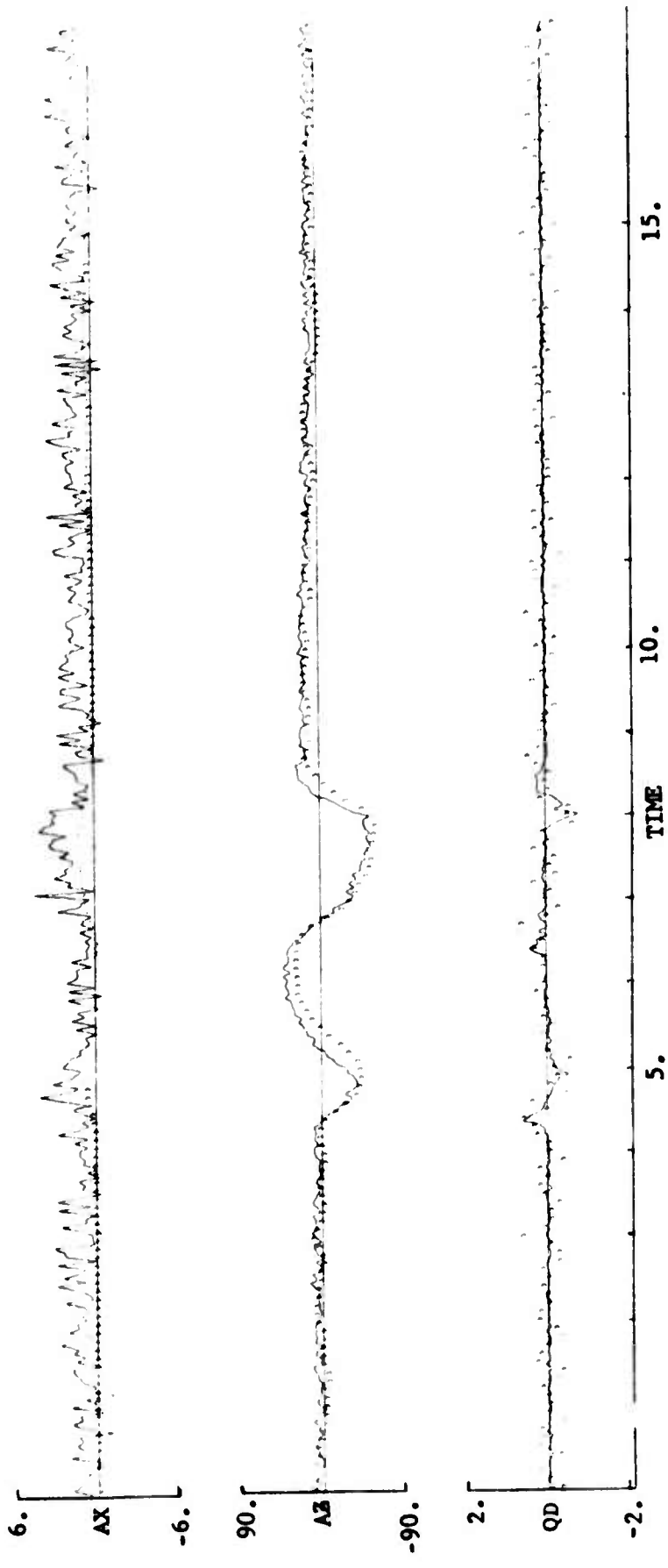

FIGURE 20 (CONT). TIME HISTORY COMPARISON DR13-1W2S2

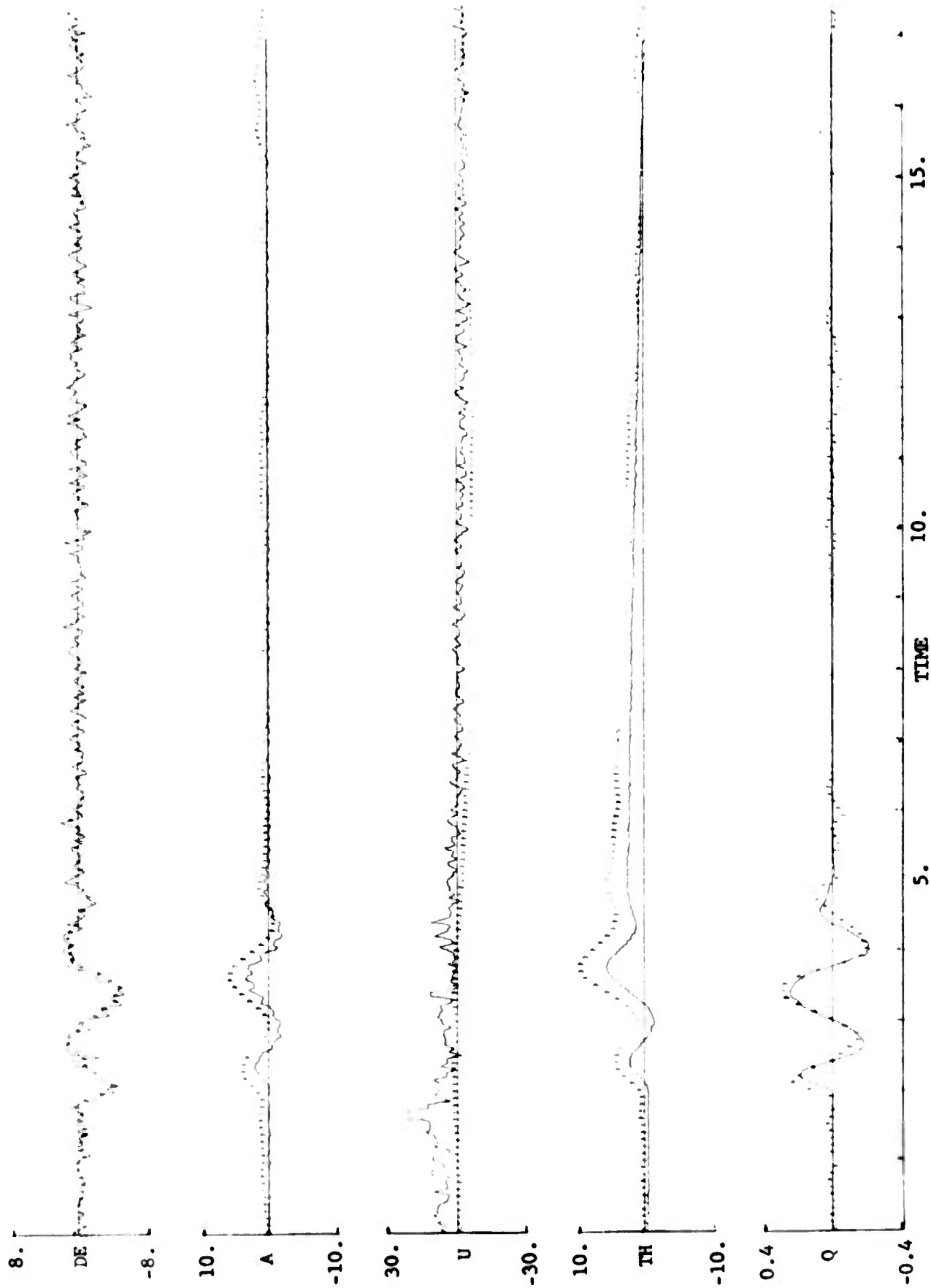

FIGURE 21. TIME HISTORY COMPARISON DR18-1W3S2

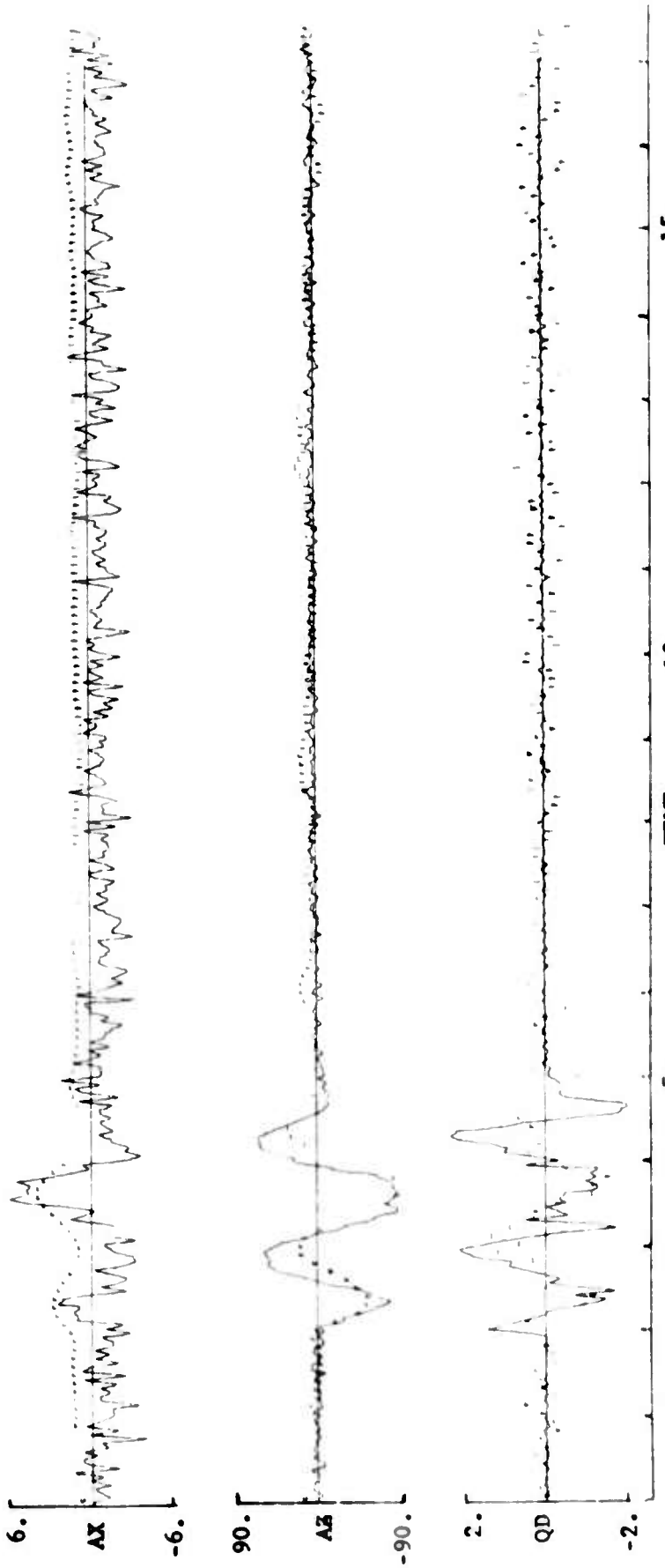

FIGURE 21 (CONT). TIME HISTORY COMPARISON DR18-1W3S2

DATA RUN 11

Figure 22 is a time history comparison for data run 11. Note that even with two iterations of smoothing, the elevator noise spikes cause considerable model response which is not present in the flight data. Figure 23 is a similar comparison for data run 11 with elevator set to zero following the significant input. Once again the angle of attack, pitch angle, and normal acceleration model responses overshoot the flight data in the time immediately following the input. The identification attempts not including elevator zeroing were not considered "final", and the results were not used. The time history comparison plots were shown to illustrate the severity of the elevator noise problem.

Unfortunately, a plot of the 70 second identification processing of data run 11 was not available due to computer malfunction. Airspeed, the quantity of particular interest, varied to -25 ft/sec and returned to approximately the original trim value during the data run. The stability derivative results (with all but the speed derivatives held at the values obtained in DR11-1W2S2DEZ) are shown in Table XVI.

DATA RUN 12

The pilot input for this data run was insufficient to cause motions large enough to permit identification of the stability derivatives principally involved in the short period motion. The intent of the input was the generation of phugoid motions, in which it succeeded. An 87.5 second record length segment of data run 12 contained 1½ cycles of phugoid motions, including velocity variations between +41 ft/sec and -30 ft/sec.

Once again, a plot of the time history comparison was unavailable, but the stability derivative results are shown in Table XVI. Start-up values for DR12-U5W3S2DEZ were not the usual a priori values, but the final results of DR11-U4W2S2DEZ.

STABILITY DERIVATIVE RESULTS

The variation in identified stability derivatives from run-to-run, and with respect to their a priori values, was similar to flight condition #1 with certain exceptions. As shown in Table XVI, results for X_α were somewhat more consistent, but still covered a wide range. Both $(C_L)_{trim}$ and C_{D_α} would be expected to be quite small for flight condition #2, and any measurement of the differences between them could certainly be subject to considerable error. The a priori value, which is larger in magnitude than any identified C_{D_α} and opposite in sign to all of the identified X_α results, could also be subject to error for the same reason. Calculation of the a priori value required the measurement of the slope of a very shallow C_D vs. α curve.

The results for M_{δ_e} were remarkably consistent. This phenomenom may indicate that the M_{δ_e} identification problems were unique to flight condition

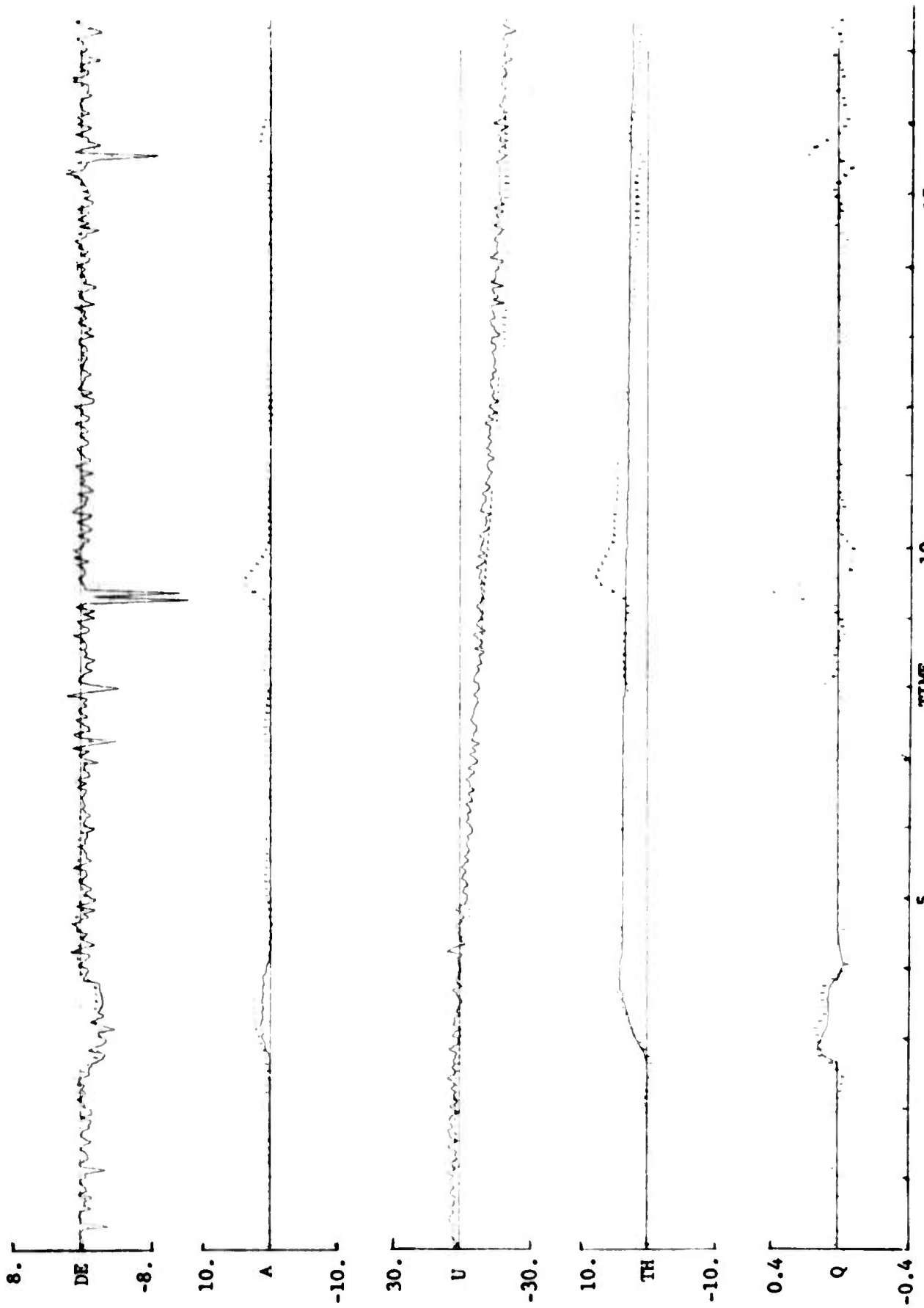

FIGURE 22. TIME HISTORY COMPARISON DR11-1W2S2

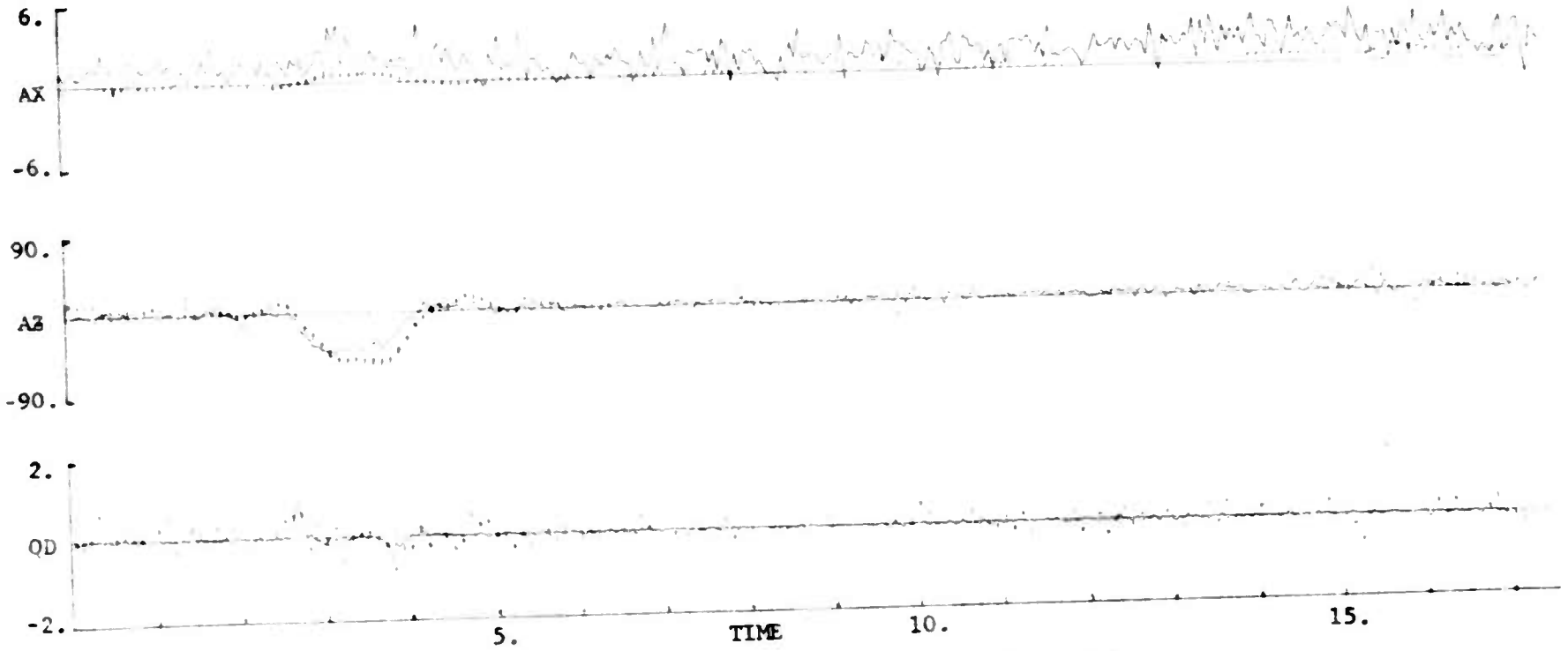

FIGURE 22 (CONT). TIME HISTORY COMPARISON DR11-1W2S2

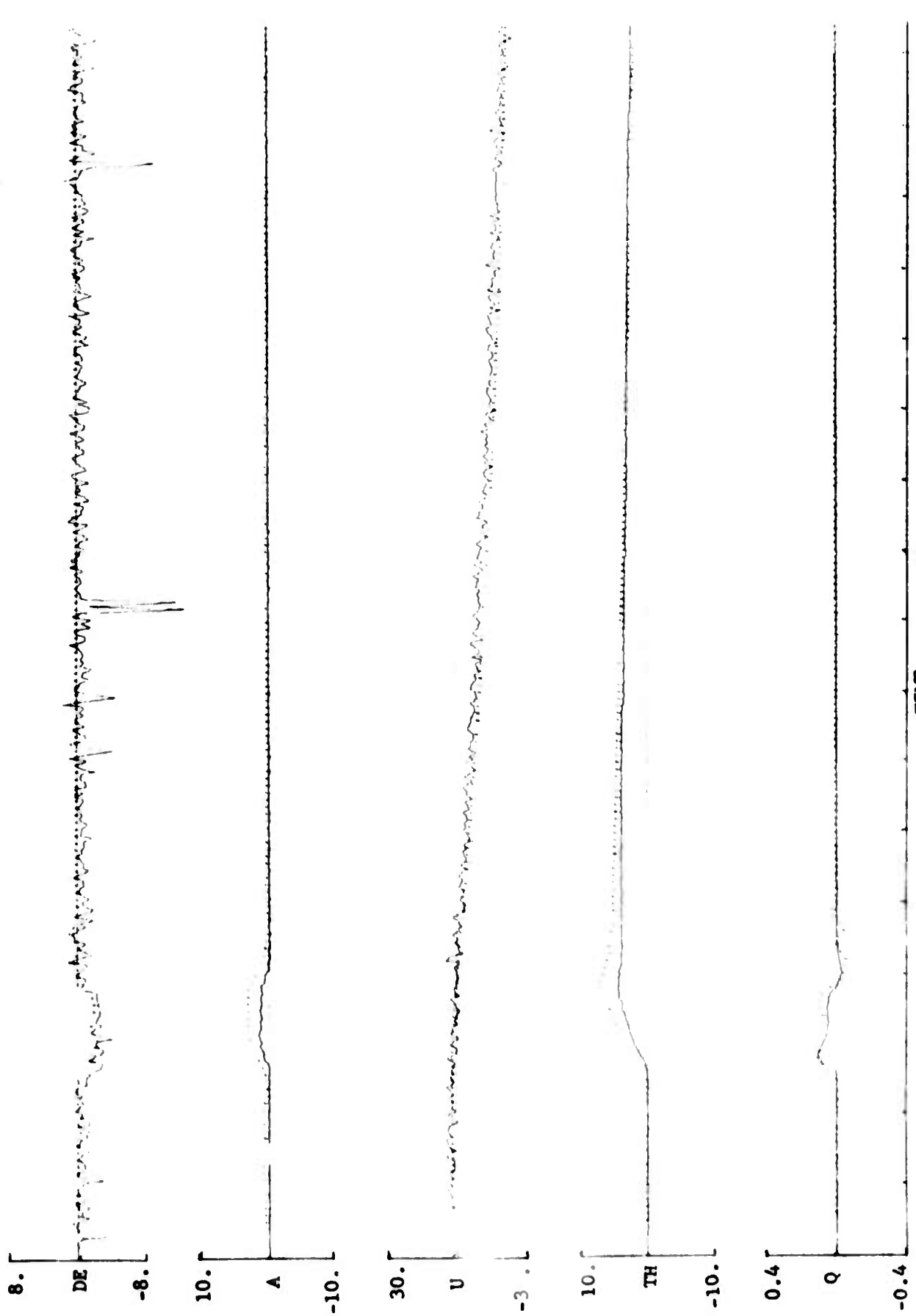

FIGURE 23. TIME HISTORY COMPARISON DR11-1W2S2DEZ

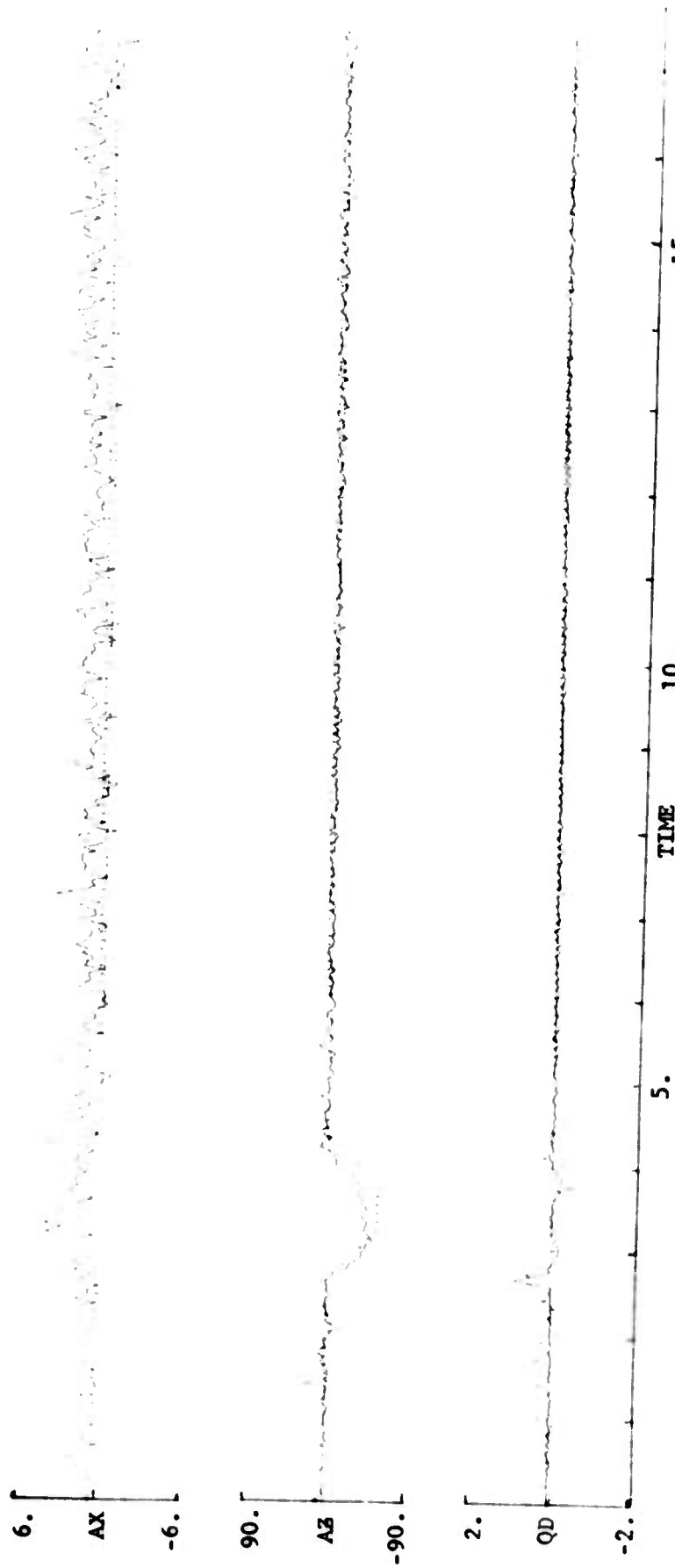

FIGURE 23 (CONT). TIME HISTORY COMPARISON DR11-1W2S2DEZ

#1, or just the opposite could be true if the algorithm were in fact simply retaining the a priori value due to a lack of sufficient information.

The M_q identification results are rather consistent, but quite different from the a priori value, the latter only having about half the magnitude of the former.

C O N C L U S I O N S

GENERAL

1. A modified Newton-Raphson parameter identification technique was acquired. This technique was shown to extract nearly perfect sets of stability derivatives from computer-generated data.

2. Carefully documented sets of flight data have been collected and provided to several contractors and agencies for the purpose of parameter identification. These data are especially suitable for parameter identification in the sense of the completeness of the measurements and the variety of selected pilot inputs. However, the signal-to-noise ratios for many of the measured quantities are not high enough for the data to be suitable as a test case for unproven identification techniques or for automatic identification without human involvement. The most serious problem is the high noise level on the control input measurement.

3. The measurement and recording systems currently available at NAVAIRDEVCEN for the acquisition of flight data for parameter identification are barely adequate for the purpose.

4. A great deal of valuable experience has been gained, and expertise developed at NAVAIRDEVCEN, in the acquisition of flight data for parameter identification purposes and in the use of parameter identification techniques.

5. No significant, consistent trends in results were observed as a function of pilot input type. Without any type of quantitative indication of identification accuracy, it is not possible to reach any conclusions from the current analysis concerning the effect of input type on identification performance.

6. Measurement of pitch angular acceleration directly with a Statham angular accelometer is a far superior method to the calculation of pitch acceleration based on nose and tail normal acceleration measurements.

FLIGHT CONDITION #1

1. Due to problems with the performance of the airspeed transducers, filtering of the airspeed measurement was necessary.

2. Proper use of the weighting matrix in the identification program, causing the weighted contributions to the fit error by the various time history matches to be equal, was essential to the performance of the identification technique.

3. Setting the value of the control input to zero following the significant pilot control input has a significant effect on the identified results, but it is not certain that this technique produces valid results, since information is destroyed as well as noise.

4. The algorithm would not converge unless the a priori stability derivatives were reasonable estimates. In the absence of sufficient information in the time histories, the identified results are heavily dependent upon the a priori values.

5. Only one data run (#3) was sufficiently long to permit a reasonable attempt at identification of the speed derivatives. Unfortunately, these data included significant atmospheric turbulence, which was not included in the model and therefore must have had an adverse effect on the identification process.

6. Based on identification results, the best estimate of X_u is -0.046, which agrees with the a priori value.

7. The stability derivative X_α was not consistently identifiable. Reduction of results to C_{D_α} still does not reveal any single value or function of $(C_L)_{trim}$. All identified C_{D_α} values were substantially smaller than the a priori value.

8. The best estimate of Z_u is -0.39, while the a priori value was -0.27.

9. Based on best results from data run segments of 17.5 seconds or less, the mean estimate for Z_α was -240.3 (compared to an a priori value of -233.8) and the standard deviation among the six numbers was 38.1.

10. The best estimate of M_u is -0.004, compared to the a priori value of zero.

11. The mean estimate, based on appropriate results, for M_α was -5.11, exactly identical to the a priori value, with a standard deviation of 0.34.

12. For M_q, the mean estimate was -1.32 and the standard deviation was 0.1. The a priori value of M_q was -1.42.

13. The mean estimate of Z_{δ_e} was -22.8 and the standard deviation was 1.81. The a priori value was -24.

14. The mean estimate of M_{δ_e} was -8.22, with a standard deviation of 0.74. The a priori estimate was -9.68. Although there was less scatter in the M_{δ_e} estimates than, for instance, Z_α estimates, the large discrepancy between the mean estimate and the a priori value was a source of concern. Reduction of the results to the nondimensional form $C_{m_{\delta_e}}$, however, led to an increase in the consistency of the identified results and an increase in the difference between the mean estimate and the a priori value.

15. The time history matches were generally good. The most serious matching problems occurred in the angle of attack time histories.

FLIGHT CONDITION #2

1. The conclusions reached for flight condition #1 concerning airspeed signal filtering, use of weighting matrix, and zeroing of control input signal are also applicable to flight condition #2.

2. The signal to noise ratio in the elevator signal was so low that a smoothing process was required before the elevator signal could reasonably be used in the identification program.

3. A priori value of X_u was -0.016. Only two estimates were obtained, -0.038 and -0.099, and insufficient agreement exists for selection of a best estimate.

4. A priori value of Z_u was -0.122. Estimates were -0.011 and -0.233, again insufficient for selection of a reasonable estimate.

5. Estimates of M_u were 0.0016 and 0.0018, which agree very well with an a priori value of 0.0017.

6. The mean estimate of X_α was 20.5, with a standard deviation of 9.97 (49% of the mean), indicating that little confidence should be placed in this estimate. The a priori value of -36.9 is in strong disagreement with the identified results.

7. The mean estimate of Z_α was -1371.6, in contrast with an a priori value of -1669.2. This discrepancy seems large for a derivative which should be easily identifiable. The standard deviation among the six appropriate estimates of Z_α was 170.4 (12% of the mean).

8. The mean estimate of M_α was -22.4, which agrees very well with the a priori value of -22.5. The standard deviation was less than 2% of the mean, indicating very consistent identification.

9. The mean estimate of M_q was -7.33, and the standard deviation of the run-to-run values was 0.67, or 9% of the mean, indicating fairly consistent results. Yet the a priori value was only -3.39 and would seem to be seriously in error.

10. The mean estimate of Z_{δ_e} was -134.5, in contrast to the a priori value of -121.3. The standard deviation was 6.8 (5% of the mean).

11. The mean estimate of M_{δ_e} was -49.3 and the standard deviation was only 0.6, or about 1%. This remarkably consistent set of identified results is in reasonable agreement with the a priori value of -52.1.

12. The time history matches were only fair. A particular pattern of excessive amplitude in the model response for angle of attack, pitch angle, and normal acceleration was obtained several times.

REFERENCES

(a) Proceedings of the Symposium on Parameter Estimation Techniques and Applications in Aircraft Flight Testing; NASA TN D7647; Apr 1974

(b) NAVMAT INSTRUCTION 5450.27; 27 Jun 1972

(c) Iliff, K. W.; Identification and Stochastic Control with Application to Flight Control in Turbulence; PhD Dissertation, University of California, Los Angeles; 1973

(d) Mehra, R. K., Stepner, D. E., and Tyler, J. S.; A Generalized Method for the Identification of Aircraft Stability and Control Derivatives from Flight Test Data; Proceedings of the 1972 Joint Automatic Control Conference, Aug 1972

(e) Chen, R. T. N., Eulrich, B. J., and Lebacqz, J. V.; Development of Advanced Techniques for the Identification of V/STOL Aircraft Stability and Control Parameters; Cornell Aeronautical Laboratory; Rept. No. BM-2820-F-1; Aug 1971

(f) Anon.; Estimated Flying Qualities for T-2B Trainer Airplane; North American Aviation, Columbus Division; Report NA64H-846; 1 Dec 1964

(g) Levine, CAPT (USMC) D., and von Husen, R.; Flying Qualities and Performance Evaluation of the T-2B Airplane; Naval Air Test Center Rept. FT-56R-68; 15 Aug 1968

(h) Anon.; Preliminary Supplemental Flight Manual, Company Model T2J-2 Prototype Aircraft; North American Aviation, Columbus Division; Rept. No. 62H-492; 30 Aug 1962

(i) North American Rockwell Corporation (Columbus Division) letter 68CL 14097, 10 Jan 1969

(j) Rediess, H. A.; An Overview of Parameter Estimation Techniques and Applications in Aircraft Flight Testing; Symposium on Parameter Estimation Techniques; NASA Flight Research Center; 24 Apr 1973

(k) Chen, R. T. N.; Input Design for Parameter Identification - Part I: A New Formulation and a Practical Solution; Flight Research Memo #497; CALSPAN Corp.; 14 Nov 1973

(l) Mehra, R. K.; Optimal Inputs for Linear System Identification; 1972 Joint Automatic Control Conference; Stanford, California; 16-18 Aug 1972

(m) Burton, R. A., and May, W. D.; Development of Digital Airframe Parameter Identification Technology; NAVAIRTESTCEN Rept. FT-77R-73; 21 Jan 1974

(n) McRuer, D., Ashkenas, I., and Graham, D.; Aircraft Dynamics and Automatic Control; Systems Technology, Inc.; Aug 1968

(o) Anon.; Estimated Aerodynamic Characteristics for Design of the T2J-1 Airplane; North American Aviation, Columbus Division; Rept. No. NA57H-580; 23 Jan 1958

(p) Iliff, K. W., and Taylor, L. W. Jr.; Determination of Stability Derivatives from Flight Data Using a Newton-Raphson Minimization Technique; NASA TN D-6579; Mar 1972

(q) Taylor, L. W. Jr., and Iliff, K. W. Systems Identification Using a Modified Newton-Raphson Method - A FORTRAN Program; NASA TN D-6734; May 1972

(r) Taylor, L. W. Jr.; Errata Sheet for Program NEWTON; private communication

(s) Harbaugh, S.; Suggested Changes to Program NEWTON Based on McDonnell-Douglas Experience; private communication

(t) Schuetz, A. J., and Bailey, D. B.; Low Speed Wind Tunnel Investigation of a .09-Scale Navy Model T-2C Subsonic Jet Trainer Aircraft From -8 to +83 Degrees Angle of Attack; NAVAIRDEVCEN Rept. No. NADC-73259-30, Dec 1973

APPENDIX A

LISTING OF PROGRAM MASSAGE

```
      PROGRAM MASSAGE (INPUT,OUTPUT,TAPE1,TAPE2,TAPE3,PUNCH)
      COMMON THOUR,TMIN,TSEC,DATA(30),IFILE,IREC,IFRAME,IPAR,INDAT(240)
C*****************************************************************************
      DATA ICOUNT,ISTRT/2,0/
C*****************************************************************************
      READ 40,CG
      PRINT 40,CG
      PRINT 140
      READ 1000,IFILER,IRECR,IFRAMER,IFILEE,IRECE,IFRAMEE
 1000 FORMAT(6I5)
      X1=(CG-37.)/12
      X2=(CG-34.)/12
      X3=(CG-207.)/12
      X4=(CG-366.5)/12
      X5=(CG-249.)/12
      X6=X5
      X7=(CG-203.)/12
      X8=(CG-56.)/12
      X9=X8
      X10=(CG-52.)/12
      X11=(CG-196.)/12
      X12=(CG-47.)/12
      X13=(CG-31.5)/12
      X14=(CG-204.)/12
      X15=X4
      Y1=-.33
      Y2=-.5
      Y3=-.083
      Y4=0
      Y5=-17.2
      Y6=+17.2
      Y7=0
      Y8=0
      Y9=0
      Y10=0
      Y11=0
       Y12=0
      Y13=-.5
      Y14=-.125
      Y15=0
```

Preceding page blank

```
      Z1=.917
      Z2=Z1
      Z3=1.75
      Z4=-.75
      Z5=-1.25
      Z6=Z5
      Z7=1.95
      Z8=-.42
       Z9=Z8
      Z10=-.21
      Z11=1.88
      Z12=-.29
      Z13=Z1
      Z14=1.54
      Z15=-.75
   4) FORMAT (F10.2)
  16) FORMAT(1X,12E10.4)
  24) FORMAT (F10.4,5X,I1,9X,I2,7X,I5,2X,8F10.4)
  23) FORMAT (5F10.4)
  16) FORMAT(1X,9E10.4)
  25) FORMAT (10F10.4)
 140) FORMAT (90HXXXXXXXXXXXXXXXXXXXXXXXXXXXXXXXXXXXXXXXXXXXXXXXXXXXXXXX
     1XXXXXXXXXXXXXXXXXXXXXXXXXXXXXXXXXXXX)
  22) CALL INPT
      IF(IFILE.EQ.IFILER.AND.IREC.EQ.IRECR.AND.IFRAME.EQ.IFRAMER)ISTRT=1
      IF(ISTRT)235,220
 235  IF(IFILE.EQ.IFILEE.AND.IREC.EQ.IRECE.AND.IFRAME.EQ.IFRAMEE)ISTRT=2
      T=TMIN*60.+TSEC
      TP=(ICOUNT-2)*.05
      VCON=(DATA(13)-DATA(12))/5.
      V25=(DATA(14)-DATA(12))/VCON
      IF(V25.LT.-.5.OR.V25.GT.5.5) GO TO 180
      V24=(DATA(15)-DATA(12))/VCON
      IF(V24.LT.-.5.OR.V24.GT.5.5) GO TO 180
      V1 =(DATA(16)-DATA(12))/VCON
      IF(V1 .LT.-.5.OR.V1 .GT.5.5) GO TO 180
      V14=(DATA(17)-DATA(12))/VCON
      IF(V14.LT.-.5.OR.V14.GT.5.5) GO TO 180
      V3 =(DATA(18)-DATA(12))/VCON
      IF(V3 .LT.-.5     .GT.5.5) GO TO 180
```

```
V2 =(DATA(19)-DATA(12))/VCON
IF(V2 .LT.-.5.OR.V2 .GT.5.5) GO TO 180
V4 =(DATA(20)-DATA(12))/VCON
IF(V4 .LT.-.5.OR.V4 .GT.5.5) GO TO 180
V13=(DATA(21)-DATA(12))/VCON
IF(V13.LT.-.5.OR.V13.GT.5.5) GO TO 180
V15=(DATA(22)-DATA(12))/VCON
IF(V15.LT.-.5.OR.V15.GT.5.5) GO TO 180
V17=(DATA(23)-DATA(12))/VCON
IF(V17.LT.-.5.OR.V17.GT.5.5) GO TO 180
V18=(DATA(24)-DATA(12))/VCON
IF(V18.LT.-.5.OR.V18.GT.5.5) GO TO 180
V16=(DATA(25)-DATA(12))/VCON
IF(V16.LT.-.5.OR.V16.GT.5.5) GO TO 180
V21=(DATA(26)-DATA(12))/VCON
IF(V21.LT.-.5.OR.V21.GT.5.5) GO TO 180
V23=(DATA(28)-DATA(12))/VCON
IF(V23.LT.-.5.OR.V23.GT.5.5) GO TO 180
V12=(DATA(29)-DATA(12))/VCON
IF(V12.LT.-.5.OR.V12.GT.5.5) GO TO 180
V19=((DATA(1)+13.)*.001323)+2.5
IF(V19.LT.-.5.OR.V19.GT.5.5) GO TO 180
V20=((DATA(2)+13.)*.001327)+2.5
IF(V20.LT.-.5.OR.V20.GT.5.5) GO TO 180
V27=((DATA(3)+21.)*.00133)+2.5
IF(V27.LT.-.5.OR.V27.GT.5.5) GO TO 180
V8=((DATA(4)+60.)*.00133)+2.5
IF(V8 .LT.-.5.OR.V8 .GT.5.5) GO TO 180
V11=((DATA(5)+29.)*.001342)+2.5
IF(V11.LT.-.5.OR.V11.GT.5.5) GO TO 180

V10=((DATA(6)+75.)*.001346)+2.5
IF(V10.LT.-.5.OR.V10.GT.5.5) GO TO 180
V9=((DATA(7)+10.)*.00133)+2.5
IF(V9 .LT.-.5.OR.V9 .GT.5.5) GO TO 180
V3=((DATA(8)+13.)*.001333)+2.5
IF(V3 .LT.-.5.OR.V3 .GT.5.5) GO TO 180
V7=((DATA(9)+23.)*.001334)+2.5
IF(V7 .LT.-.5.OR.V7 .GT.5.5) GO TO 180
V6=((DATA(10)+40.)*.001338)+2.5
IF(V6 .LT.-.5.OR.V6 .GT.5.5) GO TO 180
```

```
      V22=((DATA(11)+61.)*.01323)
      IF(V22.LT.-5.0R.V22.GT.5.)                    0 190
      P1= 13.6*(V1-2.45)
      P4=-47.8*(V4-2.45)
      P19=-4.183*(V19-2.5)
      P11= .151*(V11-2.5)
      P16= 500.0*(V16-2.4)
      ASC=100.0*V17
      K=2.0*V17
      RK=K
      ASF1=50.0*RK+10.0*V17
      ASF2=ASF1+50.
      ASF3=ASF1-50.
      DIF1=ABS(ASF1-ASC)
      DIF2=ABS(ASF2-ASC)
      DIF3=ABS(ASF3-ASC)
      IF (DIF1.LE.DIF2.AND.DIF1.LE.DIF3) P18=ASF1
      IF (DIF2.LE.DIF1.AND.DIF2.LE.DIF3) P18=ASF2
      IF (DIF3.LE.DIF2.AND.DIF3.LE.DIF1) P18=ASF3
      IF (IFILE-4) 190,200,200
  190 P5=+47.7*(V5-2.55)
      P12=+.138*(V12-2.5)
      P10=+.1446*(V10-2.48)
      GO TO 210
  200 P5=+50.11*(V5-2.55)
      P12=+.1446*(V12-2.48)
      P10=+.3216*(V10-2.53)
  210 P6=+49.5*(V6-2.55)
      P9=+6.65*(V9-2.5)
      P13=+13.05*(V13-2.5)
      P14=+12.08*(V14-2.5)
      P15=+13.8*(V15-2.5)
      P20=-4.1**(V20-2.55)
      P22=+7.***(V22-3.92)
      P23=+14.61*(V23-3.64)
      P7=-3.27*(V7-2.5)
      P8= 5.39*(V8-1.55)
      P21= 9.97*(V21-4.77)
      P2=-44.4*(V2-
      P3=-47.8*(V
```

NAVC-74181-30

```
      P24=-9.053*(V24-4.22)
      PD=(((P5-P6)*(X4-X2))-((P2-P4)*(X6-X5)))/(((Y5-Y6)*(X4-X2))-
     1      (X6-X5))
      QD=(P2-P4-PD*(Y2-Y4))/(X4-X2)
      RD=(P13-P15-PD*(Z15-Z13))/(X13-X15)

      QD2=P7
      P=P10
      Q=P11
      R=P12
      QA=P22
      PHI=P9
      TH=P8
      A=P19+4.0
       H=P16
      B=P20
      QR=P23
      QE=P21
      QB=P24
      IF (IFILE-3) 50,50,60
   50 V=(P18+4)*1.688
      GO TO 80
   60 V=(P18+8)*1.923
      GO TO 80
   70 V=(P18+6.5)*2.609
   80 A=A+1323.6*Q/V
      B=B+1340.8*R/V
      IF (IP) 30,20
   20 E=A/57.3
   30 AZ=(P3-((SIN(E)/COS(E))*(P1-Z1*QD+Y1*RD))+X3*QD-Y3*PD)/
     1      ((((SIN(E))**2)/COS(E))+COS(E))
      AX=(P1+AZ*SIN(E)-Z1*QD+Y1*RD)/COS(E)
      A=A-E*57.3
      AY=P14-X14*RD+Z14*PD
      IF (IP) 100,90
   90 QDT=QD
      QD2T=QD2
      QT=Q
      PDT=PD
      RDT=RD
      PT=P
```

```
      RT=R
      AYT=AY
      PHIT=PHI
      DAT=DA
      DRT=DR
      BT=B
      THT=TH
      AZT=AZ
      AXT=AX
      DET=DE
      VPRIME=0.
      VT=V
      DBT=DB
      HT=H
  100 DD2=DD2-QD2T
      DB=DB-DBT
      V=V-VT
      H=H-HT
      Q=Q-QT
      TH=TH-THT
      AZ=AZ-AZT
      AX=AX-AXT
      DE=DE-DET
      QD=QD-QDT
      B=B-BT
      PD=PD-PDT
      RD=RD-RDT
      P=P-PT
      R=R-RT
      AY=AY-AYT
      DA=DA-DAT
      PHI=PHI-PHIT
      DR=DR-DRT
      IF (TP) 180,170
  170 F=F*57.3
      PRINT 160, TP, F,THT,QT,QDT,QD2T,AZT,AXT,DET,DBT,VT,HT
  180 PRINT 160,TP,A,TH,Q,QD,QD2,AZ,AX,DE,DB,V,H
      IRN=2
      PUNCH 103,TP,A,TH,Q,QD2,AZ,AX,DE,V,H,IRN
  103 FORMAT(F6.2,9F8.3,I2)
```

```
      WRITE(3)      TP,A,TH,Q,QD,QD2,AZ,AX,DE,D3,V,H
C*****************************************************************************
      ICOUNT=ICOUNT+1
      IF(ISTRT.EQ.2) GOTO 130
C*****************************************************************************
      GO TO 220
  130  CONTINUE
C*****************************************************************************
C*****************************************************************************
      STOP
      END
```

```
      SUBROUTINE INPT
*
*     INPUT DATA FROM TAPE, FLOAT IT AND STORE IN COMMON.  INPT IS
*     CALLED ONCE FOR EACH FRAME OF DATA.
*     ENTRY  NONE
*     EXIT   THOUR.EQ.VALUE OF HOURS FIELD FLOATED
*            TMIN .EQ.VALUE OF MINUTES FLOATED
*            TSEC .EQ.VALUE OF SECONDS FIELD FLOATED
*            DATA .EQ.VALUE OF CHANNEL DATA FLOATED
*            IFILE.EQ.CURRENT FILE NO.
*            IREC .EQ.CURRENT RECORD NO. WITHIN FILE
*            IFRAME.EQ.CURRENT FRAME NO. WITHIN RECORD
*            IPAR .EQ. 0, IF NO PARITY ERR.
*            IPAR .EQ. 1, IF PARITY ERR
*     USES   INDAT
*     CALLS  MXRBYT
*
*
      COMMON THOUR,TMIN,TSEC,DATA(30),IFILE,IREC,IFRAME,IPAR,INDAT(240)
      DATA IFLG/1/
*
*     BRANCH  1 - FIRST TIME ENTERED
*             2 - TAPE READ REQUIRED
*             3 - FRAME ALREADY IN CORE
*
      GO TO (90,40,80),IFLG
*
*     HERE FOR FIRST TIME
*
90    NOFL=6
      IFILE=1
      IREC=0
      IFRAME=0
      IFLG=2
*
*     HERE IF TAPE READ NEEDED
*
40    BUFFER IN(1,1)(INDAT(1),INDAT(240))
      IF(UNIT(1))10,20,30
*
```

```
*       HERE FOR TAPE READ COMPLETED
*
10      IPAR=0
50      IREC=IREC+1
        IFRAME=0
        IFLG=3
*
*       HERE IF FRAME ALREADY IN CORE
*
90      IFRAME=IFRAME+1
        NPOS=(IFRAME-1)*7
*
*       GET TIME VALUES
*
        NDAT=INDAT(NPOS+1)

        THOUR=10*MXRBYT(33,2,NDAT)
       1          +MXRBYT(31,4,NDAT)
        TMIN=10*MXRBYT(27,3,NDAT)
       1         +MXRBYT(24,4,NDAT)
         TEM=10000*MXRBYT(20,4,NDAT)
       1      +1000 *MXRBYT(16,4,NDAT)
       2       +100*MXRBYT(12,4,NDAT)
       3        +10*MXRBYT(8,4,NDAT)
       4           +MXRBYT(4,4,NDAT)
        TSEC= TEM/1000.
*
*       GET CHANNEL DATA
*
        DO 60 I=1,6
        DO 70 J=1,5
        ITEM            =MXRBYT(60-(J-1)*12,12,INDAT(NPOS+I+1))
        IF (ITEM.GE.2048) ITEM=-(ITEM-2048)
        DATA((I-1)*5+J)=ITEM
70      CONTINUE
60      CONTINUE
*
*       SET IFLG FOR NEXT ENTRY.
*
        IF(IFRAME.EQ.34) IFLG=2
        RETURN
```

```
*
*       HERE WHEN EOF FOUND
*
20      IFILE=IFILE+1
        IF(IFILE.EQ.NOFL+1) STOP1
        IREC=0
        GO TO 40
*
*       HERE WHEN PARITY ERR. FOUND
*
30      PRINT 100,IFILE ,IREC,IFRAME
100     FORMAT(1X,*FILE*,I3,4X,*RECORD*,I10,4X,*FRAME*,I3,*CONTAINS PARITY
      1 ERROR*)
        IPAR=1
        GO TO 50
        END
```

APPENDIX B

LISTING OF PROGRAM NEWTON

```
      PROGRAM NEWTON (INPUT,OUTPUT,TAPE1,TAPE2)
C.....SYSTEM IDENTIFICATION PROGRAM....STABILITY DERIVATIVES FROM FLIGHT DATA..
      DIMENSION Z(7,400), U(5,400), DZ1(12),DZN(12),IP(60,4), AP(60,5)
     1,EE(12), DUD(68), APHI(68), C1(16), X2(16), XJ(16), U1(12),
     2PHI(68), D1(12), A(68), B(36), XJI(733), SUM(733),DC(30),DUM(733)
     3, F(60), G(60),  SZ(25), SJ(25), Y(15),D1S(68),YN(16)
  111 FORMAT(7X, I3,3I10,5F10.4)
  700 FORMAT(5F10.4)
  777 FORMAT(7I10)
 1001 FORMAT(11H THERE ARE ,I4,14H DATA POINTS, ,I2,38H ITERATIONS AND T
     1HE TIME INCREMENT IS ,F5.4,8H SECONDS)
 1002 FORMAT(91H      PARAMETER  GROUP      ROW      COLUMN APRIORI DEVIA
     1TION    SCALE      ANSWER  DEVIATION)
 1003 FORMAT(6H JKM =,I3,7H, NPM =,I3)
 1004 FORMAT(30H THE FIRST COLUMN IS TIME. THE NEXT ,I2,41H COLUMNS ARE
     1CONTROL VARIABLES.  THE NEXT ,I2,32H COLUMNS ARE RESPONSE VARIABLE
     2S.)
 1005 FORMAT(31H THE VALUE OF THE FIT ERROR IS ,E12.5,26H FOR THE ITERAT
     1ION NUMBER ,I3)
 1006 FORMAT(39H THE SCALING PARAMETER, FINK'S VALUE IS,F10.4)
 1010 FORMAT(F8.2,10E12.4)
 1200 FORMAT(* FINAL TIME = *,F10.4)
CIIIIIIIIIIIIIIIIIIIIIIIIIIIIIIIIIIII.....INPUT DATA (START).............I
    3 READ 777, ITR,NSKIP,NINTVL,NREAD
      READ 700, HH, FINK,UZERO
      NN=NREAD/NINTVL
      HH=HH*NINTVL
      PRINT 1001, NN, ITR, HH
      PRINT 1006, FINK
       ENN=NN
      CALL LOAD(4, A, B, D1S, F)
      CALL LOAD(3, G, SZ, SU, SU)
      CALL SPIT(A, 1HA)
      CALL SPIT(B, 1HB)
      CALL SPIT(D1S, 3HD1S)
      CALL SPIT(F, 1HF)
      CALL SPIT(G, 1HG)
      CALL SPIT(SZ, 2HSZ)
      CALL SPIT(SU, 2HSU)
      NNM1 = NN - 1
```

```
      MU = B(2) + .01
      MX = A(2) + .01
      MZ = D1S(2) + .01
      MXP1 = MX + 1
      IB = D1S(1) + .01
      IF(IB-1)78,79,78
   78 CALL SET(D1, 1,MZ)
      IJ = 4 - MZ
      DO 80 I = 1,MZ
      IJ = IJ + MZ + 1
   80 D1(I+4) = D1S(IJ)
      GO TO 81
   79 CALL MAKE(D1, D1S)
   81 CALL SPIT(D1, 2HD1)
      AJ = 1.0/ENN

      CALL ADD(AJ, D1, 0., D1, D1)
      CALL ADD(AJ, D1S, 0., D1S, D1S)
      PRINT 1002
      JKM = 1
      DO 5 NP = 1,50
      READ 111,(IP(NP,I), I = 1,4),(AP(NP,J), J = 1,3)
      PRINT111,(IP(NP,I), I = 1,4),(AP(NP,J), J = 1,3)
      AP(NP,4) = AP(NP,1)
      AP(NP,5) = 0.
      IF(IP(NP,1))6,5,5
    5 JKM = JKM + IP(NP,1)
    6 CONTINUE
      JKMM1 = JKM - 1
      NPM = NP - 1
      PRINT 1003, JKM, NPM
      II = - HH
      PRINT 1004, MU, MZ
      DO 62 I=1,NSKIP
      READ(1)(DUD(J),J=1,12)
      IF(IOCHEC(1))62,62
   62 CONTINUE
      ICOUNT=NINTVL
      I=0
  500 IF(I.GE.NN)GO TO 501
      IF(ICOUNT-NINTVL)65,66
```

```
   65 ICOUNT=ICOUNT+1
      READ(1)(UUU(J),J=1,12)
      IF(IOCHEC(1))500,500
   66 ICOUNT=1
      I=I+1
      READ(1) TIME,Z(2,I),Z(4,I),Z(3,I),UU,Z(7,I),Z(6,I),Z(5,I),U(1,I),
     C          U(2,I),Z(1,I),H
      IF(IOCHEC(1)) 503,502
  503 IF(I.LT.3) STOP 77
      DO 504 J=1,7
  504 Z(J,I)=Z(J,I-1)*2.-Z(J,I-2)
  502 U(1,I)=U(1,I)/57.296
      U(2,I)=U(2,I)/57.296
      U(3,I)=1.
      Z(2,I)=Z(2,I)/57.296
      Z(4,I)=Z(4,I)/57.296
      Z(5,I)=Z(5,I)-32.174*Z(4,I)
      Z(6,I)=Z(6,I)/(UZERO+Z(1,I))+Z(3,I)
      Z(1,I)=Z(1,I)/UZERO
      Z(5,I)=Z(5,I)/UZERO
      TT = TT + HH
CCCCCCCCCCCCCCCCCCCCCCCCCCCCCCCCCCCC.....CONDITION INPUT DATA (START)...$
      DO 63 J = 1,MZ
   63 Z(J,I) = Z(J,I)*SZ(J+4)
      DO 64 J = 1,MU
   64 U(J,I) = U(J,I)*SU(J+4)
CCCCCCCCCCCCCCCCCCCCCCCCCCCCCCCCCCCC.....CONDITION INPUT DATA (END).....$
   48 PRINT1010,TT,(U(K,I), K = 1,4U),(Z(K,I), K = 1,MZ)
      GO TO 500
  501 PRINT 1200,TIME

CIIIIIIIIIIIIIIIIIIIIIIIIIIIIIIIIIIII.....INPUT DATA (END).............$
CLLLLLLLLLLLLLLLLLLLLLLLLLLLLLLLLLLL.....ITERATION LOOP (START).........$
      DO 12 LL=1,ITR
CSSSSSSSSSSSSSSSSSSSSSSSSSSSSSSSSSSS.....SET MATRICES (START)...........$
      CALL SET(U1, MU, 1)
      CALL SET(X1, MX, 1)
      CALL SET(XJ,MX,1)
      CALL SET(Y, MZ, 1)
      CALL SET(EE,1,MZ)
      CALL SET(DZ1,1,MZ)
```

```
      CALL SET(DZN,1,MZ)
      CALL SET(SUM, JKM,JKM)
      CALL SET(XJI, JKM, MZ)
CSSSSSSSSSSSSSSSSSSSSSSSSSSSSSSSSSSS.....SET MATRICES (END)..............$
CCCCCCCCCCCCCCCCCCCCCCCCCCCCCCCCCCCC.....COMPUTE STATE TRANSITION MATRIX.
      CALL EAT(A, HH, PHI, APHI, DUM, DUD)
      JK = 0
      DO 10 NP = 1,NPM
      IG = IP(NP,2)
      JJ = IP(NP,3)
      IF(IP(NP,1)-1)71,70,71
   70 JK = JK + 1
      II = (JK-1)*JKM + JK + 4
      SUM(II) = 1./AP(NP,2)**2
      IJ = JK*JKM + 4
      SUM(IJ) = (AP(NP,1) - AP(NP,4))/AP(NP,2)**2
   71 IF(IP(NP,2) - 3)10,16,16
   16 IF(IG-5)8,10,10
    8 JI = (JK-1)*MZ + 4 + IP(NP,3)
      XJI(JI) = AP(NP,3)
      IF(LL-1)10,55,10
   55 IF(IP(NP,2)-3)10,17,20
   17 DZ1(4+JJ) = AP(NP,4)*AP(NP,3)
      GO TO 10
   20 DZN(4+JJ) = AP(NP,4)*AP(NP,3)
   10 CONTINUE
      DO 51 I = 1,MU
   51 U1(I+4) = (U(I,1) + U(I,2))*.5
      DO 24 J = 1,MX
   24 X1(J+4) = Z(J,1) - DZ1(J+4) - DZN(J+4)
C111111111111111111111111111111111111.....COMPUTE INITIAL STATE(START)...$
      CALL MULT(PHI, X1, X2)
      CALL MULT(B, U1, DUM)
      CALL MULT(APHI, DUM, DUD)
      CALL ADD(1.0,X2,1.0,DUD,X2)
      DO 47 I = 1,MX
   47 Y(I+4) = X2(I+4) + DZN(I+4)
      TT = 0.
C111111111111111111111111111111111111.....COMPUTE INITIAL STATE(END).....$
CTTTTTTTTTTTTTTTTTTTTTTTTTTTTTTTTTTT.....TIME LOOP (START)..............$
```

```
      DO 41 I = 1,NNM1
      TT = TT + HH
      JK =0
CGGGGGGGGGGGGGGGGGGGGGGGGGGGGGGG.....COMPUTE GRADIENT (START)........$
      DO 4 NP = 1,NPM

      JK = JK + IP(NP,1)
      IG = IP(NP,2)
      IF(IG-4)82,4,82
   82 II = IP(NP,3)
      JJ = IP(NP,4)
      JI = (JK-1)*MZ+4
      IF(IP(NP,1))25,83,25
   25 DO 49 J = 1,MX
   49 XJ(J+4) = XJI(JI+J)
      CALL MULT(PHI, XJ, DUM)
      DO 29 J = 1,MX
   29 XJI(JI+J) = DUM(J+4)
      IF(MZ-MX)9,83,9
    9 CALL MULT(F, XJ, DUM)
      DO 13 J = MXP1, MZ
   13 XJI(JI + J ) = DUM(J-MX+4)
   83 IJ = II + 4 - MX
      IF(IG-1)4,26,34
   26 IF(LL-1)33,33,32
   32 DO 42 J = 1,MX
      IJ = IJ + MX
      XJ(J+4) =                   APHI(IJ)*(X1(JJ+4)+X2(JJ+4))*.5*AP(NP,3)
   42 XJI(JI+J) = XJI(JI+J)  + XJ(J+4)
      GO TO 23
   33 DO 43 J = 1,MX
      IJ = IJ + MX
      XJ(J+4) =                   APHI(IJ  )*(Z(JJ,I)+Z(JJ,I+1))*.5*AP(NP,3)
   43 XJI(JI+J) = XJI(JI+J)  + XJ(J+4)
   34 IF(IG-2) 23,35,23
   35 DO 45 J = 1,MX
      IJ = IJ + MX
      XJ(J+4) =                   APHI(IJ)*(U(JJ,I)+U(JJ,I+1))*.5*AP(NP,3)
   45 XJI(JI+J) = XJI(JI+J)  + XJ(J+4)
   23 IF(MZ-MX)7,4,7
    7 IF(IG-3)84,84,85
```

```
 64 CALL MULT(F,XJ,DUM)
    DO 14 J = MXP1,MZ
 14 XJI(JI+J) = DUM(J-MX+4) + XJI(JI+J)
 85 IF(IG -5)4,15,18
 15 XJI(JI + MX + II) = XJI(JI+MX+II) + X2(JJ+4)*AP(NP,3)
    GO TO 4
 18 IF(IG-5)4,28,4
 28 XJI(JI+MX+II) = XJI(JI+MX+II) + U(JJ,I+1)*AP(NP,3)
  4 CONTINUE
    DO 53 J = 1,MU
 53 U1(J+4) = U(J,I+1)
    IF(MZ-MX)11,27,11
 11 CONTINUE
    CALL MULT(F,X2, DUM)
    CALL MULT(G, U1, DUD)
    DO 54 J = MXP1,MZ
 54 Y(J+4) = DUM(J+4-MX) + DUD(J+4-MX) + DZN(J+4)
 27 JI = (JKM-1)*MZ + 4
    DO 52 J = 1,MZ
    XJI(JI+J) = Z(J,I+1) - Y(J+4)

 52 EE(J+4) = EE(J+4) + D1(J+4)*(JI(JI+J)**2
CGGGGGGGGGGGGGGGGGGGGGGGGGGGGGGGGGGGGG.....COMPUTE GRADIENT (END).....$
    IF(LL-ITR)68,67,68
 67 IF(I-1)59,61,59
 61 PRINT 1004, MU, MZ
 59 DO 69 J = 1,MZ
 69 Y(J+4) = Y(J+4)/SZ(J+4)
    PRINT 1010,TT,(U(J,I+1), J = 1,MU),(Y(J+4), J = 1,MZ)
    YN(1)=Y(5)*UZERO
    YN(2)=Y(6)*57.296
    YN(3)=Y(7)
    YN(4)=Y(8)*57.296
    WRITE(2)TT,YN(2),YN(1),YN(4),YN(3)
 68 IF(I-NNM1)72,41,72
 72 CALL MAKE(X1, X2)
    DO 30 J = 1,MU
 30 U1(J+4) = (U(J,I+1) + U(J,I+2))*.5
CSSSSSSSSSSSSSSSSSSSSSSSSSSSSSSSSSSSS.....COMPUTE STATE (START).....$
    CALL MULT(PHI, X1, X2)
    CALL MULT(B, U1, DUD)
```

```
      CALL MULT(APMI, DDD, DUM)
      CALL ADD(1.0,X2,1.0,DUM,X2)
      DO 2 J = 1,MX
    2 Y(J+4) = X2(J+4) + DZN(J+4)
CSSSSSSSSSSSSSSSSSSSSSSSSSSSSSSSSSSSS.....COMPUTE STATE (END).............$
CEEEEEEEEEEEEEEEEEEEEEEEEEEEEEEEEEEEE.....SET UP SYSTEM OF EQUATIONS.....$
   41 CALL TRICK(XJI, D1S, SUM)
CTTTTTTTTTTTTTTTTTTTTTTTTTTTTTTTTTTTT.....TIME LOOP (END)................$
      LLM1 = LL-1
      PRINT 1005, SUM(JKM*JKM+4),LLM1
      CALL SPIT(EE,4HEE*D)
      DO 60 I = 1,MZ
   60 EE(I+4) = SQRT(EE(I+4)/(D1(I+4)*ENN))/SZ(I+4)
      CALL SPIT(EE, 3HRMS)
CDDDDDDDDDDDDDDDDDDDDDDDDDDDDDDDDDDDD)...MULT DIAG BY 1.0005 TO CONDITION.$
      CALL SET(DUM, 1, JKM)
      DO 1 J = 1,JKM
      JJ = JKM*J + 4
      IJ = (J-1)*JKM + J + 4
      DUM(J+4) = SUM(JJ)
    1 SUM(IJ) = SUM(IJ)*1.0005
      CALL SPIT(DUM, 4HGRAD)
  531 FORMAT(55H WOULD YOU BELIEVE.....                                    )
      PRINT 531
CSSSSSSSSSSSSSSSSSSSSSSSSSSSSSSSSSSSS.....SOLVE SYSTEM OF EQUATIONS......$
      CALL ADD(FINK, SUM, 0., SUM, SUM)
      IF(LL-ITR)74,73,74
   73 CALL MINR(SUM, JKM, JKM, XJI)
      CALL SET(DDD, JKMM1, 1)
      JJ = 4
      DO 75 J = 1,JKMM1
      JJ = JJ + JKM
   75 DDD(J+4) = SUM(JJ)
   74 CALL SOLVE(SUM, DC)
      CALL SPIT(DC, 2HDC)

CDDDDDDDDDDDDDDDDDDDDDDDDDDDDDDDDDDJJ.....UPDATE COEFFICIENTS (START).....$
      JK = 0
      DO 12 NP = 1,NPM
      IG = IP(NP,2)
      II = IP(NP,3)
```

```
      JJ = IP(NP,4)
      JK = JK + IP(NP,1)
      IF(JK)12,12,50
   50 IF(IP(NP,1)-1)57,56,57
   56 AP(NP,4) = AP(NP,4) + DC(JK+4)*AP(NP,3)
   57 IF(IG-1)12,19,21
   19 IJ = (II-1)*MX + JJ + 4
      A(IJ) = A(IJ) + DC(JK+4)*AP(NP,3)
      GO TO 12
   21 IF(IG-2)12,22,37
   22 IJ = (II-1)*MU + JJ + 4
      B(IJ) = B(IJ) + DC(JK+4)*AP(NP,3)
   37 IF(IG-3)12,36,38
   36 DZ1(II+4) = DZ1(II+4) + DC(JK+4)*AP(NP,3)
   38 IF(IG-4)12,39,31
   39 DZN(II+4) = DZN(II+4) + DC(JK+4)*AP(NP,3)
   31 IF(IG-5)12,40,44
   40 IJ = (II-1)*MX + JJ + 4
      F(IJ) = F(IJ) + DC(JK+4)*AP(NP,3)
   44 IF(IG-6)12,46,12
   46 IJ = (II-1)*MU + JJ + 4
      G(IJ) = G(IJ) + DC(JK+4)*AP(NP,3)
CUUUUUUUUUUUUUUUUUUUUUUUUUUUUUUUUUUUJJ.....UPDATE COEFFICIENTS (END).....$
   12 CONTINUE
CLLLLLLLLLLLLLLLLLLLLLLLLLLLLLLLLLLLLL.....ITERATION LOOP (END).....$
      CALL SPIT(A, 1HA)
      CALL SPIT(B, 1HB)
      CALL SPIT(DZ1, 3HDZ1)
      CALL SPIT(DZN, 3HDZN)
      CALL SPIT(F, 1HF)
      CALL SPIT(G, 1HG)
      CALL MAKE(DUM, XJI)
      CALL INVR(XJI, SUM)
      CALL MULT(SUM, DUM, XJI)
      CALL SPIT(XJI, 4HS-1S)
      CALL MULT(SUM, DUD, XJI)
      CALL SPIT(XJI, 5H DC" )
      PRINT 1002
      JK = 0
      DO 56 NP = 1,NPM
```

```
      IF(IP(NP,1)-1)58,77,58
   77 JK = JK + 1
      IJ = (JK-1)*JKMM1 + JK + 4
      AP(NP,5) = SQRT(SUM(IJ)/FINK)
   58 PRINT 111,(IP(NP,J), J = 1,4),(AP(NP,J), J = 1,5)
      STOP
      END
```

```
      SUBROUTINE ADD(P, A, Q, B, C)
C     VECTOR FORMAT
      DIMENSION A(1), B(1), C(1)
      N = A(3) + 4.01
      DO 1 I = 5,N
    1 C(I) = P*A(I) + Q*B(I)
      C(1) = A(1)
      C(2) = A(2)
      C(3) = A(3)
      C(4) = A(4)
      RETURN
      END
```

```
      SUBROUTINE EAT(A, T, PHI, APHI, A2, A3)
C     VECTOR FORMAT
      DIMENSION A(1), PHI(1), APHI(1), A2(1), A3(1)
  123 FORMAT(55H MATRIX IS NOT SQUARE FOR EAT, STUPID.....
      II = A(1) + .01
      JJ = A(2) + .01
      IF(II-JJ)4,3,4
    3 CALL SET(PHI, II, II)
      CALL SET(APHI, II, II)
      DO 1 I = 1,II
      IJ = (I-1)*II + I + 4
    1 PHI(IJ) = 1.0
      CALL MAKE(A2, PHI)
      G = 1.0
      DO 2 I = 1,6
      BB = I
      G = G*T/BB
      CALL ADD(1.0, APHI, G, A2, APHI)
      CALL MULT(A, A2, A3)
      CALL MAKE(A2, A3)
      CALL ADD(1., PHI, G, A2, PHI)
    2 CONTINUE
      GO TO 5
    4 PRINT 123
    5 RETURN
      END
```

```
      SUBROUTINE INVR(A, B)
C     VECTOR FORMAT, DIAGONAL ELEMENTS MUST BE NON-ZERO.
      DIMENSION A(1), B(1)
  101 FORMAT(E15.7)
      N = A(1) + .01
      CALL SET(B, N, N)
      DO 6 I = 1,N
      IJ = (I-1)*N + I + 4
    6 B(IJ) = 1.0
      DETA = 1.0
      DO 3 K = 1,N
      KP1 = K + 1
      KK = (K-1)*N + K + 4
      AKK1 = 1.0/A(KK)
      DETA = DETA*A(KK)
      DO 5 J = 1,N
      IJ = (K-1)*N + J + 4
    5 B(IJ) = B(IJ)*AKK1
      DO 1 J = K,N
      IJ = (K-1)*N + J + 4
    1 A(IJ) = A(IJ)*AKK1
      DO 2 KI = 1,N
      IF(K - KI)7,2,7
    7 KIK = (KI-1)*N + K + 4
      AKIK = A(KIK)
      DO 4 L = 1,N
      KL = (K-1)*N + L + 4
      KIL = (KI-1)*N + L + 4
      B(KIL) = B(KIL) - AKIK*B(KL)
    4 CONTINUE
      IF(K-N)8,9,8
    8 DO 10 L = KP1,N
      KL = (K-1)*N + L + 4
      KIL = (KI-1)*N + L + 4
      A(KIL) = A(KIL) - AKIK*A(KL)
   10 CONTINUE
    9 CONTINUE
    2 CONTINUE
    3 CONTINUE
      PRINT 101, DETA
      RETURN
      END
```

```
      SUBROUTINE LOAD(N, A, B, C, D)
C     VECTOR FORMAT
      DIMENSION A(1), B(1), C(1), D(1)
      CALL LODE(A)
      IF(M-1)8,8,2
    2 CALL LODE(B)
      IF(M-2)8,8,4
    4 CALL LODE(C)
      IF(M-3)8,8,6
    6 CALL LODE(D)
    8 RETURN
      END
```

```
      SUBROUTINE LODE(A)
C     VECTOR FORMAT
      DIMENSION A(1)
  700 FORMAT(7F10.3)
  444 FORMAT(7X,I3,7X,I3)
      READ  444, II, JJ
      A(1) = II
      A(2) = JJ
      A(3) = II*JJ
      A(4) = 0.
      IF(A(3))2,3,2
    2 CONTINUE
      L = 4 - JJ
      DO 1 I = 1,II
      L = L + JJ
    1 READ  700,(A(L+J), J = 1,JJ)
    3 CONTINUE
      RETURN
      END
```

```
      SUBROUTINE MINR(A, I, J, B)
C     VECTOR FORMAT
      DIMENSION A(1), B(1)
      M = A(1) + .01
      N = A(2) + .01
      IF(I)11,10,11
   10 I = 99999
      MM1 = M
      GO TO 12
   11 MM1 = M - 1
   12 IF(J)13,14,13
   14 J = 99999
      NM1 = N
      GO TO 9
   13 NM1 = N - 1
    9 DO 1 K = 1,M
      DO 1 L = 1,N
      IF(I-K)2,8,3
    2 II = K - 1
      GO TO 4
    3 II = K
    4 IF(J-L)5,8,6
    5 JJ = L-1
      GO TO 7
    6 JJ = L
    7 B(II*NM1 + JJ - NM1 + 4) = A(K*N + L - N + 4)
    8 CONTINUE
    1 CONTINUE
      B(1) = MM1
      B(2) = NM1
      B(3) = MM1*NM1
      B(4) = 0.
      RETURN
      END
```

```
      SUBROUTINE MAKE(A, B)
C     VECTOR FORMAT
      DIMENSION A(1), B(1)
      N = B(1)*B(2) + 4.01
      DO 1 I = 1,N
    1 A(I) = B(I)
      RETURN
      END
```

```
      SUBROUTINE MULT(A, B, C)
C     VECTOR FORMAT - NEITHER A NOR B CAN BE EQUIVALENT TO C
      DIMENSION A(1), B(1), C(1)
      II = A(1) + .01
      JJ = B(2) + .01
      KK = A(2) + .01
      LL = B(1) + .01
      CALL SET(C, II, JJ)
      IF(KK - LL)12,11,12
   12 PRINT 123
  123 FORMAT(55H MATRICES INCOMPATIBLE FOR MULT, DUM-DUM....          )
   11 DO 1 I = 1,II
      DO 1 J = 1,JJ
      DO 1 K = 1,KK
      IJ = (I-1)*JJ + J + 4
      IK = (I-1)*KK + K + 4
      KJ = (K-1)*JJ + J + 4
    1 C(IJ) = C(IJ) + A(IK)*B(KJ)
      C(1) = A(1)
      C(2) = B(2)
      C(3) = II*JJ
      C(4) = 0.
      RETURN
      END
```

```
      SUBROUTINE SOLVE(A, C)
C    VECTOR FORMAT
      DIMENSION A(1), C(1)
  101 FORMAT(E15.7)
      N = A(1) - .99
      NM1 = N - 1
      NP1 = N + 1
      NP3 = N - 3
      DO 6 K = 1,NM1
      AKK1 = 1./A(K*NP1 + K - NP3)
      K1 = K + 1
      DO 6 KI = K1,N
      AKIK = A(KI*NP1 + K - NP3)*A(K1
      DO 6 L = K1,NP1
      KIL = KI*NP1 + L - NP3
    6 A(KIL) = A(KIL) - AKIK*A(K*NP1 + L - NP3)
      DETA = A(5)
      C(N+4) = A(NP1*NP1 - NP3)/A(N*NP1 + 3)
      DO 16 I = 2,N
      NI1 = N - I + 1
      C(NI1 + 4) = A(NI1*NP1 + 4)
      NI2 = NI1 + 1
      DO 8 J = NI2,N
    8 C(NI1+4) = C(NI1+4) - C(J+4)*A(NI1*NP1 + J - NP3)
      C(NI1+4) = C(NI1+4)/A(NI1*NP1 + NI1 - NP3)
   16 DETA = DETA*A(I*NP1 + I - NP3)
      PRINT 101, DETA
      C(1) = 1.0
      C(2) = A(1) - 1.0
      C(3) = C(2)
      C(4) = 0.0
      RETURN
      END
```

```
      SUBROUTINE SPIT(A, B)
C     VECTOR FORMAT
      DIMENSION A(1)
  505 FORMAT(5E12.4)
  321 FORMAT(6H MATRIX ,A5,4HHAS ,I4,10H ROWS AND ,I4,8H COLUMNS)
      II = A(1) + .01
      JJ = A(2) + .01
      PRINT 321, B, II, JJ
      L = 4 - JJ
      IF(II)3,3,2
    2 DO 1 I = 1,II
      L = L + JJ
    1 PRINT 505,(A(L+J), J = 1,JJ)
    3 RETURN
      END
```



```
      SUBROUTINE SET(A, II, JJ)
C     VECTOR FORMAT
      DIMENSION A(1)
      A(1) = II
      A(2) = JJ
      A(3) = II*JJ
      A(4) = 0.
      N = II*JJ + 4
      DO 1 I = 5,N
    1 A(I) = 0.0
      RETURN
      END
```

```
      SUBROUTINE TRICK(A, B, C)
C     VECTOR FORMAT
      DIMENSION A(1), B(1), C(1)
      IB = B(1) + .01
      JB = B(2) + .01
      II = A(1) + .01
      JJ = A(2) + .01
      IF((IB-1)*(JB-1))3,4,3
    4 CONTINUE
      DO 1 J = 1,II
      DO 1 I = 1,J
      IJ = (I-1)*II + J + 4
      DO 2 K = 1,JJ
    2 C(IJ) = C(IJ) + A(I*JJ+K-JJ+4)*A(J*JJ+K-JJ+4)*B(K+4)
    1 C(J*II + I - II + 4) = C(IJ)
      RETURN
    3 CONTINUE
      DO 11 J = 1,II
      DO 11 I = 1,J
      IJ = (I-1)*II + J + 4
      DO 12 K = 1,JJ
      IK = (I-1)*JJ + K + 4
      DO 12 L = 1,JJ
      KL = (K-1)*JJ + L + 4
      JL = (J-1)*JJ + L + 4
   12 C(IJ) = C(IJ) + A(IK)*B(KL)*A(JL)
   11 C(J*II + I - II + 4) = C(IJ)
      RETURN
      END
```

APPENDIX C

IDENTIFICATION RESULTS (UNREDUCED)

Unreduced Derivatives:

$$X'_{\tilde{w}} = \frac{X_{\tilde{w}}}{U}$$

$$Z'_{\tilde{w}} = \frac{Z_{\tilde{w}}}{U_o - Z_{\dot{\tilde{w}}}}$$

$$M'_u = M_u + \frac{M_{\dot{\tilde{w}}} Z_u}{U_o - Z_{\dot{\tilde{w}}}}$$

$$M'_{\tilde{w}} = M_{\tilde{w}} + \frac{M_{\dot{\tilde{w}}} Z_{\tilde{w}}}{U_o - Z_{\dot{\tilde{w}}}}$$

$$M'_q = M_q + M_{\dot{\tilde{w}}} \left[\frac{U_o + Z_q}{U_o - Z_{\dot{\tilde{w}}}} \right]$$

$$Z'_{\delta_e} = \frac{Z_{\delta_e}}{U_o - Z_{\dot{\tilde{w}}}}$$

$$M'_{\delta_e} = M_{\delta_e} + \frac{M_{\dot{\tilde{w}}} Z_{\delta_e}}{U_o - Z_{\dot{\tilde{w}}}}$$

Initial Conditions: X_o, Z_o, M_o

For run number coding refer to page 52.

Preceding page blank

TABLE C-I
IDENTIFICATION RESULTS (FLIGHT CONDITION #1)

Derivative Name	Start-Up	Run No. DR2-1W1	DR2-1W2	DR2-1W3
X_u	-.046	-.066	-.074	-.076
X'_{α}	-.087	-.049	-.046	-.041
Z_u	-.27	.040	.062	.069
Z'_{α}	-.877	-1.142	-1.16	-1.17
M'_u	1.59	.28	.23	.21
M'_{α}	-4.59	-4.95	-4.99	-5.02
M'_q	-1.95	-1.74	-1.76	-1.77
Z'_{δ_e}	-.092	-.090	-.082	-.081
M'_{δ_e}	-9.63	-9.16	-9.24	-9.28
X_o	-	$-.2 \times 10^{-2}$	$-.3 \times 10^{-2}$	$-.3 \times 10^{-2}$
Z_o	-	$.8 \times 10^{-2}$	$1. \times 10^{-2}$	$.1 \times 10^{-1}$
M_o	-	$-.2 \times 10^{-1}$	$-.2 \times 10^{-1}$	$-.2 \times 10^{-1}$
Run Time	-	17.5	17.5	17.5
Trim Velocity	-	266.5	266.5	266.5

TABLE C-I (CONTINUED)
IDENTIFICATION RESULTS (FLIGHT CONDITION #1)

Derivative Name	Start-Up	Run No. DR3-1	DR3-1W1	DR3-1W2
X_u	-.046	-.046	-.028	-.046
X'_α	-.087	-.087	-.047	-.023
Z_u	-.27	-.27	-.26	-.28
Z'_α	-.877	-.877	-.903	-.954
M'_u	1.59	1.60	.935	-.020
M'_α	-4.59	-4.59	-4.54	-4.46
M'_q	-1.95	-1.95	-1.97	-1.75
Z'_{δ_e}	-.092	-.092	-.089	-.088
M'_{δ_e}	-9.63	-9.61	-7.56	-7.15
X_o	-	-0.8×10^{-3}	-0.3×10^{-2}	-0.2×10^{-2}
Z_o	-	0.4×10^{-3}	0.1×10^{-1}	0.2×10^{-1}
M_o	-	-0.6×10^{-4}	-0.2×10^{-1}	-0.2×10^{-1}
Run Time	-	17.5	17.5	17.5
Trim Velocity	-	246.7	246.7	246.7

TABLE C-I (CONTINUED)
IDENTIFICATION RESULTS (FLIGHT CONDITION #1)

Derivative Name	Start-Up	Run No. DR3-2W	DR3-2W2	DR3-U2W1
X_u	-.046	-.046	-.047	-.054
X'_α	-.087	-.048	-.030	-.023
Z_u	-.27	-.356	-.373	-.414
Z'_α	-.877	-.831	-.817	-.954
M'_u	1.59	-.57	-.61	-.73
M'_α	-4.59	-4.45	-4.34	-4.46
M'_q	-1.95	-2.13	-2.19	-1.75
Z'_{δ_e}	-.092	-.090	-.089	-.090
M'_{δ_e}	-9.63	-7.07	-7.10	-7.15
X_o	-	-0.2×10^{-2}	-0.3×10^{-2}	-0.2×10^{-2}
Z_o	-	0.2×10^{-1}	0.2×10^{-1}	0.2×10^{-1}
M_o	-	-0.1×10^{-1}	-0.2×10^{-1}	-0.2×10^{-1}
Run Time	-	35	35	35
Trim Velocity	-	246.7	246.7	246.7

TABLE C-I (CONTINUED)
IDENTIFICATION RESULTS (FLIGHT CONDITION #1)

Derivative Name	Start-Up	Run No. DR3-U3W1	DR3-U3W2	DR3-1W1DEZ
X_u	-.046	-.046	-.046	-.044
X'_{α}	-.087	-.023	-.023	+.002
Z_u	-.27	-.338	-.387	-.22
Z'_{α}	-.877	-.954	-.954	-.804
M'_u	1.59	-.62	-.84	.75
M'_{α}	-4.59	-4.46	-4.46	-4.69
M'_q	-1.95	-1.75	-1.75	-2.03
Z'_{δ_e}	-.092	-.090	-.090	-.092
M'_{δ_e}	-9.63	-7.15	-7.15	-7.66
X_o	-	-0.2×10^{-2}	0.1×10^{-2}	-0.5×10^{-2}
Z_o	-	0.1×10^{-1}	0.2×10^{-1}	0.1×10^{-1}
M_o	-	-0.2×10^{-1}	-0.2×10^{-1}	-0.2×10^{-1}
Run Time		52.5	52.5	17.5
Trim Velocity		246.7	246.7	246.7

TABLE C-I (CONTINUED)
IDENTIFICATION RESULTS (FLIGHT CONDITION #1)

Derivative Name	Start-Up	Run No. DR4-1W1	DR4-1W2	DR4-1W3	DR4-1W4
X_u	-.046	-.023	-.014	-.020	-.036
X'_α	-.087	-.057	-.038	-.043	-.042
Z_u	-.27	-.16	-.20	-.22	-.22
Z'_α	-.877	-.922	-.904	-.887	-.879
M'_u	1.59	-.67	-.83	-.93	-.96
M'_α	-4.59	-4.30	-4.27	-4.24	-4.22
M'_q	-1.95	-1.72	-1.76	-1.79	-1.81
Z'_{δ_e}	-.092	-.096	-.088	-.090	-.091
M'_{δ_e}	-9.63	-8.08	-8.11	-8.18	-8.21
X_o	-	$.2 \times 10^{-2}$	$.9 \times 10^{-3}$	$-.1 \times 10^{-3}$	$-.7 \times 10^{-3}$
Z_o	-	$-.4 \times 10^{-3}$	$-1. \times 10^{-3}$	$-.2 \times 10^{-2}$	$-.2 \times 10^{-2}$
M_o	-	$.6 \times 10^{-2}$	$.3 \times 10^{-2}$	$-.4 \times 10^{-3}$	$-.3 \times 10^{-2}$
Run Time		17.5	17.5	17.5	17.5
Trim Velocity		253.2	253.2	253.2	253.2

TABLE C-I (CONTINUED)
IDENTIFICATION RESULTS (FLIGHT CONDITION #1)

Derivative Name	Start-Up	Run No. DR5-1W1	DR5-1W2	DR5-1W3
X_u	-.046	.034	.035	.034
X'_{α}	-.087	.023	.024	.020
Z_u	-.27	-.35	-.36	-.35
Z'_{α}	-.877	-.919	-.922	-.941
M'_u	1.59	1.29	1.29	1.25
M'_{α}	-4.59	-4.80	-4.81	-4.86
M'_q	-1.95	-1.87	-1.88	-1.85
Z'_{δ_e}	-.092	-.113	-.113	-.103
M'_{δ_e}	-9.63	-8.66	-8.67	-8.60
X_o	-	$.7 \times 10^{-3}$	$.7 \times 10^{-3}$	$.7 \times 10^{-3}$
Z_o	-	$.60 \times 10^{-2}$	$.6 \times 10^{-2}$	$.6 \times 10^{-2}$
M_o	-	$-1. \times 10^{-2}$	$-1. \times 10^{-2}$	$-.1 \times 10^{-1}$
Run Time	-	17.5	17.5	17.5
Trim Velocity	-	255.7	255.7	255.7

TABLE C-I (CONTINUED)
IDENTIFICATION RESULTS (FLIGHT CONDITION #1)

Derivative Name	Start-Up	Run No. DR6-1W1	DR6-1W2	DR6-1W2SH	DR6-1W3SH
X_u	-.046	.024	.025	.018	0
X'_w	-.087	-.052	-.055	-.044	-.034
Z_u	-.27	-.38	-.38	-.25	-.24
Z'_w	-.877	-.941	-.945	-.937	-.927
M'_u	1.59	.56	.54	.59	.47
M'_w	-4.59	-4.51	-4.53	-4.54	-4.41
M'_q	-1.95	-1.76	-1.79	-1.81	-1.86
Z'_{δ_e}	-.092	-.094	-.096	-.089	-.086
M'_{δ_e}	-9.63	-6.74	-6.81	-7.97	-8.10
X_o	-	$.2 \times 10^{-2}$	$.2 \times 10^{-2}$	$.2 \times 10^{-2}$	$.2 \times 10^{-2}$
Z_o	-	$-.1 \times 10^{-1}$	$-.1 \times 10^{-1}$	$-.1 \times 10^{-1}$	$-.1 \times 10^{-1}$
M_o	-	$.1 \times 10^{-1}$	$.2 \times 10^{-1}$	$.2 \times 10^{-1}$	$.2 \times 10^{-1}$
Run Time		17.5	17.5	10.0	10.0
Trim Velocity		251.6	251.6	251.6	251.6

TABLE C-II
IDENTIFICATION RESULTS (FLIGHT CONDITION #2)

Derivative Name	Start-Up	Run No. DR10-1W1S1	DR10-1W2S1	DR10-1W2S2
X_u	-.016	-.0034	.0017	.0010
$X'_{\sim}$	-.054	.0065	.011	.010
Z_u	-.12	+.179	+.156	+.155
$Z'_{\sim}$	-2.46	-1.89	-2.05	-2.06
M'_u	1.34	-.375	-.63	-.63
M'_{α}	-18.6	-19.07	-19.0	-19.0
M'_q	-4.96	-8.59	-8.15	-8.04
Z'_{δ_e}	-.18	-.19	-.19	-.19
M'_{δ_e}	-51.8	-49.0	-49.4	-49.8
X_o	-	$.15 \times 10^{-3}$	$.3 \times 10^{-3}$	$.3 \times 10^{-3}$
Z_o	-	$-.5 \times 10^{-2}$	$-.5 \times 10^{-2}$	$-.5 \times 10^{-2}$
M_o	-	$.6 \times 10^{-3}$	$.5 \times 10^{-2}$	$.5 \times 10^{-2}$
Run Time	-	17.5	17.5	17.5
Trim Velocity	-	683.7	683.7	683.7

TABLE C-II (CONTINUED)
IDENTIFICATION RESULTS (FLIGHT CONDITION #2)

Derivative Name	Start-Up	Run No. DR11-1W1S2	DR11-1W2S2	DR11-1W1S2DEZ
X_u	-.016	-.026	-.038	-.004
X'_{α}	-.054	.012	.028	.020
Z_u	-.12	.029	.092	.172
Z'_{α}	-2.46	-2.28	-2.13	-1.80
M'_u	1.34	.78	.751	.32
M'_{α}	-18.6	-19.0	-19.1	-19.1
M'_q	-4.96	-9.78	-9.05	-7.29
Z'_{δ_e}	-.18	-.18	-.19	-.20
M'_{δ_e}	-51.8	-48.8	-49.1	-50.3
X_o	-	$-.2 \times 10^{-3}$	$-.5 \times 10^{-3}$	$.2 \times 10^{-3}$
Z_o	-	$.2 \times 10^{-1}$	$.2 \times 10^{-1}$	$.1 \times 10^{-1}$
M_o	-	$-.4 \times 10^{-2}$	$-.7 \times 10^{-2}$	$-.4 \times 10^{-2}$
Run Time	-	17.5	17.5	17.5
Trim Velocity	-	679.2	679.2	679.2

TABLE C-II (CONTINUED)
IDENTIFICATION RESULTS (FLIGHT CONDITION #2)

Derivative Name	Start-Up	Run No. DR11-1W2S2DEZ	DR11-U4W1S2DEZ	DR11-U4W2S2DEZ
X_u	-.016	-.006	-.117	-.099
X'_{α}	-.054	.017	.017	.017
Z_u	-.12	.175	.158	-.011
Z'_{α}	-2.46	-2.00	-2.00	-2.00
M'_u	1.34	.259	1.07	1.12
M'_{α}	-18.6	-19.3	-19.3	-19.3
M'_q	-4.96	-8.69	-8.69	-8.69
Z'_{δ_e}	-.18	-.20	-.20	-.20
M'_{δ_e}	-51.8	-49.3	-49.3	-49.3
X_o	-	$.2 \times 10^{-3}$	$-.5 \times 10^{-3}$	$-.2 \times 10^{-3}$
Z_o	-	$.1 \times 10^{-1}$	$.5 \times 10^{-2}$	$.87 \times 10^{-3}$
M_o	-	$-.6 \times 10^{-2}$	$-.1 \times 10^{-1}$	$.6 \times 10^{-2}$
Run Time	-	17.5	70	70
Trim Velocity	-	679.2	679.2	679.2

TABLE C-II (CONTINUED)
IDENTIFICATION RESULTS (FLIGHT CONDITION #2)

Derivative Name	Start-Up	Run No. DR12-U5W1S2DEZ	DR12-U5W2S2DEZ	DR12-U5W3S2DEZ
X_u	-.016	-.038	-.040	-.038
X'_{α}	-.054	-.054	-.054	.017
Z_u	-.12	-.207	-.215	-.233
Z'_{α}	-2.46	-2.03	-2.03	-2.00
M'_u	1.34	1.40	1.28	1.57
M'_{α}	-18.6	-22.0	-22.0	-19.3
M'_q	-4.96	-7.0	-7.0	-8.69
Z'_{δ_e}	-.18	-.2	-.2	-.20
M'_{δ_e}	-51.8	-50.	-50.	-49.3
X_o	-	$-.2 \times 10^{-2}$	$-.2 \times 10^{-2}$	$-.1 \times 10^{-2}$
Z_o	-	$-.5 \times 10^{-2}$	$-.5 \times 10^{-2}$	$-.6 \times 10^{-2}$
M_o	-	$.8 \times 10^{-2}$	$.1 \times 10^{-2}$	$.4 \times 10^{-2}$
Run Time	-	87.5	87.5	87.5
Trim Velocity	-	669.9	669.9	669.9

TABLE C-II (CONTINUED)
IDENTIFICATION RESULTS (FLIGHT CONDITION #2)

Derivative Name	Start-Up	Run No. DR13-1W1S2	Run No. DR13-1W2S2
X_u	-.016	-.029	-.027
X'_α	-.054	+.027	+.028
Z_u	-.12	+.106	+.093
Z'_α	-2.46	-2.06	-1.98
M'_u	1.34	+.91	+.70
M'_α	-18.6	-19.7	-19.4
M'_q	-4.96	-9.15	-9.29
Z'_{δ_e}	-.18	-.19	-.20
M'_{δ_e}	-51.8	-48.3	-48.6
X_o	-	$-.3 \times 10^{-3}$	$-.3 \times 10^{-3}$
Z_o	-	$.2 \times 10^{-1}$	$.2 \times 10^{-1}$
M_o	-	$-.2 \times 10^{-1}$	$-.9 \times 10^{-2}$
Run Time	-	17.5	17.5
Trim Velocity	-	680.8	680.8

TABLE C-II (CONTINUED)
IDENTIFICATION RESULTS (FLIGHT CONDITION #2)

Derivative Name	Start-Up	Run No. DR14-1W1S1SH	DR14-1W2S2SH	DR14-1W3S2SH
X_u	-.016	.044	.052	.053
X'_α	-.054	.043	.042	.041
Z_u	-.12	+.111	+.021	-.021
Z'_α	-2.46	-2.02	-2.28	-2.41
M'_u	1.34	.40	.73	.91
M'_α	-18.6	-19.5	-19.3	-19.2
M'_q	-4.96	-10.36	-9.78	-9.65
Z'_{δ_e}	-.18	-.20	-.19	-.18
M'_{δ_e}	-51.8	-47.7	-48.6	-48.7
X_o	-	$.2 \times 10^{-2}$	$.2 \times 10^{-2}$	$.2 \times 10^{-2}$
Z_o	-	$.1 \times 10^{-1}$	$.1 \times 10^{-1}$	$.1 \times 10^{-1}$
M_o	-	$-.1 \times 10^{-1}$	$-.1 \times 10^{-1}$	$-.1 \times 10^{-1}$
Run Time	-	15.0	15.0	15.0
Trim Velocity	-	687.2	687.2	687.2

TABLE C-II (CONTINUED)
IDENTIFICATION RESULTS (FLIGHT CONDITION #2)

Derivative Name	Start-Up	Run No. DR18-1W1S2	DR18-1W2S2	DR18-1W3S2
X_u	-.016	+.044	+.036	.024
$X'_{\sim}$	-.054	+.050	.050	.048
Z_u	-.12	+.022	-.021	+.005
$Z'_{\sim}$	-2.46	-1.66	-1.44	-1.64
M'_u	1.34	+1.94	1.29	1.00
$M'_{\sim}$	-18.6	-21.0	-19.7	-19.3
M'_q	-4.96	-9.23	-8.88	-8.62
Z'_{δ_e}	-.18	-.21	-.21	-.21
M'_{δ_e}	-51.8	-45.4	-48.7	-49.4
X_o	-	$.8 \times 10^{-3}$	$.6 \times 10^{-3}$	$.9 \times 10^{-3}$
Z_o	-	$.3 \times 10^{-1}$	$.4 \times 10^{-1}$	$.2 \times 10^{-1}$
M_o	-	$-.3 \times 10^{-1}$	$-.9 \times 10^{-2}$	$-.5 \times 10^{-2}$
Run Time	-	17.5	17.5	17.5
Trim Velocity	-	682.8	682.8	682.8

TABLE C-II (CONTINUED)
IDENTIFICATION RESULTS (FLIGHT CONDITION #2)

Derivative Name	Start-Up	Run No. DR19-1W	Run No. DR19-1W2
X_u	-.016	-.097	-.075
$X'_\sim$	-.054	+.062	+.036
Z_u	-.12	-.116	-.013
$Z'_\sim$	-2.46	-2.00	-1.98
M'_u	1.34	-.123	+.276
$M'_\sim$	-18.6	-20.0	-19.55
M'_q	-4.96	-9.91	-9.51
Z'_{δ_e}	-.18	-.19	-.20
M'_{δ_e}	-51.8	-45.8	-48.2
X_o	-	$-.2 \times 10^{-2}$	$-.2 \times 10^{-2}$
Z_o	-	$-.2 \times 10^{-1}$	$-.3 \times 10^{-1}$
M_o	-	$+.2 \times 10^{-1}$	$+.8 \times 10^{-2}$
Run Time	-	17.5	17.5
Trim Velocity	-	690.0	690.0

Note: "S" followed by digit indicates degree of smoothing for elevator signal

☆U. S. GOVERNMENT PRINTING OFFICE: 1975—603-811/1201 Reg. No. 2-1